

Appendix C. Development of Geologic Framework of Regional Groundwater Flow Model

C.1. High-Resolution Geologic Model

The high-resolution geologic model is a set of 12 high-resolution surface models of individual surfaces, here referred to as *high-resolution surface models* (Table C-1), representing the top elevations of each of the 11 model hydrostratigraphic units and the bottom elevation of the Mt. Simon Unit. Each high-resolution surface model consists of a point-feature shapefile containing an estimate of the elevation of the surface at each point in the regional model domain. Each model was produced by interpolation of point-estimates of the top elevation of the unit (*interpolation source data*), derived from a variety of sources, followed by post-processing of the interpolation results. The accuracy of each high-resolution surface model is greatest in the area of active model cells east of the Mississippi River.

Because the finite-difference groundwater flow modeling approach requires that the models of all hydrostratigraphic units extend across the entire model domain, each of the 11 high-resolution surface models includes estimates of the surface elevation both in areas where the unit is present and in areas where it is absent. Top-elevation estimates in the area of absence of a hydrostratigraphic unit are essentially equal to those of the underlying unit, implying a thickness of zero for the unit in its area of absence. The high-resolution surface model of the top of the Upper Bedrock Unit is equivalent to a model of bedrock surface, which is present in the real world throughout the regional model domain. Likewise, the high-resolution surface model of the base of the Mt. Simon Unit is equivalent to a model of the Precambrian surface, which is also present throughout the model domain.

Except for the high-resolution surface model of the top of the Quaternary Unit—a special case developed from surface-elevation data and Lake Michigan bathymetric data—each high-resolution surface model was developed through interpolation of three general types of source data (Figure C-1). In areas east of the Mississippi River (the active cells of the regional model), structure data were used as estimates of the top elevation of the unit in areas where the unit is present, but not exposed at the bedrock surface. In areas west of the Mississippi River, structure data were used as estimates of the top elevation of the unit in all areas where the unit is present, whether or not it is exposed at the bedrock surface. Estimates of bedrock-surface elevation were employed as interpolation source data in areas of bedrock-surface exposure east of the Mississippi River. For the model of the top of the Upper Bedrock Unit, these consist principally of data derived from bedrock-surface topographic maps. For models of the other units, the bedrock-surface estimates consist of point data selected and clipped from the model of the Upper Bedrock Unit, which was completed early in the process. Estimates of the elevation of the underlying unit were generally used as interpolation source data in areas of absence of a unit. These consist of point data selected and clipped from the high-resolution surface model of the underlying unit developed earlier in the overall process.

Following interpolation, the provisional high-resolution surface model was adjusted using the previously developed high-resolution surface model of an overlying unit, or, more commonly, previously developed high-resolution surface models of both an overlying and underlying unit. Because the procedure of developing each high-resolution surface model employed previously developed high-resolution surface models, order of development of the high-resolution surface models was important to compiling an accurate high-resolution geologic

model (Table C-2). For example, high-resolution surface modeling of the top of the Upper Bedrock Unit employed data from the high-resolution surface model of the top of the Quaternary Unit, requiring that the Quaternary Unit model be completed first. The portion of each high-resolution surface model corresponding to the area of active cells east of the Mississippi River was clipped as an *active-cell high-resolution surface model* and was employed for development of the irregular-grid geologic model.

Most of the data processing leading to the high-resolution geologic model was conducted using ArcGIS version 9.1 (Environmental Systems Research Institute, 2005) and Surfer version 8 (Golden Software Inc., 2002). The terms shapefile and coverage as used in this report refer to proprietary data formats employed in ArcGIS.

Table C-1. Specialized Terminology Employed in Discussion of Geological Modeling

<i>Term</i>	<i>Definition</i>
Active-cell high-resolution surface model	Point-shapefile created from a <i>high-resolution surface model</i> containing estimates of the elevation of a hydrostratigraphic horizon at nodes in the part of the regional model domain east of the Mississippi River.
High-resolution geologic model	Set of 12 <i>high-resolution surface models</i> of the tops of each of the 11 hydrostratigraphic units and the bottom of the Mt. Simon Unit.
High-resolution surface model	Point-shapefile containing estimates of the elevation of a hydrostratigraphic horizon at nodes spaced 762 m (2500 ft) apart across the entire regional model domain.
Interpolation source data	Data sources for point-format estimates of the elevation of a hydrostratigraphic horizon that are interpolated to develop a <i>provisional high-resolution surface model</i> . Examples include high-resolution surface models, hardcopy structure-contour or bedrock-topography maps, polyline-feature shapefiles depicting bedrock topography, and point-shapefiles created by adding or subtracting thickness and structure data.
Irregular-grid geologic model	Set of 12 <i>irregular-grid surface models</i> , in Microsoft Excel format, of the tops of each of the 11 hydrostratigraphic units and the bottom of the Mt. Simon Unit.
Irregular-grid surface model	Estimates of the elevation of a hydrostratigraphic horizon for each active cell in the irregular finite-difference groundwater flow modeling grid in Microsoft Excel format. Elevation estimates are adjusted from a provisional irregular-grid surface model to accommodate a minimum model layer thickness of one foot.
Provisional high-resolution surface model	Point-shapefile containing results of interpolation of <i>interpolation source data</i> that have not been adjusted to remove <i>stratigraphic violations</i> .
Provisional irregular-grid surface model	Polygon-shapefile containing estimates of the elevation of a hydrostratigraphic horizon for each active cell in the irregular finite-difference groundwater flow modeling grid. Elevation estimates are averages for each cell of estimated elevations in an active-cell high-resolution surface model.
Stratigraphic violation	An inconsistency between two or more depictions of geologic structure (for example, hardcopy structure-contour maps, polyline-format digital structure-contour data, point-format digital interpolated elevation results, etc.) implying that one surface is at a higher elevation than another surface that is stratigraphically higher.

Table C-2. Order of Development and Interpolation Source Data of High-Resolution Surface Models

<i>Order</i>	<i>High-Resolution Surface Model (HRSM)</i>	<i>General Description of Interpolation Source Data</i>		
		<i>Unit is Present (Not Exposed at Bedrock Surface)</i>	<i>Unit Exposed at Bedrock-Surface</i>	<i>Unit Absent</i>
1	Top of Quaternary Unit (Land Surface)	NA ¹	NA	NA
2	Top of Upper Bedrock Unit (Bedrock Surface)	NA	Bedrock-surface elevation data	Bedrock-surface elevation data; Top of Quaternary Unit (HRSM) in driftless area
3	Base of Mt. Simon Unit (Precambrian Surface)	Precambrian top-elevation estimates	Top of Upper Bedrock Unit (Bedrock Surface) (HRSM) ²	NA
4	Top of Mt. Simon Unit	Mt. Simon Unit top-elevation estimates	Top of Upper Bedrock Unit (Bedrock Surface) (HRSM)	Base of Mt. Simon Unit (Precambrian Surface) (HRSM)
5	Top of Silurian-Devonian Carbonate Unit (First Iteration)	Silurian-Devonian Carbonate Unit top-elevation estimates	Top of Upper Bedrock Unit (Bedrock Surface) (HRSM)	Top of Mt. Simon Unit (HRSM)
6	Top of Eau Claire Unit	Eau Claire Unit top-elevation estimates	Top of Silurian-Devonian Carbonate Unit (First Iteration) (HRSM)	Top of Mt. Simon Unit (HRSM)
7	Top of Ironton-Galesville Unit	Ironton-Galesville Unit top-elevation estimates		Top of Eau Claire Unit (HRSM)
8	Top of Potosi-Franconia Unit	Potosi-Franconia Unit top-elevation estimates		Top of Ironton-Galesville Unit (HRSM)
9	Top of Prairie du Chien-Eminence Unit	Prairie du Chien-Eminence Unit top-elevation estimates		Top of Potosi-Franconia Unit (HRSM)
10	Top of Ansell Unit	Ansell Unit top-elevation estimates		Top of Prairie du Chien-Eminence Unit (HRSM)
11	Top of Galena-Platteville Unit	Galena-Platteville Unit top-elevation estimates		Top of Ansell Unit (HRSM)
12	Top of Maquoketa Unit	Maquoketa Unit top-elevation estimates		Top of Galena-Platteville Unit (HRSM)
13	Top of Silurian-Devonian Carbonate Unit (Second Iteration)	Silurian-Devonian Carbonate Unit top-elevation estimates	Top of Upper Bedrock Unit (Bedrock Surface) (HRSM)	Top of Maquoketa Unit (HRSM)

¹NA: not applicable

²Used in areas of Precambrian bedrock-surface exposure.

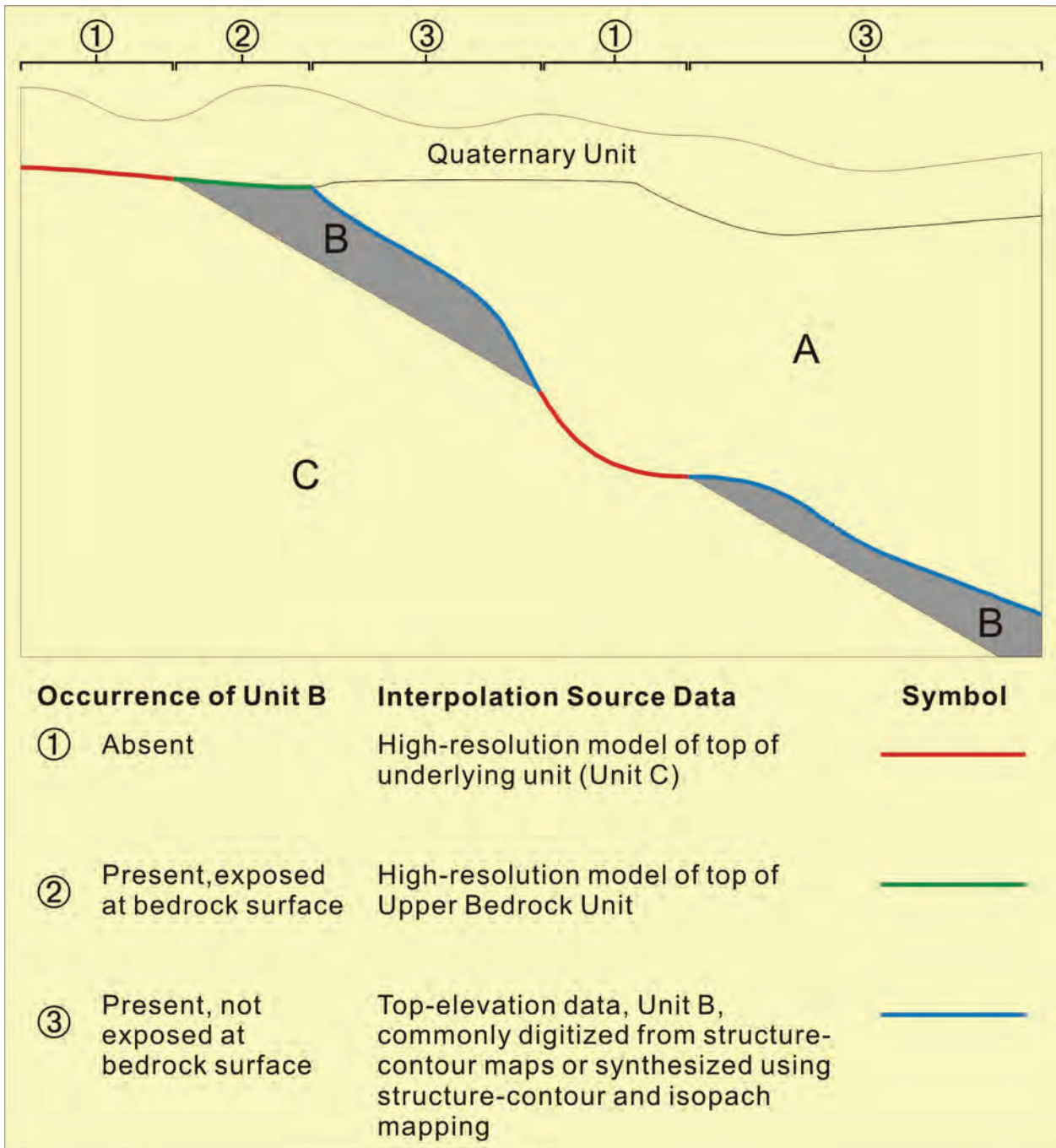


Figure C-1. General categories of source data employed for interpolation in area of active model cells.

C.1.1. Development of Required Geologic Mapping Elements

The high-resolution geologic modeling methodology required development and compilation of (1) mapping of bedrock-surface exposures of the hydrostratigraphic units; (2) mapping of areas of absence of the hydrostratigraphic units; and (3) mapping of fault features to be used as breaklines in the interpolation procedure. As described in the preceding section, mapping of areas of bedrock-surface exposure and areas of absence were employed to select elevation data from previously developed high-resolution surface models for use in the interpolation process. Mapping of fault features allowed the interpolation process to replicate escarpments along the selected faults.

C.1.1.1. Bedrock-Surface Exposures

Delineation of areas of bedrock-surface exposure—areas of outcrop and Quaternary subcrop—relied heavily on GIS-format state geologic maps of Illinois (Illinois Department of Natural Resources, 1996a) and Indiana (Gray et al., 2002) as well as a GIS-format geologic map of the Lake Superior area of Michigan, Minnesota, and Wisconsin (Cannon et al., 1997). Bedrock-surface exposures were delineated only in the portion of the regional model domain east of the Mississippi River because the trans-Mississippi area was designated as inactive. In the trans-Mississippi area, where estimated elevations of tops of hydrostratigraphic units are irrelevant, interpolation source data in areas of bedrock-surface exposure are based on structure-contour maps.

With one exception, the use of different mapping units by the authors of the geologic maps of Illinois, Indiana, and the Lake Superior area was not problematic, since the hydrostratigraphic units employed in the modeling effort are often aggregations of the lithostratigraphic mapping units used in the maps (Table C-3). The exception pertains to the Cambrian lithostratigraphic units, in which both the Illinois and Lake Superior-area geologic mapping aggregate into a single Cambrian mapping unit (Cambrian rocks are not exposed at the bedrock surface in Indiana). The regional modeling effort, however, includes Cambrian lithostratigraphic units in several hydrostratigraphic units, and development of the high-resolution geologic model consequently required that bedrock-surface exposures be delineated for these units. Numerous published and unpublished resources were employed to subdivide the mapped Cambrian bedrock-surface exposure into exposures of hydrostratigraphic units used in the modeling effort. The resulting maps of bedrock-surface exposures were saved as polygon-shapefiles for later use in data processing.

Except for a single outlier where the Franconia Formation crops out (Willman et al., 1975), Cambrian rocks crop out or subcrop the Quaternary in a small portion of Illinois immediately south of the Sandwich Fault Zone, where Cambrian bedrock-surface exposure includes the upper portion of the Franconia Formation, the Potosi Dolomite, and the Eminence Formation (Kolata et al., 1978; Willman et al., 1975). No published or unpublished resource displays the areas of bedrock-surface exposure of these formations within the Cambrian bedrock-surface exposure south of the Sandwich Fault. However, it is reasonable to conclude that rocks assigned in this paper to the Potosi-Franconia Unit make up most of the areal extent of exposure. This conclusion is based on the fact that the uneroded Potosi Dolomite thickness in the area—on the order of 150 ft—is about three times greater than that of the Eminence Formation (Willman et al., 1975), together with the fact that an unknown thickness of the Franconia Formation is reportedly exposed here. In the absence of detailed mapping of the Cambrian exposure, then, it is assumed that the entire area of the mapped Cambrian bedrock-surface exposure south of the

Sandwich Fault is a bedrock-surface exposure of the Potosi-Franconia Unit. For purposes of geologic modeling, this assumption results in an underestimation of the bedrock-surface exposure of the Prairie du Chien-Eminence Unit and an overestimation of the bedrock-surface exposure of the Potosi-Franconia Unit, since a portion of the mapped Cambrian bedrock-surface exposure must be occupied by dolomites of the Eminence Formation. The bedrock-surface exposure of the Prairie du Chien-Eminence Unit was assumed to be equivalent to the mapped area of Prairie du Chien exposure. From a hydrologic standpoint, however, this inaccuracy is probably of little importance, because the dolomites of both the Potosi-Franconia and Prairie du Chien-Eminence Units are hydraulically similar, and the mapping errors are compensatory: the overall bedrock-exposure of the two units honors the geologic mapping.

Unpublished structure-contour mapping (United States Geological Survey [USGS], Wisconsin District, personal communication, 2002), used for developing a regional groundwater-flow model of the Cambrian and Ordovician aquifers of the U.S. upper Midwest (Young, 1992), permitted the large Cambrian bedrock-surface exposure in Wisconsin to be disaggregated into bedrock-surface exposures of hydrostratigraphic units employed in the present modeling study. This mapping included delineations of areas of absence of equivalents of the Eau Claire Unit, Ironton-Galesville Unit, and Potosi-Franconia Unit.

The areas of absence illustrated on these maps were digitized for the present study, and these were displayed in an ArcGIS map file together with the Wisconsin Cambrian bedrock-surface exposure from Cannon et al. (1997). The area of bedrock-surface exposure of the Potosi-Franconia Unit was then approximated by erasing the area of absence of the Potosi-Franconia Unit (digitized from the unpublished USGS mapping) from the Cambrian bedrock-surface exposure (Cannon et al., 1997). Similarly, the area of bedrock-surface exposure of the Ironton-Galesville Unit was approximated as the portion of the Cambrian bedrock-surface exposure where the unpublished mapping showed (1) the Ironton-Galesville Unit to be present and (2) the Potosi-Franconia Unit to be absent. The bedrock-surface exposure of the Eau Claire Unit was approximated as the portion of the Cambrian bedrock-surface exposure where the unpublished mapping showed (1) the Eau Claire Unit to be present, (2) the Ironton-Galesville Unit to be absent, and (3) the Potosi-Franconia Unit to be absent. Finally, the bedrock-surface exposure of the Mt. Simon Unit was approximated as the portion of the Cambrian bedrock-surface exposure where the unpublished mapping showed the Eau Claire, Ironton-Galesville, and Potosi-Franconia Units to all be absent.

As was the case with the assumption regarding mapped Cambrian bedrock-surface exposures in Illinois, this set of assumptions regarding the Wisconsin exposure probably overestimates the bedrock-surface exposure of the Potosi-Franconia Unit at the expense of that of the Prairie du Chien-Eminence Unit. The Cambrian Eminence Formation and equivalent Jordan Formation in Wisconsin must occupy a portion of the mapped Cambrian bedrock-surface exposure, yet the assumption employed here assigns this area to the bedrock-surface exposure of the Potosi-Franconia Unit. Unlike the stratigraphically deeper units, a suitable map illustrating the area of absence of the Prairie du Chien-Eminence Unit in Wisconsin was not available, so—as was the assumption in Illinois—the area of exposure of the Prairie du Chien-Eminence Unit was assumed to be the mapped area of exposure of the Prairie du Chien Group only.

Table C-3 summarizes the aggregation of mapped geologic units in the Illinois, Indiana, and Lake Superior area geologic mapping into bedrock-surface exposures of the hydrostratigraphic units employed in the study. Offsets of contacts between mapped units at boundaries between the areas covered by the geologic maps were minor and not corrected since

these offsets would ultimately be of little importance following the averaging process leading to the irregular-grid geologic model. The resulting maps of bedrock-surface exposure areas were saved as ArcGIS polygon-shapefiles. They were generally created by selecting and—in ArcGIS Editor— copying polygons from the Illinois, Indiana, and Lake Superior area GIS-format geologic maps and pasting them into a polygon-shapefile developed for the bedrock-surface exposure of each hydrostratigraphic unit. The polygons within each of these shapefiles were then clipped using a polygon-shapefile of the regional model domain and, for clarity and ease of use, combined into a single feature.

The highly disruptive but very limited effects of the Des Plaines and Kentland Disturbances were removed from the bedrock-surface exposure mapping, effectively removing their effects from the resulting high-resolution and irregular-grid geologic models. The bedrock-surface manifestations of these features were removed because their local-scale structural effects are so poorly understood that the regional-scale structure-contour mapping that is the basis for much of the geologic modeling ignores them. Without detailed contour mapping of the subsurface structure of these features, use of the conflicting bedrock-surface exposure patterns and structure-contour data in the geologic-modeling procedure presented here would lead to an improbable rendering of the geologic structure. Removal of these probable impact features from the geologic models was viewed as acceptable for purposes of this project since their effect on regional groundwater circulation is probably negligible. The bedrock-exposure mapping of the Des Plaines Disturbance shown in the mapping of the Illinois Department of Natural Resources (1996a) was altered to remove effects of the feature on bedrock-surface geology by cutting polygons in the Disturbance representing rocks assigned to the Upper Bedrock, Maquoketa, and Ancell Units from the shapefiles developed to show bedrock-surface exposure of these units and pasting the cut polygons into the shapefile representing bedrock-surface exposure of the Silurian-Devonian Carbonate Unit. A similar approach was employed to alter the real-world bedrock-exposure pattern at the Kentland Disturbance. Here, polygon in the Disturbance representing rocks assigned to the Maquoketa Unit were cut and pasted into the shapefile representing the bedrock-surface exposure of the Silurian-Devonian Carbonate Unit. The bedrock-surface exposure patterns of the Des Plaines Disturbance and Kentland Disturbance were thus altered to resemble the bedrock surface of the surrounding, undisturbed areas.

The geologic modeling procedure required that bedrock-surface exposure patterns be assumed in areas for which bedrock-surface geologic mapping is not available, principally the area of Lake Michigan, and in Wisconsin, Lakes Winnebago, Butte des Morts, Winneconne, and Poygan, for which bedrock-surface geology is not mapped by Cannon et al. (1997). The only unmapped contact that was estimated under the area of Lake Michigan was that between the Upper Bedrock Unit and the Silurian-Devonian Carbonate Unit. This was estimated with professional judgment informed by the mapping of adjacent onshore areas by Cannon et al. (1997), Gray et al. (2002), and the Illinois Department of Natural Resources (1996a). Professional judgment was also employed to estimate contacts at the bases of the Silurian-Devonian Carbonate Unit, Maquoketa Unit, Galena-Platteville Unit, Ancell Unit, Prairie du Chien-Eminence Unit, Potosi-Franconia Unit, Ironton-Galesville Unit, and Eau Claire Unit under the areas of Lakes Winnebago, Butte des Morts, Winneconne, and Poygan. The estimated positions of these contacts are based on the mapping of Cannon et al. (1997) and the bedrock-surface exposure patterns estimated for Cambrian hydrostratigraphic units described previously.

C.1.1.2. Areas of Absence

Delineations of areas of absence were employed to select points as interpolation source data from a previously developed high-resolution surface model of an underlying unit. Areas of absence may be broadly subdivided into two categories. The first category consists of areas where older, stratigraphically deeper units are exposed at the bedrock surface. For example, the Eau Claire Unit is absent in areas where the Mt. Simon Unit and Precambrian rocks are exposed at the bedrock surface. The second category consists of areas where a unit is absent from the subsurface interval beneath the bedrock surface, either as a consequence of nondeposition or complete removal by erosion. For example, the Prairie du Chien-Eminence Unit is absent from a large area of northern Illinois and southern Wisconsin where it was completely removed by erosion prior to deposition of the Ansell Unit and its equivalents. In this area of absence, the Ansell Unit rests directly on the Potosi-Franconia and older units. Delineation of the areas of absence of each hydrostratigraphic unit required, then, aggregation of mapping showing bedrock-surface exposures of all older units (the first category of areas of absence) together with mapping showing areas of absence in the subsurface interval that is deeper than the bedrock surface (the second category).

For each hydrostratigraphic unit, mapping of bedrock-surface exposures of the older hydrostratigraphic units was compiled, with one exception, from the polygon-shapefiles depicting these exposures developed as described in the preceding section of this report. The exception is the Quaternary Unit, which is absent from a large driftless area in the northwestern part of the regional model domain that includes extreme northwestern Illinois and much of southwestern Wisconsin. The area of absence of the Quaternary Unit was mapped by digitizing as a polygon the driftless area of Wisconsin from a hardcopy Quaternary geologic map of Wisconsin (Wisconsin Geological and Natural History Survey and Wisconsin Department of Administration State Planning Office, 1976), digitizing as a polygon the driftless area of Illinois from a polyline-shapefile illustrating the bedrock-topography of Illinois (Illinois Department of Natural Resources, 1996b), and merging the two.

The second category of areas of absence are known with less certainty than are the first category, which are better understood from observation of outcrops and the logs of large numbers of shallow wells penetrating the bedrock surface. Nonetheless, resources are available, including structure-contour, isopach, and geologic mapping of significant unconformities (subcrop mapping), that allow an approximation of these areas of absence.

Unpublished structure-contour mapping (USGS, Wisconsin District, personal communication, 2002), used for developing a regional groundwater-flow model of the Cambrian and Ordovician aquifers of the U.S. upper Midwest (Young, 1992), illustrated approximate areas of absence of the Mt. Simon Unit, Eau Claire Unit, Ironton-Galesville Unit, Potosi-Franconia Unit, and Prairie du Chien-Eminence Unit in Wisconsin. These were digitized from the hardcopy maps as separate polygon shapefiles.

In Illinois, erosion preceding deposition of the Tippecanoe, Kaskaskia, and Absaroka Sequences resulted in complete removal, in certain areas, of some of the hydrostratigraphic units employed in this study; published subcrop mapping of each of these sequences was employed to delineate areas of absence. Mapping by Willman et al. (1975) shows that non-deposition was only a small influence on the configuration of areas of absence in Illinois.

Tippecanoe-Sequence subcrop mapping by Buschbach (1964) and Willman et al. (1975) was used as a basis for delineating areas of absence of the Prairie du Chien-Eminence Unit in northern Illinois (Figure C-2, Figure C-3). Unfortunately, the aggregation of lithostratigraphic

units into subcrop-mapping units employed in these maps is inconsistent. The Tippecanoe-Sequence subcrop map of Buschbach (1964), which is limited in scope to a seven-county area of northeastern Illinois, employs lithostratigraphic mapping units that are directly applicable to this study, lumping the Eminence Formation with the Gunter Sandstone and Oneota Dolomite (the lower members of the Prairie du Chien Group) so that the Potosi Dolomite subcrop shown in the map illustrates precisely the area of absence of the Prairie du Chien-Eminence Unit of this study. The map of Willman et al. (1975), which is not only more recently published—and presumably more accurate—than that of Buschbach (1964), but also covers all of northern Illinois, lumps the Eminence Formation and Potosi Dolomite into a mapping unit that is problematic in that it includes parts of two hydrostratigraphic units employed in the present study. The subcrop patterns of the Oneota-Gunter-Eminence and Potosi mapping units of Buschbach (1964) strongly resemble those of the Oneota-Gunter and Eminence-Potosi mapping units of Willman et al. (1975), respectively, in the northeastern Illinois area mapped in both studies.

The failure of these studies to adjust their subcrop mapping to the use of differing mapping units that aggregate the Eminence Formation with the overlying lower Prairie du Chien Group on the one hand (Buschbach, 1964), and with the underlying Potosi Dolomite on the other (Willman et al., 1975), suggests that the similar lithologies of the Potosi Dolomite, Eminence Formation, and Prairie du Chien Group render these units problematic to distinguish in drilling records. For purposes of groundwater flow modeling, the similar lithologies and comparable depth of burial of all of these units suggest that they are hydraulically comparable.

In the absence of more recent Tippecanoe-Sequence subcrop mapping that makes use of mapping units that are consistent with hydrostratigraphic units employed in the present study, then the authors have chosen to employ the more areally extensive subcrop map of Willman et al. (1975) as a guide to areas of absence of the Prairie du Chien-Eminence Unit, digitizing as a polygon-shapefile the mapped Eminence-Potosi and Franconia subcrops as approximations of areas of absence of the Prairie du Chien-Eminence Unit. A similar assumption was employed to delineate bedrock-surface exposures of the Prairie du Chien-Eminence and Potosi-Franconia Units, as discussed previously. If the subcrop map of Willman et al. (1975) is accurate, the described use of the map would result in an underestimation of the area of absence of the Prairie du Chien-Eminence Unit and an overestimation of the area of absence of the Potosi-Franconia Unit, since a portion of the mapped Eminence-Potosi subcrop must be occupied by dolomites of the Eminence Formation. The subcrop of the Prairie du Chien-Eminence Unit is assumed to be equivalent to the mapped area of the Prairie du Chien subcrop. From a hydrologic standpoint, however, this inaccuracy is probably of little importance, because the dolomites of both the Potosi-Franconia and Prairie du Chien-Eminence Units are hydraulically similar, and the mapping errors are compensatory: the overall Tippecanoe-Sequence subcrop of the two units honors the geologic mapping.

The approximate areas of absence of the Prairie du Chien-Eminence Unit in Wisconsin (digitized from unpublished mapping (USGS, Wisconsin District, personal communication, 2002) and in Illinois [digitized from Tippecanoe-Sequence subcrop mapping (Willman et al., 1975)] were revised slightly using professional judgment informed by a generalized mapping by Droste and Shaver (1983) and Droste and Patton (1985). This revision was necessary because the original digitized outlines, reflecting the mapped areas of the source data, abruptly terminate the areas of absence along the Illinois-Wisconsin boundary. Revision resulted in a more plausible estimation of the area of absence of the Prairie du Chien-Eminence Unit that crosses the state boundary and extends beneath a large part of southern Lake Michigan.

Kaskaskia-Sequence subcrop mapping (Willman et al., 1975) shows an area of extreme western Illinois where middle Devonian carbonates—the basal rocks of the Kaskaskia Sequence in that area—rest directly on the Galena Group. In this area the Maquoketa Group and Silurian dolomites have been completely removed by pre-Kaskaskia erosion. In terms of the hydrostratigraphic nomenclature employed in this study, the Silurian-Devonian Carbonate Unit rests directly on the Galena-Platteville Unit in this area, and the Maquoketa Unit is absent. The area where the Kaskaskia Sequence is subcropped by the Galena Group depicted by Willman et al. (1975) was therefore digitized as a polygon-shapefile showing an area of absence of the Maquoketa Unit.

Absaroka-Sequence subcrop mapping (Willman et al., 1975) show adjacent subcrop belts in an area of north-central Illinois where Pennsylvanian rocks of the Absaroka Sequence rest directly on the Ancell Group, the Galena and Platteville Groups, and the Maquoketa Group. In the Ancell Group subcrop, the Upper Bedrock Unit rests directly on the Ancell Unit, and the Silurian-Devonian Carbonate Unit, Maquoketa Unit, and Galena-Platteville Unit are absent, having been completely removed by erosion prior to deposition of the Absaroka Sequence. The Upper Bedrock Unit rests directly on the Galena-Platteville Unit where the Absaroka Sequence is subcropped by the Galena and Platteville Groups, and the Silurian-Devonian Carbonate Unit and Maquoketa Unit are absent. Finally, in the Maquoketa Group subcrop, the Upper Bedrock Unit rests directly on the Maquoketa Unit, and the Silurian-Devonian Carbonate Unit is absent. Thus, the Ancell Group subcrop, the Galena and Platteville Group subcrop, and the Maquoketa subcrop depicted by Willman et al. (1975) were digitized as a single polygon-shapefile illustrating an area of absence of the Silurian-Devonian Carbonate Unit. The Galena and Platteville Group subcrop as well as the Ancell Group subcrop were digitized as a polygon-shapefile illustrating an area of absence of the Maquoketa Unit. Lastly, the Ancell Group subcrop was digitized as a polygon-shapefile delineating an area of absence of the Galena-Platteville Unit.

With a single exception, all of the hydrostratigraphic units beneath the Quaternary Unit were deposited across all of Illinois, so that the principal generator of areas of absence in Illinois has been erosion during the periods of time between deposition of the Sauk, Tippecanoe, Kaskaskia, and Absaroka Sequences. A comparatively small area of absence of the Silurian-Devonian Carbonate Unit resulting partly from non-deposition is present in the southwestern part of the regional model domain in western Illinois along the Mississippi River. In this area, pre-Kaskaskia erosion completely removed Silurian dolomites, and Middle Devonian carbonates—the basal rocks of the Kaskaskia Sequence in the region—were not deposited. This area of absence of the Silurian-Devonian Carbonate Unit was delineated by processing polygon-shapefiles digitized from maps by Willman et al. (1975) showing the outline of the area of non-deposition of the Middle Devonian carbonates and the outline of the Maquoketa and Galena Group subcrops of the Kaskaskia Sequence. These shapefiles were processed by clipping the portion of the polygon delineating the area of non-deposition of the Middle Devonian carbonates within the polygon showing the Maquoketa and Galena Group subcrops of the Kaskaskia Sequence.

Areas of absence through erosion or nondeposition belonging to the second category described previously—those lying below the bedrock surface—do not significantly affect the distribution of the hydrostratigraphic units in Indiana and Michigan. Rupp (1991) reported that the Ancell Group in Indiana is missing in places that are areally small and poorly known and therefore are not documented in his structure-contour and isopach maps of the unit. Because the

level of detail required by the groundwater flow model is low, particularly in the model farfield of Indiana, like Rupp, these comparatively small areas of absence have been ignored. Pre-Tippecanoe, pre-Kaskaskia and pre-Absaroka erosion has affected the distribution of some lithostratigraphic units in Indiana and Michigan, but it has not completely removed any of the aggregate hydrostratigraphic units (Droste and Patton, 1985; Droste and Shaver, 1983; Rupp, 1991).

Areas of absence were delineated to a limited extent in the inactive portion of the regional model domain west of the Mississippi River. If such areas of absence were identified in the unpublished structure-contour maps used extensively for interpolation source data in this area (USGS, Wisconsin District, personal communication, 2002), their outlines were digitized as polygon-shapefiles as areas of absence. Areas of absence were delineated in the southwestern part of Minnesota because that area is covered by the Lake Superior area geologic mapping of Cannon et al. (1997; Droste and Patton, 1985) used for delineation of bedrock-surface exposures and areas of absence in Michigan and Wisconsin, but no special effort was made to digitize areas of absence from geologic maps covering the portions of Iowa and Missouri within the regional model domain. This sacrifice, made to address time and budget constraints, was viewed as acceptable chiefly because geologic model accuracy in the inactive portion of the groundwater flow model corresponding to the trans-Mississippi River area is irrelevant to the functioning of the groundwater flow model. The inclusion of points from the high-resolution surface model of an underlying unit for representation of a unit's elevation in an area of absence of the unit might, in some cases, have resulted in a small improvement in high-resolution surface model accuracy along the western boundary of the area of active cells (the Mississippi River). This improvement in high-resolution surface model accuracy would have a negligible effect on the irregular-grid model and on groundwater flow modeling results in the model nearfield.

Table C-3. Key to Aggregation of Geologic Mapping Units to Hydrostratigraphic Units

<i>Hydrostratigraphic Unit</i>	<i>Illinois (Illinois Department of Natural Resources, 1996a)</i>	<i>Indiana (Gray et al., 2002)</i>	<i>Lake Superior Area (Michigan and Wisconsin) (Cannon et al., 1997)</i>	
Upper Bedrock Unit	All Cretaceous units All Pennsylvanian units All Mississippian units All Upper Devonian units	All Pennsylvanian units All Mississippian units Ellsworth Shale (Devonian) Antrim Shale (Devonian) New Albany Shale (Devonian)	All Jurassic units All Pennsylvanian units All Mississippian units Ellsworth Shale (Devonian) Antrim Shale (Devonian)	
Silurian-Devonian Carbonate Unit	All Middle Devonian units All Silurian units	Muscatatuck Group (Devonian) All Silurian units	Traverse Group (Devonian) All Silurian units	
Maquoketa Unit	Maquoketa Group (Ordovician)	All Ordovician units	Maquoketa Formation (Ordovician)	
Galena-Platteville Unit	Galena-Platteville Group (Ordovician)	(Not exposed at bedrock surface)	Sinnipee Group (Ordovician)	
Ancell Unit	Ancell Group (Ordovician)		Ancell Group (Ordovician)	
Prairie du Chien-Eminence Unit	Prairie du Chien Group (Ordovician) (see text)		Prairie du Chien Group (Ordovician) (see text)	
Potosi-Franconia Unit	All Cambrian units (see text)		None. The aggregate Cambrian mapping unit was subdivided as described in the text.	
Ironton-Galesville Unit	(Not exposed at bedrock surface)			
Eau Claire Unit				
Mt. Simon Unit				
Precambrian (not a modeled hydrostratigraphic unit)		All Precambrian units		

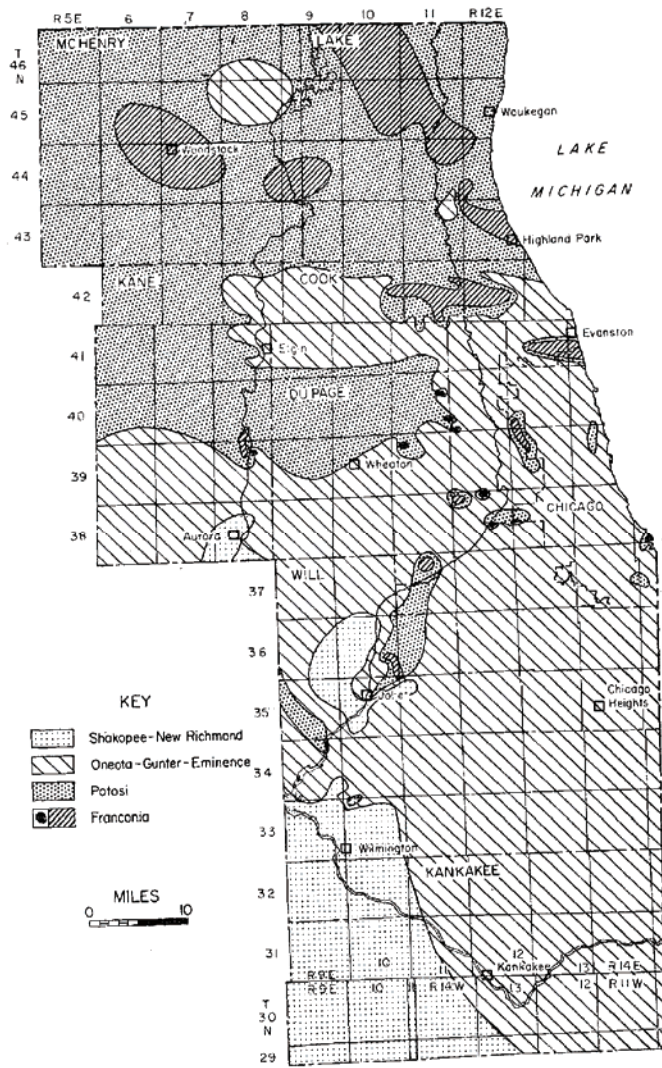


Figure C-2. Tippecanoe-Sequence subcrop map of northeastern Illinois (Buschbach, 1964). The Shakopee, New Richmond, Oneota, and Gunter units are formations within the Prairie du Chien Group.

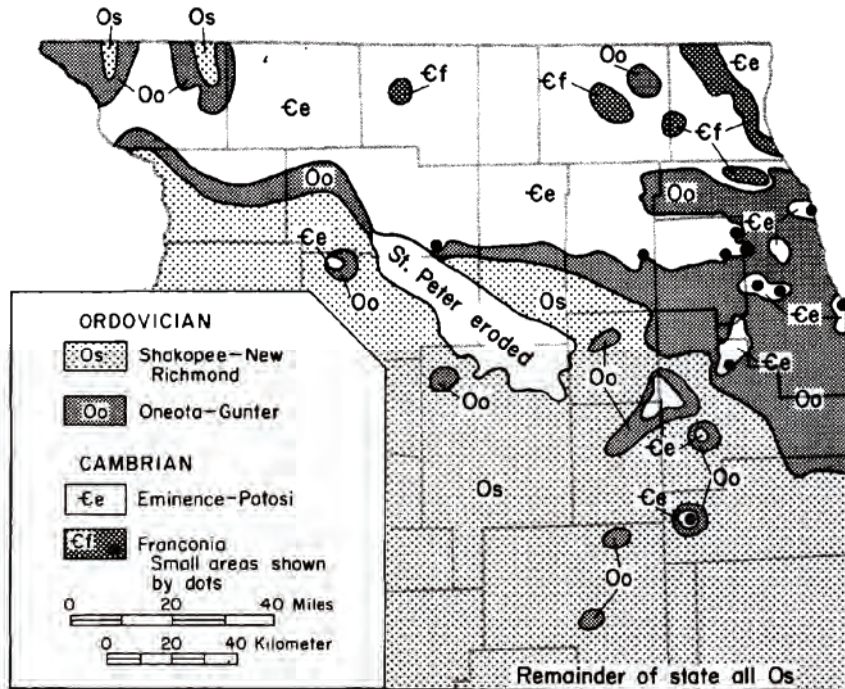


Figure C-3. Tippecanoe-Sequence subcrop map of northern Illinois (Willman et al., 1975). The Shakopee, New Richmond, Oneota, and Gunter units are formations within the Prairie du Chien Group.

C.1.1.3. Faults to be Modeled as Breakline Features

The interpolation algorithm selected for development of many of the high-resolution surface models, inverse distance to a power, permits the incorporation of faults into the interpolation process as features known as *breaklines*. In estimating a value at a given location, the search pattern of the interpolation algorithm is restricted from searching the input data on the opposite side of a breakline.

Faults were selected for explicit treatment as breaklines if they were included on structure-contour mapping used as source data for the project. All other faulting affecting the regional model domain is assumed to be represented accurately enough for purposes of groundwater flow modeling through structure contouring. The faults included as breaklines are the Plum River Fault and Sandwich Fault Zones in Illinois and the Royal Center, Fortville, and Mt. Carmel Faults in Indiana (Figure C-4). These faults offset the tops of the Silurian-Devonian Carbonate Unit and all underlying units. The Plum River Fault and the Sandwich Fault Zone, simplified to a single trace, were digitized from mapping by Visocky et al. (1985). Incorporation of the Sandwich Fault Zone in the geologic modeling as a single surface, rather than as a set of surfaces, required some simplification, using professional judgment, of the outcrop patterns illustrated in geologic mapping by the Illinois Department of Natural Resources (1996a) in the immediate vicinity of the fault zone. Indiana fault locations were digitized from mapping by Rupp (1991).

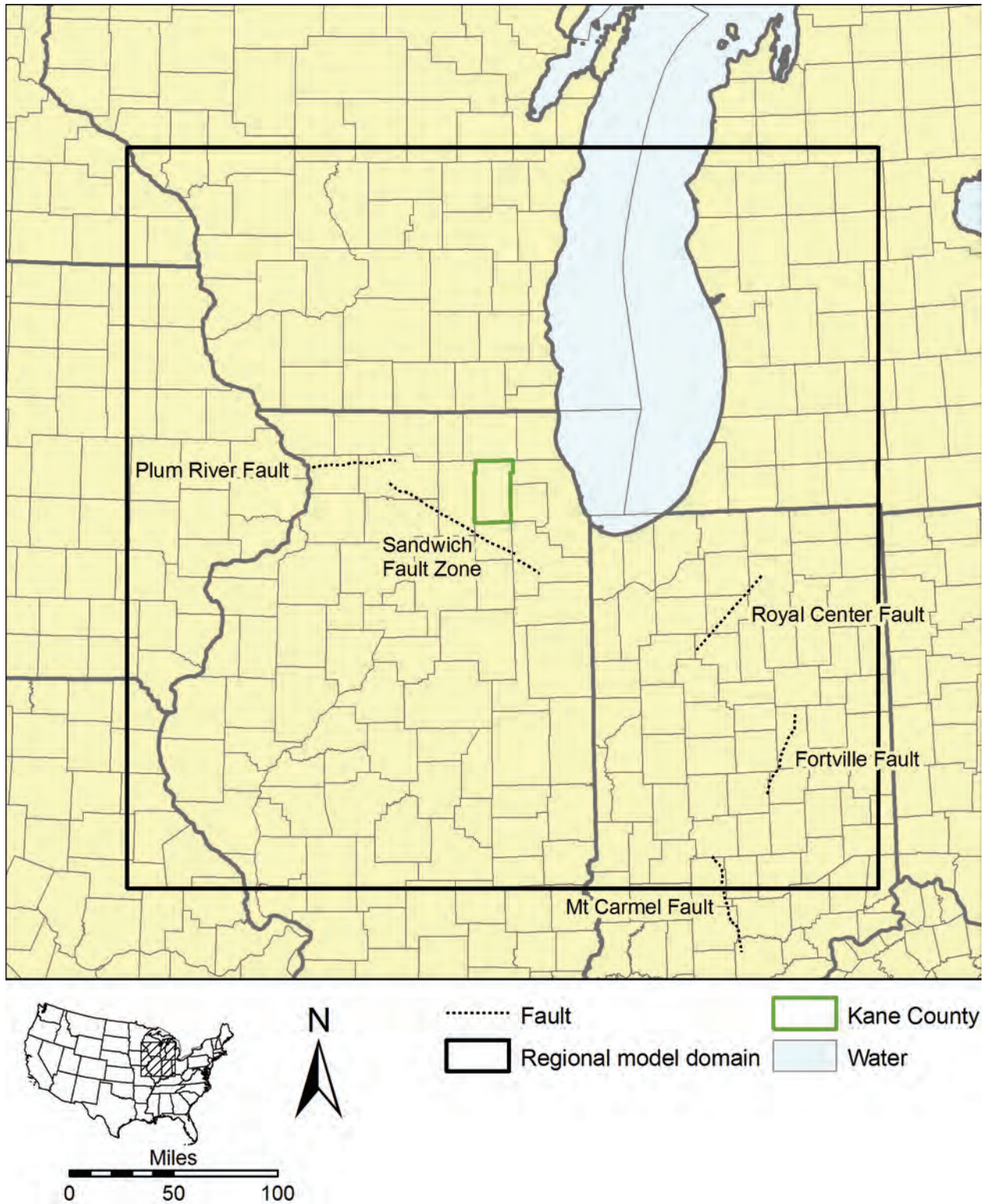


Figure C-4. Faults included as surfaces of displacement.

C.1.2. *Compilation of Interpolation Source Data*

The general procedure for developing each high-resolution surface model began with compiling estimates, as ArcGIS point-shapefiles in a consistent projection and coordinate system, of the top elevation of the surface from available digital and hardcopy sources. These compiled estimates constitute the *interpolation source data* that were interpolated to generate the high-resolution surface model. If available, digital source data, such as digital bedrock-surface topographic mapping, often required projection and transformation to the Lambert conic conformal projection used for the project (referred to as the *Illimap projection* in this report) as well as conversion from raster to vector-point format or conversion from vector-polyline to vector-point format. Hardcopy source data required digitization as polylines, followed by conversion to a vector-point format.

Source data were irregularly employed from areas outside of the regional model domain. If they were available, and if time and budget constraints permitted, source data were employed from areas outside the regional model domain, but the high-resolution and, ultimately, the irregular-grid model were developed only for the area of active model cells (i.e., the portion of the regional model domain east of the Mississippi River). The selected interpolation algorithms consider the source data from outside the regional model domain only in a limited fashion, but their inclusion in the interpolation process marginally improves the model accuracy along the edges of the regional model domain.

Most of the hardcopy maps digitized for the project are contoured maps of the tops of the hydrostratigraphic units employed in the study, either bedrock-topography or structure-contour maps. In a few cases, however, structure-contour maps were not available for the tops of hydrostratigraphic units, requiring digitization of isopach maps of one or more lithostratigraphic units and synthesis of the missing structure data. This synthesis was accomplished through a process of addition or subtraction of the thickness data to or from an adjacent, previously generated, high-resolution surface model or a digitized structure-contour map of another lithostratigraphic surface. For example, since a structure-contour map of the top of the Eau Claire Group in Indiana was not available, but an isopach map of the Eau Claire Group was available, the isopach map was digitized, and the thickness data were then interpolated. The interpolated thickness data—a thickness model of the Eau Claire Group—was then added to the previously generated high-resolution surface model of the Mt. Simon Unit to synthesize top elevation data for the Eau Claire Unit in Indiana. These data were in turn used as source data for interpolation of the high-resolution surface model of the Eau Claire Unit. Top-elevation data that were synthesized by adding or subtracting thickness data to or from a structure-contour map were saved as a point-feature shapefile.

In many cases, it was necessary for digitized structure-contour and isopach maps to be augmented, using professional judgment, with additional contours to provide enough data for ensuing interpolation procedures to generate geologically plausible results from the interpolation source data. This augmentation was made necessary because experiments with the selected interpolation algorithms showed that data derived from the relatively widely separated contours on some of the digitized maps did not adequately constrain the interpolation results. Specifically, the interpolation results using only the contour data digitized from the source maps sometimes strayed from the values of adjacent contours in the maps so that the resulting surface was not a plausible model of the data represented by the map. Interpolated surfaces based only on the map contours were especially implausible in the case of elevations interpolated in the vicinity of faults, where the search pattern of the selected interpolation algorithm is restricted to only one

side of the fault, further limiting the already sparse availability of data on which to base the interpolation result. Time and budget constraints sometimes limited the labor-intensive augmentation process to the model nearfield and to portions of the regional model domain near faults. The added contours were constructed to depict simple surfaces honoring the map contours with minimal added perturbations between the map contours.

Some editing of contours digitized from structure-contour maps used as source data was necessary to correct *stratigraphic violations* and adjust elevations in the vicinity of areas of absence. For purposes of this report, a *stratigraphic violation* occurs between two depictions of geologic structure (e.g., hardcopy structure-contour maps, polyline-format digital structure-contour data, point-format digital interpolated elevation results, etc.) when they imply that one surface is at a higher elevation than another surface that is stratigraphically higher. For example, a stratigraphic violation occurs where structure-contour maps of the tops of the Ancell Group and the Platteville Group show that the top of the Ancell Group is at a higher elevation than the top of the Platteville Group. Adjustment of contours was also necessary in the vicinity of areas of absence delineated in some structure-contour maps employed as source data. Although consistent mapping requires that structure contours at the edge of an area of absence show the elevation of the top of a mapped unit to be the same as that shown on a structure-contour map of the immediately underlying stratigraphic unit, some maps employed as source data for this study rarely meet this requirement. Thus, the digitized structure contours were repositioned, in as minimal a way as possible, to consistently and plausibly depict elevations in the vicinity of mapped areas of absence.

Before using them as interpolation source data, the elevation estimates in both point- and polyline-feature shapefiles were erased from a buffer area along state boundaries and—if fault features had displaced the surface to be modeled—from a narrow buffer on either side of faults. This removal of source data was necessary to eliminate direct juxtaposition of structure interpretations by different state and federal mapping authorities, causing differences in interpretations between mapping authorities to be resolved by the interpolation algorithm. Direct juxtaposition of competing interpretations would result in an implausible simulation of surface by the interpolation process. One buffer was employed to erase data in a 50,000-ft buffer *outside* the Illinois boundary. Erasing these data effectively forces the interpolation process to give priority to interpretations by Illinois mapping authorities in areas near the Illinois boundary. Prioritization was preferred for Illinois-based interpretations because they probably are more accurate for the parts of the model nearfield (northeastern Illinois) abutting Indiana, Lake Michigan, and Wisconsin than would be interpretations resolved mathematically by the interpolation algorithm. As the center of the Chicago metropolitan area, northeastern Illinois has been the subject of numerous geologic studies, and the authors preferred that the interpolation results prioritize interpretations of Illinois mapping authorities in the region. A second buffer was employed to erase data in a 50,000-ft strip straddling the Indiana-Michigan boundary and the Lake Michigan shoreline of Indiana, Michigan, and Wisconsin. By erasing data from a 25,000-ft strip on each side of the boundaries separating these areas, this buffer results in the interpolation algorithm giving equal priority to the competing interpretations on either side of the boundaries.

Since digitizing of structure contours and editing of the digitized polylines representing them results in polyline vertices being placed precisely on fault features employed as breaklines, polyline segments were erased in a 7,000-ft buffer on either side of the fault features to eliminate vertices located directly on the faults. Vertices located precisely on the fault features would interfere with the interpolation process, because the search pattern of the algorithm seeks

elevation data on one side of a fault, and a vertex located precisely on the fault would be employed by the algorithm to estimate elevations on both sides of the fault, resulting in implausible interpolation results. Buffers were employed to erase polyline segments along faults as a step in compiling the interpolation source data for all high-resolution surface models except those of the tops of the Quaternary and Upper Bedrock Units, which are unaffected by displacement along the faults.

After erasing point data and polyline segments from along state boundaries and, if necessary, from fault areas, an ArcGIS tool was employed to convert the polyline-shapefiles to point-shapefiles consisting of the polyline vertices. Fields were added to the attribute tables of these point-feature shapefiles to hold the x - and y -coordinates of the individual points, and another ArcGIS tool was used to populate these fields with the coordinates. If not already present, such fields were also added to the attribute tables of any point-feature shapefiles developed using thickness data for use as interpolation source data, and these fields were populated with x - and y -coordinates of the points. At the conclusion of this step, all interpolation source data consisted of point-feature shapefiles containing fields for x - and y -coordinates and a field for the elevation of the hydrostratigraphic unit to be modeled. All of these point-feature shapefiles were then exported in text format, and in Surfer, the contents of the files were appended to one another and saved in comma-delimited (.csv) format.

As previously discussed, digital source data were employed from previously completed high-resolution surface models for development of each high-resolution surface model (Table C-2). These data were selected from the previously completed high-resolution surface models using polygon-shapefiles depicting the areas of bedrock-surface exposure and absence of the surface to be modeled. The selected features were then exported in text format. In Surfer, the contents of these text files were then appended to the .csv file described in the previous paragraph, and the combined file was used as input for the interpolation process.

A polygon-shapefile of the bedrock-surface exposures of the unit was employed to select points from the previously developed high-resolution surface model of the top of the Upper Bedrock Unit (which is equivalent to a model of the bedrock surface) that fall within the bedrock-surface exposures. For example, points for development of the high-resolution surface model of the top of the Eau Claire Unit were selected from the high-resolution surface model of the top of the Upper Bedrock Unit if they fell within the polygons included in the shapefile of the bedrock-surface exposures of the Eau Claire Unit. Use of these data in the interpolation process forces the interpolation to duplicate bedrock-surface configuration in the area of bedrock-surface exposure.

Polygon-shapefiles of areas of absence were used to select points from a previously developed high-resolution surface model of an underlying unit. For example, points for development of the Eau Claire high-resolution surface model were selected from the high-resolution surface model of the top of the Mt. Simon Unit if they fell within polygons included in the shapefile of areas of absence of the Eau Claire Unit. These data force the interpolation process to duplicate the configuration of the top of the underlying unit in the areas of absence. Such duplication provides laterally extensive elevation estimates covering areas of real-world absence—a requirement of finite-difference groundwater flow modeling—and implies zero thickness, essentially, in the areas of absence. Later data processing, done in conjunction with development of the irregular-grid geologic model, assigns a minimum thickness of 1 ft to each unit in its area of absence.

C.1.3. Interpolation

A provisional high-resolution surface model was then interpolated from the compiled interpolation source data. Different interpolation algorithms employing different parameters were employed for the high-resolution surface models. A kriging algorithm was employed if the real-world surface was not displaced by faulting, but an inverse-distance algorithm was used if fault escarpments were present on the surface. The kriging algorithm was preferred if the interpolation process was not intended to duplicate fault escarpments because it provides a more realistic simulation of a geologic surface. Otherwise, the inverse-distance algorithm was employed since this algorithm can take into account breakline features and thereby generate a simulated surface that includes escarpments along faults.

A 2500-ft interpolation-node spacing was employed in all interpolations, and bounding coordinates were selected so that the interpolation results for all high-resolution surface models were consistently located at the same x - and y -coordinates. In most cases, the bounding coordinates were selected so that the area covered by the interpolation results was equivalent to the regional model domain, but in some cases, interpolation results were desired for smaller parts of the regional model domain, such as the Lake Michigan basin, and the bounding coordinates were adjusted accordingly. Parameters of the principal interpolation algorithms employed are shown in Table C-4 and Table C-5.

The quality of the interpolation resulting in each provisional high-resolution surface model was assessed using a cross-validation process (Table C-6). The cross-validation process reports statistics based on the interpolation error at a subset of N source data points (residual Z). Surfer computes each residual Z by removing the first observation from the subset of source data and using the remaining data and the specified algorithm to interpolate a value at the first observation location. The interpolation error is calculated using the following relationship:

$$\text{interpolation error} = \text{interpolated value} - \text{observed value}$$

The first observation is then returned to the dataset, and the interpolation error is computed with the second observation removed from the subset of source data. The process is then repeated with the third, fourth, fifth observations, etc., and removed all the way up to and including the N th observation. With completion of this process, N interpolation errors have been computed, and statistics are generated based on these errors, the most significant of which are included in Table C-6. These statistics show that the selected interpolation algorithms adequately predict an observed value when the observation has been removed from the interpolation source data and all other interpolation source data are retained. Correlation statistics show the spatial correlations between the residual Z and the (x, y) coordinates and elevation (z -coordinate) of the removed source data point are near zero.

C.1.4. Processing of Provisional High-Resolution Surface Models

Each provisional high-resolution surface model was adjusted, generally using previously generated high-resolution surface models of one overlying and one underlying surface (Table C-7). The previously generated high-resolution surface models were employed as upper and lower constraints on plausible values of the elevation of the provisional high-resolution surface model that was the subject of the adjustment. Less typically, the provisional high-resolution surface model was adjusted using only a single previously generated high-resolution surface model of an

overlying surface as an upper constraint on the plausibility of the provisional high-resolution surface model that was the subject of the adjustment.

This adjustment was undertaken to eliminate stratigraphic violations between the provisional high-resolution surface model and the high-resolution surface models of the overlying and underlying units. These stratigraphic violations occur for two main reasons. The most numerous stratigraphic violations fall in the immediate vicinity of areas of absence of the unit that is the subject of the adjustment, where interpolation source data were imported from the high-resolution surface model of the underlying unit. Because the interpolation algorithms employed for this study are not designed to strictly honor the input data, comparison of the provisional high-resolution surface model in an area of absence with the high-resolution surface model of the underlying unit (the very data used as a source for the provisional high-resolution surface model) reveals numerous small differences—both positive and negative, and always less than 0.3 m (1 ft)—between the surface models. It is the negative differences that are identified as stratigraphic violations and that are the basis for adjustment of the provisional high-resolution surface model.

The second category of stratigraphic violations result from stratigraphic violations inherited from the structure-contour mapping digitized as source data for development of the high-resolution surface models. Many, perhaps most, of these structure-contour maps were not developed in concert with one another so as to assure an absence of stratigraphic violations. Structure-contour mapping used as source data for the project was selected with care so as to avoid stratigraphic violations, but for many areas the available structure-contour mapping is limited. In some cases where structure-contour mapping was unacceptable, structure data for use as interpolation sources were synthesized by adding or subtracting thickness data to or from structure data. In other cases, the mapping—after digitization—was edited manually, based on professional judgment, to eliminate stratigraphic violations. But in still other cases in the model farfield far from northeastern Illinois, source data were not synthesized or corrected to circumvent stratigraphic violations. Stratigraphic violations between the provisional high-resolution surface model and the high-resolution surface models of overlying and underlying surfaces resulting from violations in the source data typically affect smaller areas than the first category of violations and are restricted to the model farfield, but the violations may exceed 30 m (100 ft).

As mentioned in the preceding paragraph, the interpolation process sometimes generates provisional elevation estimates in areas of absence that imply a small (<0.3 m or 1 ft) thickness of the unit. For purposes of this project, this error is acceptable, because it is a requirement of the finite-difference groundwater flow modeling code that model layers be present at all locations within the model domain, even in areas of real-world absence. Model layers are therefore assigned a consistently applied minimum thickness in such areas of absence. In this project, that minimum thickness is 1 ft. Since the thicknesses implied in areas of absence are less than the 1 ft minimum thickness, the small implied thicknesses in areas of absence are ignored, and not corrected, in the provisional high-resolution surface models. In fact, with development of the irregular-grid model, these implied thicknesses—rather than being eliminated—are increased to 1 ft to satisfy groundwater flow-modeling requirements.

Adjustments were made to the provisional high-resolution surface model in ArcGIS after converting the interpolation results to a point-feature shapefile. Examples of these adjustments are illustrated as a plot (Figure C-5) and unrelated table (Figure C-6). The fields X (the *x*-coordinate), Y (the *y*-coordinate, and PROV (the provisional interpolated elevation value) are the

values imported from the text file holding the Surfer interpolation results. A long-integer field INDEX was added to the attribute table, as it was for all previously generated high-resolution interpolation results, and the field was populated with a unique, location-based index value using the formula $INDEX = (X \times 10000000) + Y$.

This is the same formula used for populating the INDEX field in all previously generated high-resolution interpolation results. Since the interpolations were constrained so as to give results at a consistent set of locations, the INDEX field was employed to join the attribute table to previously generated high-resolution surface models of the stratigraphically nearest-available overlying and underlying units. For example, if the subject of the data processing was a provisional high-resolution surface model of the Eau Claire Unit, the shapefile attribute table was joined to the attribute table of the high-resolution surface models of the Silurian-Devonian Carbonate Unit (the stratigraphically nearest-available high-resolution surface model of an overlying unit, since such models were not yet generated for hydrostratigraphic units between the Silurian-Devonian Carbonate Unit and the Eau Claire Unit) and the Mt. Simon Unit (the underlying unit).

Fields were added to the attribute table of the provisional high-resolution surface model to hold elevations of the underlying and overlying units from the joined tables for use as lower and upper constraints on plausible values for the provisional high-resolution surface model (LOW and UPP, respectively, in Figure C-6). The added fields were populated with elevations of the underlying and overlying units. The table join was then removed.

Three additional fields were added to the attribute table of the provisional high-resolution surface model and then populated. One was a field to hold a value calculated as the difference between the provisional high-resolution interpolation results and the final high-resolution surface elevation of the stratigraphically nearest-available underlying unit (field PROV_LOW in Figure C-6). The second was a field for a value calculated as the difference between the final high-resolution surface elevation of the stratigraphically nearest-available overlying unit and the provisional high-resolution interpolation results (field UPP_PROV in Figure C-6). The last field (FINAL in Figure C-6) was added to hold the elevations of the high-resolution surface model determined from the provisional values and the imported elevations from the high-resolution surface models of the stratigraphically nearest-available overlying and underlying units.

Records in the attribute table were selected for which provisional interpolated elevations were lower than the high-resolution surface model of the underlying surface (see records in Figure C-6 for which the field PROV_LOW is negative). Since such elevations imply that the thickness of the unit that is the subject of the data processing is negative at the selected points, an adjustment of the provisional interpolated elevation at the selected points was necessary. Thus, the elevation of the high-resolution surface model of the stratigraphically nearest-available underlying unit was employed as the elevation of the high-resolution surface model of the unit that was the subject of the data processing. In the example in Figure C-6, then, the value of the field FINAL was calculated for the selected records as the value in the field LOW. In the same way, records in the attribute table were selected for which provisional interpolated elevations were higher than the high-resolution surface model of the overlying surface (see records in Figure C-6 for which the field UPP_PROV is negative). For the selected records, the elevation of the high-resolution surface model of the stratigraphically nearest-available overlying unit was employed as the elevation of the high-resolution surface model of the unit that was the subject of the data processing. Referring to the example (Figure C-6), the value in the field FINAL was calculated for the selected records as the value in the field UPP. For all other records in the

attribute table of the provisional high-resolution surface model—those for which the provisional interpolated elevation was between the imported elevations from the high-resolution surface models of the stratigraphically nearest-available overlying and underlying units —the provisional interpolated elevation was employed as the elevation in the high-resolution surface model. In the example (Figure C-6), the field FINAL for such records was populated with the elevation in the field PROV. The high-resolution surface model consists of the x- and y-coordinates together with the adjusted interpolated elevations—that is, the data in the fields X, Y, and FINAL in the example (Figure C-6).

The adjustment process was the final step in development of each high-resolution surface model. Point features located west of the Mississippi River (the inactive portion of the regional model) were then erased from each high-resolution surface model using a polygon-shapefile delineating the portion of the regional model domain west of the Mississippi River. This step created the active-cell high-resolution surface model, which was used to develop the irregular-grid geologic model.

Table C-4. Parameters of Kriging Algorithm Having Output Grid Coincident with Regional Model Domain

<i>Gridding Method</i>	<i>Kriging</i>
Kriging Type	Point
Polynomial Drift Order	0
Kriging std. deviation grid	no
Output Grid	
Minimum x	2361500 ft
Maximum x	4269000 ft
Minimum y	2236000 ft
Maximum y	4116000 ft
x and y spacing	2500 ft
Semi-Variogram Model	
Component Type	Linear
Anisotropy Angle	0
Anisotropy Ratio	1
Variogram Slope	1
Search Parameters	
Search Ellipse Radius #1	600000 ft
Search Ellipse Radius #2	600000 ft
Search Ellipse Angle	0
Number of Search Sectors	8
Maximum Data Per Sector	8
Maximum Empty Sectors	6
Minimum Data	3
Maximum Data	64

Table C-5. Parameters of Inverse Distance Algorithm Having Output Grid Coincident with Regional Model Domain

<i>Gridding Method</i>	<i>Inverse Distance to a Power</i>
Weighting Power	1
Smoothing Factor	0
Anisotropy Ratio	1
Anisotropy Angle	0
Output Grid	
Minimum x	2361500 ft
Maximum x	4269000 ft
Minimum y	2236000 ft
Maximum y	4116000 ft
x and y spacing	2500 ft
Search Parameters	
Search Ellipse Radius #1	2280000 ft
Search Ellipse Radius #2	2280000 ft
Search Ellipse Angle	0
Number of Search Sectors	8
Maximum Data Per Sector	8
Maximum Empty Sectors	6
Minimum Data	3
Maximum Data	64

Table C-6. Cross-Validation Statistics for Interpolations of Elevation Data

<i>Surface</i>	<i>Univariate Cross-Validation Statistics</i>			<i>Inter-Variable Correlation with Residual Z at Validation Points</i>		
	<i>Median Abs. Deviation of Residual Z</i>	<i>Mean of Residual Z</i>	<i>Root Mean Square of Residual Z</i>	<i>X</i>	<i>Y</i>	<i>Z</i>
Top of Quaternary Unit	0.009	-0.013	1.817	-0.045	-0.020	0.002
Top of Upper Bedrock Unit (Preliminary Onshore Surface Model)	0.639	-0.267	10.426	-0.002	-0.024	-0.167
Top of Upper Bedrock Unit (Preliminary Lake Michigan Surface Model)	23.440	0.348	51.289	0.025	-0.043	-0.305
Top of Silurian-Devonian Carbonate Unit (Second Iteration)	7.338	0.034	30.729	0.011	-0.012	-0.120
Top of Silurian-Devonian Carbonate Unit (First Iteration)	8.955	0.877	31.883	-0.003	0.017	-0.137
Top of Maquoketa Unit	7.094	1.900	29.689	0.004	-0.046	-0.019
Top of Galena-Platteville Unit	15.102	0.903	46.515	-0.098	-0.054	-0.007
Top of Ancell Unit	4.217	0.164	36.201	0.019	-0.000 ¹	-0.100
Top of Prairie du Chien-Eminence Unit	6.261	-2.275	42.590	0.039	0.009	-0.115
Top of Potosi-Franconia Unit	2.967	1.169	35.794	0.004	0.031	-0.157
Top of Ironton-Galesville Unit	2.068	0.648	29.070	-0.025	0.037	-0.072
Top of Eau Claire Unit	2.028	0.702	28.089	-0.014	-0.008	-0.138
Top of Mt. Simon Unit	9.733	-4.713	74.259	-0.026	0.017	-0.100
Base of Mt. Simon Unit	27.173	0.649	113.785	-0.010	-0.024	-0.186

¹ Between 0 and -0.0005

Table C-7. High-Resolution Surface Models Used As Constraints for Adjustment of Provisional High-Resolution Surface Models

<i>Order</i>	<i>Provisional High-Resolution Surface Model</i>	<i>High-Resolution Surface Models used as Constraints</i>	
		<i>Lower Constraint</i>	<i>Upper Constraint</i>
1	Top of Quaternary Unit (Land Surface)	None	None
2	Top of Upper Bedrock Unit (Bedrock Surface)	None	Top of Quaternary Unit (Land Surface)
3	Base of Mt. Simon Unit (Precambrian Surface)	None	Top of Upper Bedrock Unit (Bedrock Surface)
4	Top of Mt. Simon Unit	Base of Mt. Simon Unit (Precambrian Surface)	Top of Upper Bedrock Unit (Bedrock Surface)
5	Top of Silurian-Devonian Carbonate Unit (First Iteration)	Top of Mt. Simon Unit	Top of Upper Bedrock Unit (Bedrock Surface)
6	Top of Eau Claire Unit	Top of Mt. Simon Unit	Top of Silurian-Devonian Carbonate Unit (First Iteration)
7	Top of Ironton-Galesville Unit	Top of Eau Claire Unit	Top of Silurian-Devonian Carbonate Unit (First Iteration)
8	Top of Potosi-Franconia Unit	Top of Ironton-Galesville Unit	Top of Silurian-Devonian Carbonate Unit (First Iteration)
9	Top of Prairie du Chien-Eminence Unit	Top of Potosi-Franconia Unit	Top of Silurian-Devonian Carbonate Unit (First Iteration)
10	Top of Ansell Unit	Top of Prairie du Chien-Eminence Unit	Top of Silurian-Devonian Carbonate Unit (First Iteration)
11	Top of Galena-Platteville Unit	Top of Ansell Unit	Top of Silurian-Devonian Carbonate Unit (First Iteration)
12	Top of Maquoketa Unit	Top of Galena-Platteville Unit	Top of Silurian-Devonian Carbonate Unit (First Iteration)
13	Top of Silurian-Devonian Carbonate Unit (Second Iteration)	Top of Maquoketa Unit	Top of Upper Bedrock Unit (Bedrock Surface)

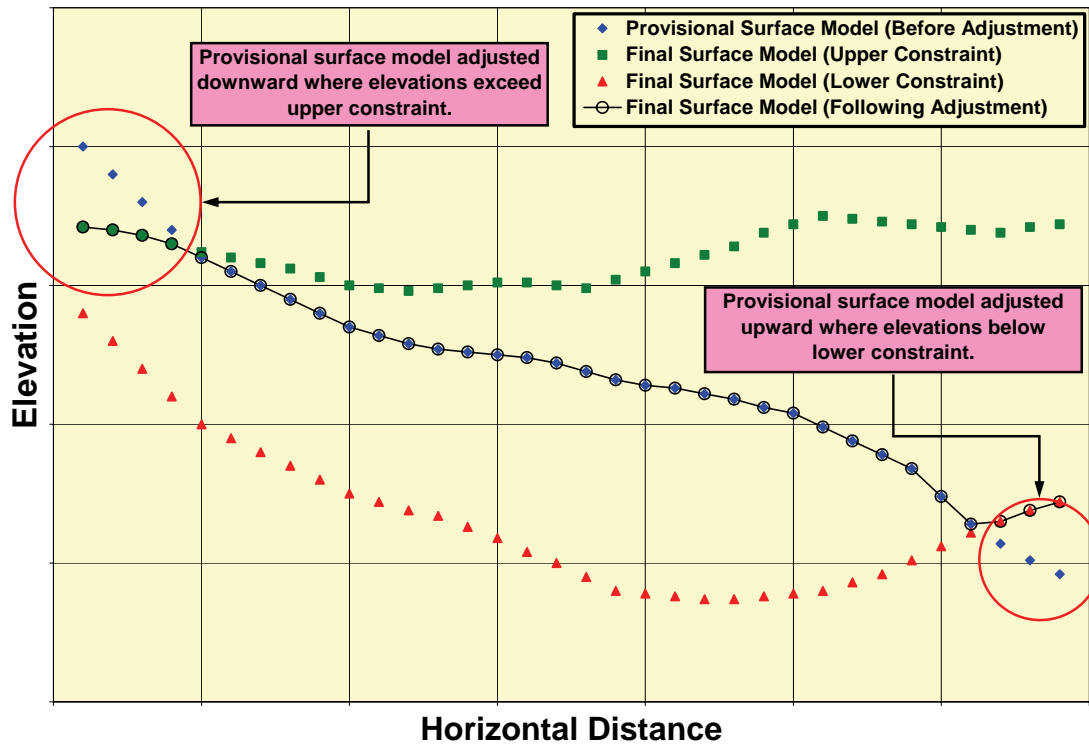


Figure C-5. Plot illustrating adjustment of provisional high-resolution surface model.

Attributes of h1_res_data_proc_example_5

FID	Shape*	X	Y	PROV	INDEX	LOW	UPP	PROV_LOW	UPP_PROV	FINAL
0	Point	3904000	3396000	-2921.142271	390400003396000	-2920.222266	-684.797747	-0.920005	2226.344524	-2920.222266
1	Point	2476500	2343500	-1228.112684	247650002343500	-1227.245693	575.353946	-0.867001	1803.466639	-1227.245693
2	Point	3941500	3476000	-3493.930467	394150003476000	-3493.394981	-811.352991	-0.535488	2682.577475	-3493.394981
3	Point	3941500	3388500	-3063.127405	394150003388500	-3062.669136	-703.959467	-0.488270	2359.167919	-3062.669136
4	Point	3884000	3428500	-2914.279026	388400003428500	-2914.033260	-588.043541	-0.245766	2226.235485	-2914.033260
5	Point	3925000	3391000	-3013.069214	392500003391000	-3012.883546	-702.288991	-0.085669	2310.776623	-3012.883546
6	Point	3144000	3668500	476.12	314400003668500	476.127469	854.42	-0.007469	378.3	476.127469
7	Point	3149000	3666000	500.24	314900003666000	500.245932	846.58	-0.005932	346.34	500.245932
8	Point	3146500	3668500	489.28	314650003668500	489.285030	840.26	-0.005030	350.98	489.285030
9	Point	3151500	3666000	520.83	315150003666000	520.833958	851.66	-0.003958	330.83	520.833958
10	Point	2929000	3876000	902.260365	292900003876000	902.231	902.231	0.029365	-0.029365	902.231
11	Point	2621500	4073500	876.548819	262150004073500	876	876	9.858674	-0.548819	876
12	Point	2959000	3898500	902.889445	295900003898500	881.141589	902.23	21.547856	-0.459445	902.23
13	Point	2684000	3978500	843.173856	268400003978500	812.410111	842.99	30.763745	-0.183856	842.99
14	Point	2924000	3668500	912.863264	292400003668500	882.012389	912.07	30.850876	-0.793264	912.07
15	Point	2884000	3741000	784.570829	288400003741000	890.161130	783.99	94.409699	-0.580829	783.99
16	Point	3134000	3976000	754.745092	313400003976000	855.374368	754.59	99.370725	-0.155092	754.59
17	Point	2806500	3736000	771.806570	280650003736000	861.614089	771	110.182481	-0.806570	771
18	Point	2889000	3736000	768.904502	288900003736000	853.594607	768	115.309895	-0.904502	768
19	Point	2536500	3916000	630.504975	253650003916000	489.844858	629.92128	140.680117	-0.583695	629.92128
20	Point	2609000	3971000	788.747877	260900003971000	624.984511	788	163.783366	-0.747877	788
21	Point	2369000	4098500	603.007951	236900004098500	471.470216	602.72960	191.609730	-0.350271	602.72960
22	Point	2576500	3936000	742.382341	257650003936000	542.117675	742	200.264665	-0.382341	742
23	Point	2394000	2236000	-1068.287458	239400002236000	-1410.849234	432.142156	342.561776	1500.429614	-1068.287458
24	Point	2396500	2236000	-1070.378768	239650002236000	-1415.638467	432.789242	345.259699	1503.168011	-1070.378768
25	Point	2398000	2236000	-1074.175361	239800002236000	-1420.685740	433.320089	346.510379	1507.495450	-1074.175361
26	Point	2389000	2236000	-1052.360989	238900002236000	-1399.392617	431.207785	347.031628	1483.568774	-1052.360989
27	Point	2391500	2236000	-1058.986086	239150002236000	-1406.206657	431.544288	347.214571	1490.530374	-1058.986086
28	Point	2384000	2236000	-1044.359403	238400002236000	-1394.010246	430.122543	349.650844	1474.481946	-1044.359403
29	Point	2386500	2236000	-1047.166353	238650002236000	-1398.726849	430.692622	351.560496	1477.858975	-1047.166353
30	Point	2381500	2236000	-1038.372873	238150002236000	-1391.944905	429.691235	353.572032	1468.064109	-1038.372873
31	Point	2379000	2236000	-1033.749894	237900002236000	-1387.674198	429.210846	353.924304	1462.960740	-1033.749894
32	Point	2376500	2236000	-1029.177168	237650002236000	-1383.395942	428.733161	354.218774	1457.910328	-1029.177168
33	Point	2374000	2236000	-1022.004626	237400002236000	-1381.793375	428.251095	359.788749	1450.285721	-1022.004626
34	Point	2369000	2236000	-1007.394989	236900002236000	-1375.406380	427.251070	368.011390	1434.646060	-1007.394989
35	Point	2371500	2236000	-1012.359906	237150002236000	-1380.429586	427.724624	368.089681	1440.084529	-1012.359906
36	Point	2364000	2236000	-993.710198	236400002236000	-1366.453619	426.191508	372.743421	1419.901706	-993.710198
37	Point	2366500	2236000	-1001.373619	236650002236000	-1375.365430	426.631890	373.991811	1428.205509	-1001.373619
38	Point	2361500	2236000	-985.713216	236150002236000	-1362.609495	425.904805	376.896279	1411.618021	-985.713216

Record: 14 | Show: All | Selected | Records (0 out of 39 Selected.) | Options

Figure C-6. Adjustment of provisional high-resolution surface model to lower (red box) and upper (green box) constraints based on previously developed high-resolution surface models of underlying and overlying units.

C.1.5. Development of High-Resolution Surface Models

C.1.5.1. Top of Quaternary Unit (Land Surface)

Development of the high-resolution model of the top of the Quaternary Unit required separate development of high-resolution surface models for the onshore area—that is, the area not occupied by Lake Michigan—and for Lake Michigan. These separate models were then combined into a single high-resolution model covering the entire area. For the onshore area, land surface elevation was estimated as the median elevation, based on USGS Digital Elevation Models (DEMs), in each 2500-by-2500 ft cell of the high-resolution grid. Since the DEM elevations represent the lake surface in the area of Lake Michigan, development of the high-resolution model of the top of the Quaternary Unit required separate construction of a model of the bottom of Lake Michigan based largely on digital Lake Michigan bathymetric mapping (National Oceanic and Atmospheric Administration Satellite and Information Service, 1996). This interpolation was conducted using a kriging algorithm designed for a rectangular area surrounding the southern part of Lake Michigan (Table C-8). Interpolation source data consisted of the digitized lake bottom elevation data and onshore land-surface elevation data obtained from DEMs. The high-resolution surface model of the top of the Quaternary Unit was completed by substituting the interpolated lake-bottom elevations for the water-surface elevations computed from the DEMs for the area of Lake Michigan.

C.1.5.2. Top of Upper Bedrock Unit (Bedrock Surface)

The second high-resolution surface model generated depicts the top of the Upper Bedrock Unit and is equivalent to a high-resolution surface model of the bedrock surface. The bedrock surface represents the surface underlying the glacial drift and—in a few major river valleys in the region—the surface underlying post-glacial alluvium. The process of developing the high-resolution surface model of the top of the Upper Bedrock Unit required development of separate preliminary high-resolution surface models of the top of the Upper Bedrock Unit in (1) the onshore part of the regional model domain (the *preliminary onshore high-resolution surface model of the top of the Upper Bedrock Unit*) and (2) the Lake Michigan part of the domain (the *preliminary Lake Michigan high-resolution surface model of the top of the Upper Bedrock Unit*). These preliminary models were then combined into a provisional high-resolution surface model of the top of the Upper Bedrock Unit, which was then adjusted to eliminate stratigraphic violations.

Several sets of source data were compiled to generate the preliminary onshore high-resolution surface model of the top of the Upper Bedrock Unit (Figure C-7). Sources include an Arc/Info coverage of bedrock-surface topography in Illinois based on Herzog et al. (1994) (Illinois Department of Natural Resources, 1996b), converted to shapefile format; polyline-feature shapefiles depicting bedrock-surface topography in Indiana (Indiana Geological Survey, personal communication, 2003) and in the seven-county southeastern Wisconsin area (Wisconsin Geological and Natural History Survey, personal communication, 2003), referenced to the Illimap projection; and a hardcopy map of bedrock-surface topography in the lower peninsula of Michigan (Western Michigan University Department of Geology, 1981), digitized for the project.

For the area of absence of the Quaternary Unit (the driftless area of southwestern Wisconsin and northwestern Illinois), source data for development of the preliminary onshore

high-resolution surface model of the top of the Upper Bedrock Unit were copied from the high-resolution surface model of the top of the Quaternary Unit using a polygon-shapefile of the driftless area described previously.

Since faulting has not affected the bedrock surface, a kriging algorithm was employed for the interpolation with parameters as specified in Table C-4. The interpolation results—by default saved in the Surfer grid format—were exported from Surfer in text format. This text file was subsequently imported to ArcGIS, where it was saved in point-shapefile format, a step marking completion of the preliminary onshore high-resolution surface model of the top of the Upper Bedrock Unit.

Fewer source data were available for developing the preliminary high-resolution Lake Michigan Upper Bedrock model (Figure C-8). Of greatest importance was a point-feature shapefile giving estimates of bedrock-surface elevation at locations in southern Lake Michigan that was provided by the Wisconsin Geological and Natural History Survey (personal communication, 2002). These data were employed in construction of a groundwater flow model covering the southeastern Wisconsin area (Feinstein et al., 2003). A second point-feature shapefile was developed from points marking the terminations at the boundary of Lake Michigan of polylines in the digital bedrock-surface maps of Illinois (Illinois Department of Natural Resources, 1996b), southeastern Wisconsin (Wisconsin Geological and Natural History Survey, personal communication, 2003), Indiana (Indiana Geological Survey, personal communication, 2003), and the hardcopy bedrock-topographic map of the lower peninsula of Michigan digitized for this project (Western Michigan University Department of Geology, 1981).

A kriging algorithm designed for a smaller output grid covering only the Lake Michigan area was employed for interpolation (Table C-8). Interpolation results were exported as a text file, which was then imported into ArcGIS and saved in point-shapefile format. The points in the resulting shapefile lying in the area outside of Lake Michigan were then erased using a polygon-shapefile of Lake Michigan, a step that marked completion of the preliminary high-resolution Lake Michigan bedrock-surface model.

The two preliminary high-resolution surface models of the top of the Upper Bedrock Unit—one of the onshore area and one of the Lake Michigan area—were then combined into a single shapefile. For the most part, the interpolated elevations along the interface between the points in the two shapefiles (that is, those points located along the Lake Michigan coast) were consistent with one another, but inconsistencies in the source data of the two interpolations resulted in significant disagreement in the interpolated elevations in the far northeastern part of Lake Michigan within the regional model domain. For this reason, a simple combination of the preliminary high-resolution onshore and Lake Michigan Upper Bedrock models would have resulted in an unlikely bedrock-surface configuration in this part of Lake Michigan. Thus, the final combination of the preliminary high-resolution surface model of the top of the Upper Bedrock Units was manually adjusted to include a small portion of the preliminary high-resolution onshore Upper Bedrock model within the area of Lake Michigan, where otherwise the preliminary high-resolution Lake Michigan Upper Bedrock model was employed (Figure C-9). To combine the two preliminary high-resolution surface models, the point features from the areas of the two models shown in Figure C-9 were selected, copied, and pasted into a new point-feature shapefile. Combination of the two preliminary high-resolution surface models of the Upper Bedrock Unit completed the provisional high-resolution surface model of the top of the Upper Bedrock Unit.

The provisional high-resolution surface model of the top of the Upper Bedrock Unit was then adjusted using the high-resolution surface model of the top of the Quaternary Unit as an upper constraint, marking completion of the high-resolution surface model of the Upper Bedrock Unit. The portion of the high-resolution surface model of the top of the Upper Bedrock Unit west of the Mississippi River was then erased to create the active-cell high-resolution surface model of the top of the Upper Bedrock Unit.

Table C-8. Parameters of Kriging Algorithm Having Output Grid Coincident with Lake Michigan Region

<i>Gridding Method</i>	<i>Kriging</i>
Kriging Type	Point
Polynomial Drift Order	0
Kriging std. deviation grid	no
Output Grid	
Minimum x	3424000 ft
Maximum x	3894000 ft
Minimum y	3128500 ft
Maximum y	4116000 ft
x and y spacing	2500 ft
Semi-Variogram Model	
Component Type	Linear
Anisotropy Angle	0
Anisotropy Ratio	1
Variogram Slope	1
Search Parameters	
Search Ellipse Radius #1	433000 ft
Search Ellipse Radius #2	433000 ft
Search Ellipse Angle	0
Number of Search Sectors	8
Maximum Data Per Sector	8
Maximum Empty Sectors	6
Minimum Data	3
Maximum Data	64

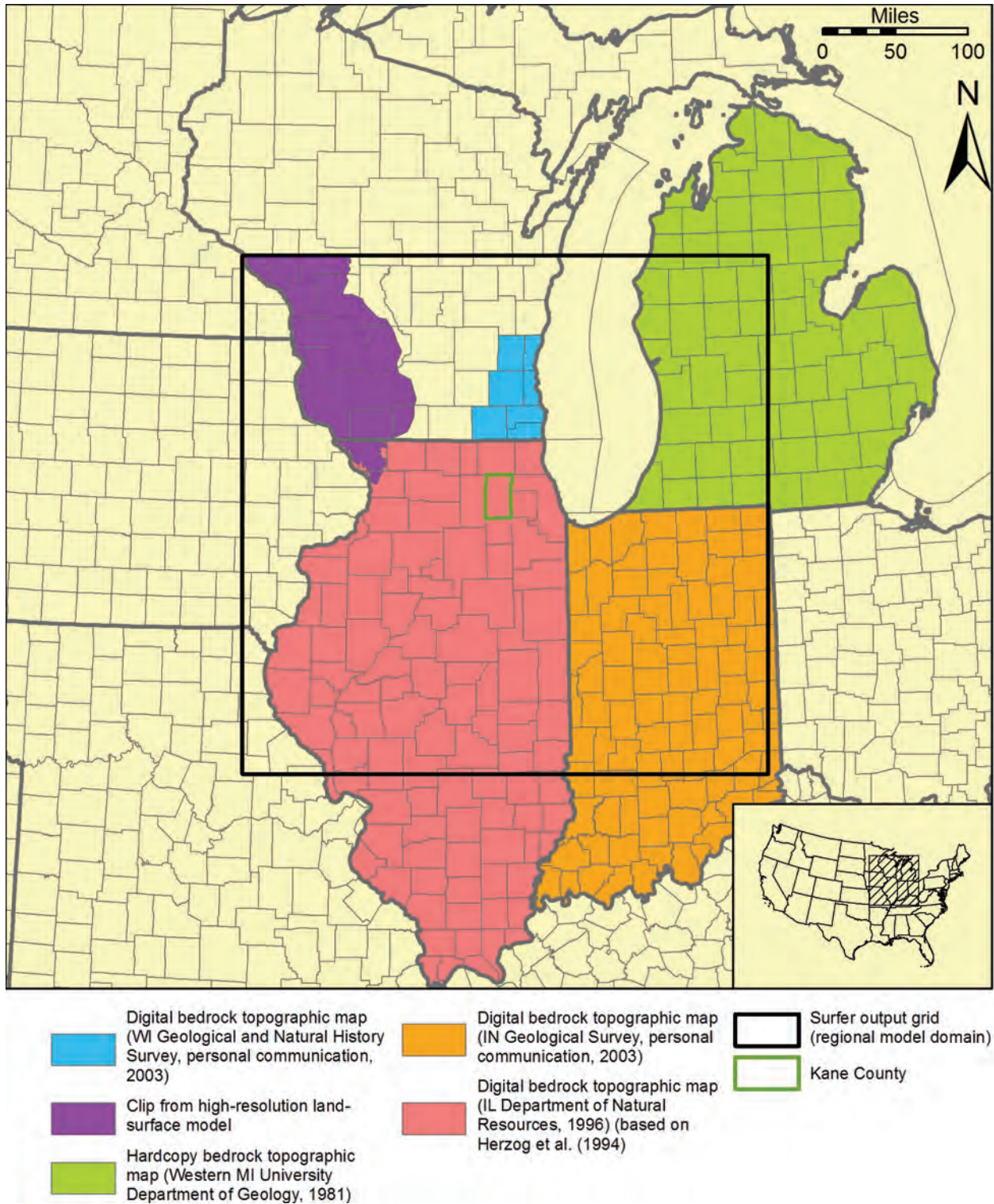
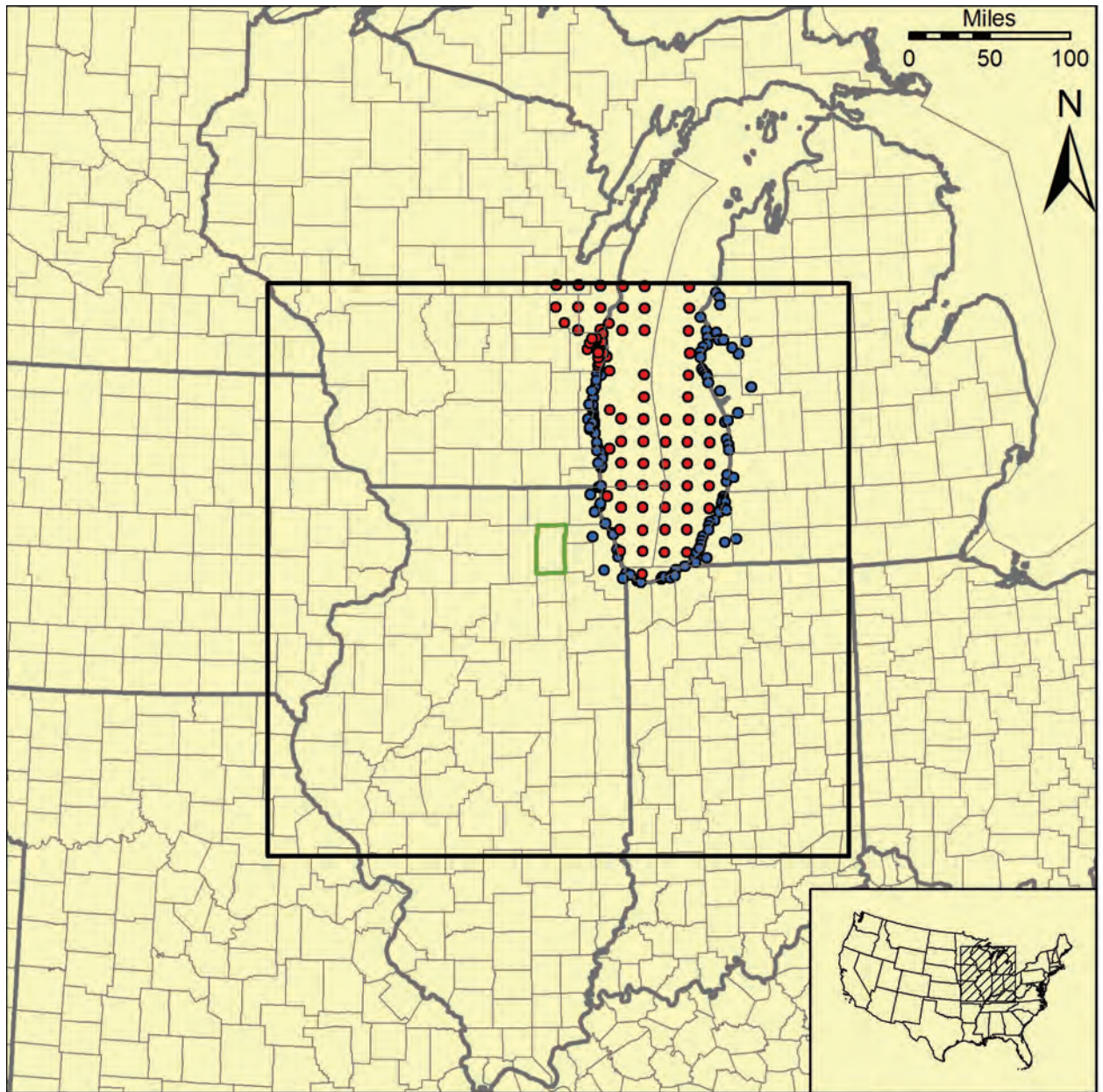


Figure C-7. Sources of data for the preliminary onshore high-resolution surface model of the top of the Upper Bedrock Unit.



- Shapefile of estimated bedrock-surface elevation in southern Lake Michigan area (WI Geol and Natural History Survey, personal communication, 2002)
 - Shapefile of bedrock-surface elevations estimated from digital and hardcopy bedrock-surface mapping (IL Dept of Natural Resources, 1996; WI Geol and Natural History Survey, personal communication, 2003; IN Geol Survey, personal communication, 2003; Western MI Univ Dept of Geology, 1981).
- Surfer output grid (regional model domain)
 Kane County

Figure C-8. Sources of data for preliminary Lake Michigan high-resolution surface model of the top of the Upper Bedrock Unit.

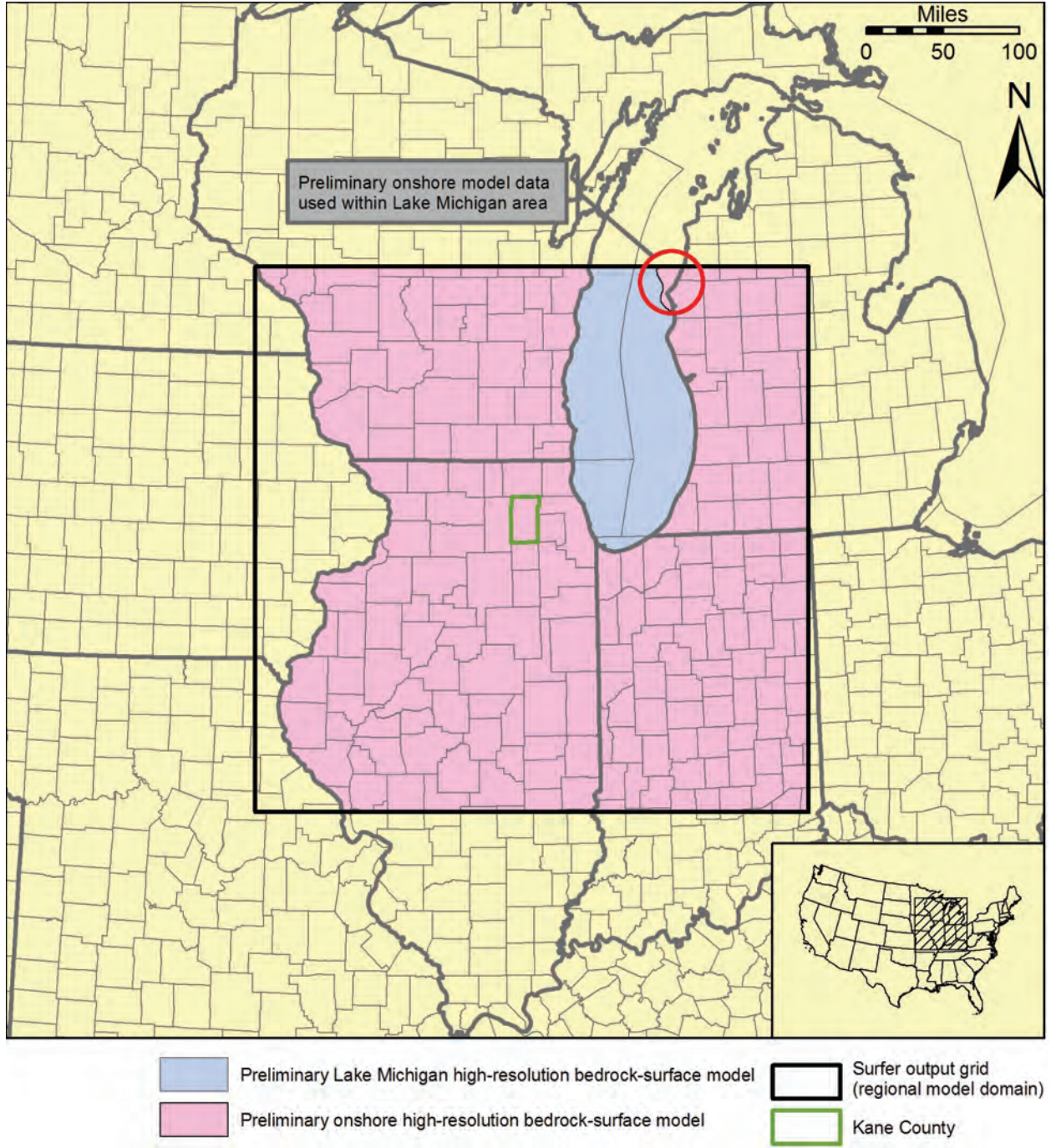


Figure C-9. Development of final high-resolution surface model of top of Upper Bedrock Unit from preliminary onshore and Lake Michigan models.

C.1.5.3. Base of Mt. Simon Unit (Precambrian Surface)

Structure-contour mapping of the Precambrian surface was digitized and employed as interpolation source data for development of the high-resolution surface model of the base of the Mt. Simon Unit for all areas except the Lower Peninsula of Michigan, most of Lake Michigan, and areas of bedrock-surface exposure of the Precambrian (Figure C-10). Structure contours digitized as polylines from the Precambrian structure-map of Visocky et al. (1985) were augmented with additional contours, positioned using professional judgment in a high-priority area encompassing the model nearfield and the Plum River Fault and Sandwich Fault Zone. The contours digitized from an unpublished structure-contour map of the Precambrian surface (USGS, Wisconsin District, personal communication, 2002) were edited to correct stratigraphic violations of digitized structure contours of overlying hydrostratigraphic units and for consistency with structure-contour maps of overlying and underlying units in the vicinity of mapped areas of absence. This mapping was not employed as the basis for the high-resolution surface model in northern Illinois, where the mapping of Visocky et al. (1985)—which is based on local studies and is presumed to be more accurate in that area—was used. The USGS mapping was employed in central Illinois, but it was edited to adjust contour positions to those along the southern border of the northern Illinois area where the data of Visocky et al. (1985) were used. Contours digitized from a structure-contour map of the Precambrian surface in Indiana (Rupp, 1991) required no editing and were not augmented.

Source data for the Michigan portion of the high-resolution surface model of the base of the Mt. Simon Unit were synthesized by effectively subtracting an isopach map of the Mt. Simon Formation from a structure-contour map of the Mt. Simon. Both maps were developed by Bricker et al. (1983). More recently published Precambrian structure-contour mapping in Michigan (Catacosinos and Daniels, 1991) was not employed as source data for the high-resolution surface model because of numerous, severe stratigraphic violations between this map and structure-contour maps of shallower horizons developed by Bricker et al. (1983) that are used extensively as source data for the high-resolution surface models of these shallower horizons. Both the Mt. Simon isopach map and structure-contour map of Bricker et al. (1983) were digitized as polyline-shapefiles. Each shapefile was then augmented with additional contours, positioned using professional judgment between the locations of the published contours. A point-shapefile was then generated from the two polyline-shapefiles containing the structure and thickness contours using an ArcGIS tool to calculate the intersections of the polylines in these shapefiles. A field was added to the attribute table of the resulting point-shapefile to represent the estimated Mt. Simon base elevation, and this field was calculated as the difference between the Mt. Simon top elevation and the Mt. Simon thickness—fields that were inherited from the parent polyline-shapefiles.

Scant geologic data is available for the area of Lake Michigan. The Precambrian structure-contour mapping of Catacosinos and Daniels (1991) was digitized and employed for a small amount of Mt. Simon base elevation data in the eastern part of Lake Michigan, but for the most part, structure contours were estimated using professional judgment for the entire area of Lake Michigan within the regional model domain. The contours were constructed to depict a simple surface, with minimal added perturbations, that completely honors the Mt. Simon base-elevation data in surrounding areas as shown in Figure C-10.

For areas of bedrock-surface exposure of the Precambrian, source data for development of the high-resolution surface model of the base of the Mt. Simon Unit were obtained from the

previously developed high-resolution surface model of the top of the Upper Bedrock Unit if they were located within polygons of a shapefile of the Precambrian bedrock-surface exposures.

Since faulting has affected the Precambrian surface, the inverse-distance algorithm (Table C-5) was employed for interpolation of the source data, with breaklines included in a .bln file developed from the shapefile containing the five fault features discussed previously (Section C.1.1.3). This provisional high-resolution surface model of the base of the Mt. Simon Unit was then adjusted using the high-resolution surface model of the top of Upper Bedrock Unit as an upper constraint. The portion of the resulting high-resolution surface model of the base of the Mt. Simon Unit west of the Mississippi River was then erased to create the active-cell high-resolution surface model of the base of the Mt. Simon Unit.

C.1.5.4. Top of Mt. Simon Unit

Structure-contour mapping of the top of the Mt. Simon Sandstone was digitized and employed as source data for development of the high-resolution surface model of the top of the Mt. Simon Unit for all areas except the northern half of Illinois, Lake Michigan, and areas of bedrock-surface exposure of the Mt. Simon Unit (Figure C-11). Structure contours digitized as polylines from the Michigan Mt. Simon structure map of Bricker et al. (1983) were augmented with contours, positioned using professional judgment between the contours appearing in the published map. Contours digitized from an unpublished structure-contour map of the Precambrian surface (USGS, Wisconsin District, personal communication, 2002) were edited to correct stratigraphic violations of digitized structure contours of overlying hydrostratigraphic units and for consistency with structure-contour maps of overlying and underlying units in the vicinity of mapped areas of absence. This mapping was not employed as the basis for the high-resolution surface model in northern Illinois, where the local Eau Claire structure-contour mapping of Visocky et al. (1985) was used in conjunction with Illinois statewide mapping of Eau Claire thickness (Willman et al., 1975) to synthesize Mt. Simon structure data. The unpublished USGS mapping was employed in central Illinois, but it was edited to adjust contour positions to those along the southern border of the northern Illinois area where the data of Visocky et al. (1985) and Willman et al. (1975) were used. Contours digitized from a structure-contour map of the Precambrian surface in Indiana (Rupp, 1991) required no editing and were not augmented.

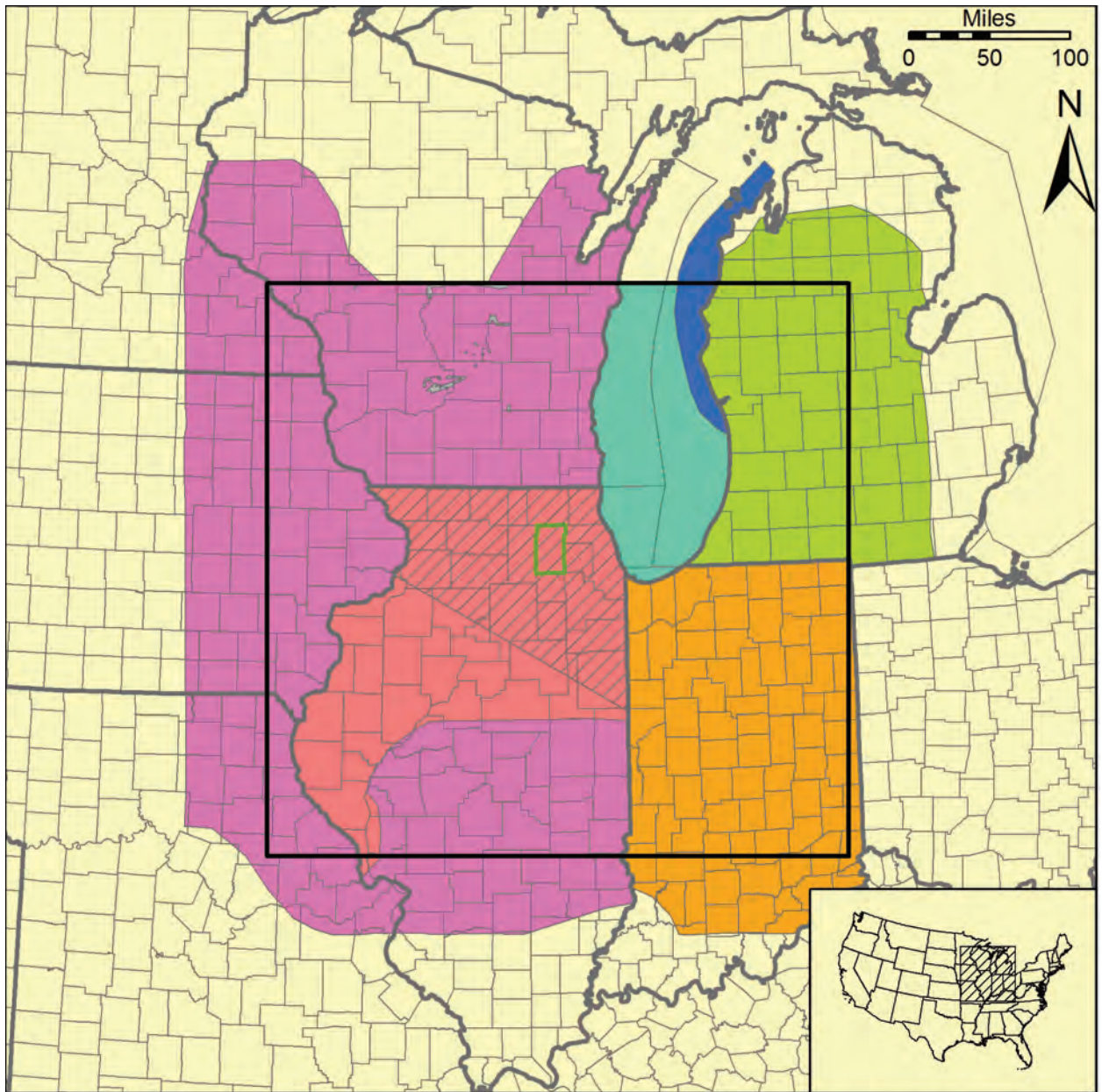
Source data for the northern Illinois portion of the high-resolution surface model of the top of the Mt. Simon Unit were obtained by effectively subtracting an isopach map of the Eau Claire Formation (Willman et al., 1975) from a structure-contour map of the Eau Claire (Visocky et al., 1985). Visocky et al. (1985) published a structure-contour map of the top of the Elmhurst-Mt. Simon Aquifer in northern Illinois, but since this map shows the top elevation of the basal Elmhurst Member of the Eau Claire Formation, not that of the Mt. Simon Sandstone (the top of the Mt. Simon Unit of the present study), the step of subtracting a thickness map of the Eau Claire from a structure-contour map was taken to develop a more accurate Mt. Simon Sandstone structure map consistent with the definition of the *Mt. Simon Unit* employed in this study. To accomplish this, the Eau Claire structure-contour map (Visocky et al., 1985) was first digitized as a polyline-shapefile. The Eau Claire isopach map (Willman et al., 1975) was then scanned, and the scanned image was registered to the digitized Eau Claire structure-contour map. With both the digitized structure-contour map and scanned thickness map displayed on screen, a Mt. Simon structure map was constructed manually, using the approximate elevation of the top of the Mt. Simon at intersections of structure contours and isopachs as a guide. The constructed contours were then augmented with additional contours, positioned using professional judgment between the contours appearing in the published map. This augmentation process was limited to

a high-priority area encompassing the model nearfield and the Plum River Fault and Sandwich Fault Zone and was necessary to permit the interpolation algorithm to generate a geologically plausible surface from the source data.

Structure contours were estimated using professional judgment for the entire area of Lake Michigan within the regional model domain. The contours were constructed to depict a simple surface, with minimal added perturbations, that completely honors the Mt. Simon top-elevation data in surrounding areas as shown in Figure C-11.

Interpolation source data for areas of bedrock-surface exposures of the Mt. Simon Unit were generated by selecting and exporting point-features located within these exposures from the previously-developed high-resolution surface model of the top of the Upper Bedrock Unit. Similarly, interpolation source data for areas of absence of the Mt. Simon Unit were generated by selecting and exporting point-features located within these areas from the previously developed high-resolution surface model of the base of the Mt. Simon Unit.

Since faulting has affected the top of the Mt. Simon Unit, the inverse-distance algorithm (Table C-5) was employed for interpolation of the source data, with breaklines included in a .bln file developed from the shapefile containing the five fault features discussed previously (Section C.1.1.3). The provisional high-resolution surface model of the top of the Mt. Simon Unit was then adjusted using the high-resolution surface models of the top of the Upper Bedrock Unit and the base of the Mt. Simon Unit as upper and lower constraints, respectively. The portion of the resulting high-resolution surface model of the top of the Mt. Simon Unit west of the Mississippi River was then erased to create the active-cell high-resolution surface model of the top of the Mt. Simon Unit.











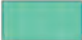
- | | | | | | |
|---|---|---|---|---|--|
|  | High-resolution model of Upper Bedrock Unit (Precambrian bedrock-surface exposures) |  | Precambrian top structure (Rupp, 1991) |  | Surfer output grid (regional model domain) |
|  | Precambrian top structure (Catacosinos and Daniels, 1991) |  | Precambrian top structure (Visocky et al., 1985), augmented where hatched |  | Kane County |
|  | Mt Simon Ss top structure (augmented) minus Mt. Simon Ss thickness (augmented) (Bricker et al., 1983) |  | Precambrian top structure (US Geological Survey, WI Dist, personal communication, 2002), edited | | |
| | |  | Estimated | | |

Figure C-10. Sources of data for high-resolution surface model of base of Mt. Simon Unit.

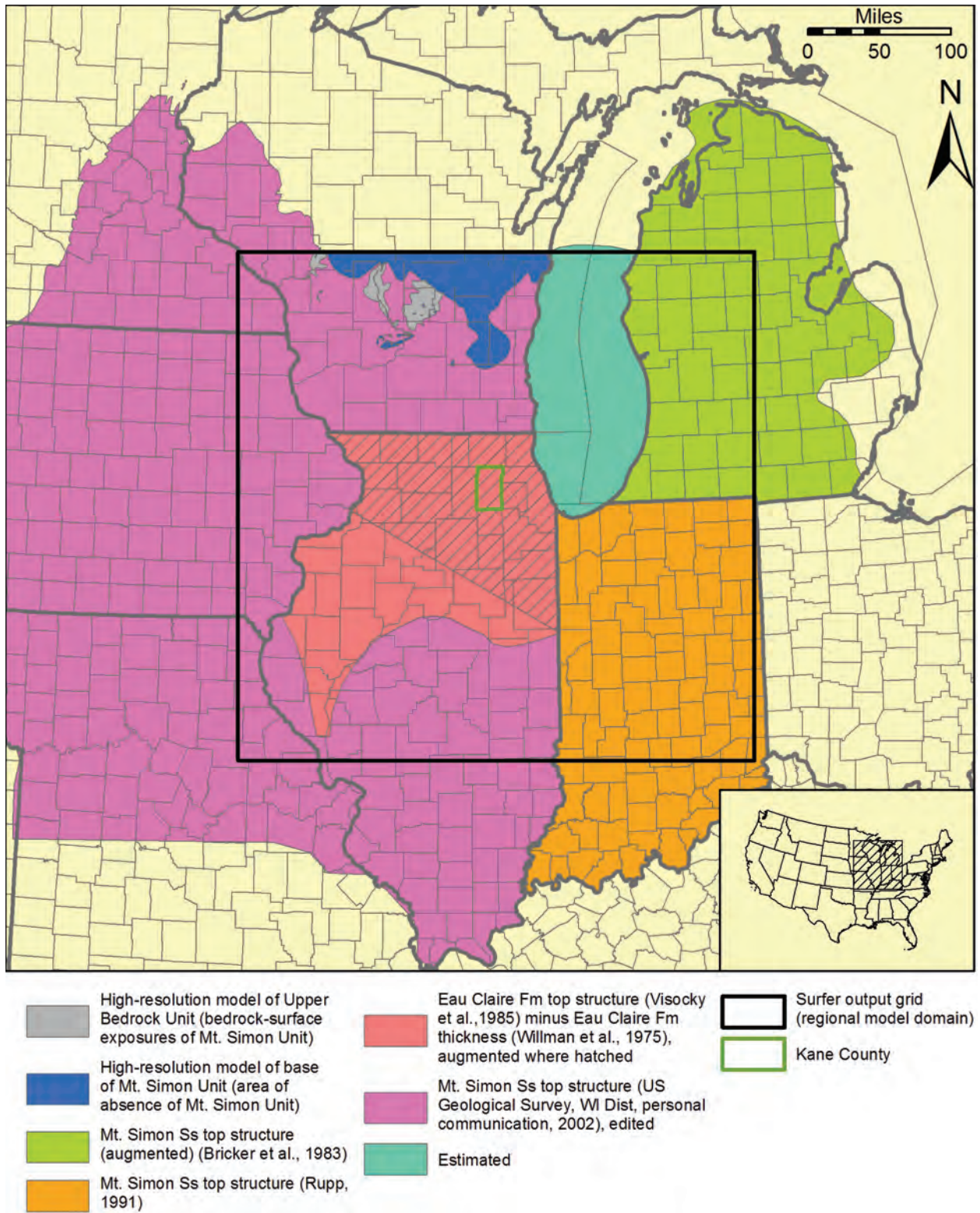


Figure C-11. Sources of data for high-resolution surface model of top of Mt. Simon Unit.

C.1.5.5. Top of Silurian-Devonian Carbonate Unit (First Iteration)

A first-iteration high-resolution surface model of the top of the Silurian-Devonian Carbonate Unit was developed for use as input to the development of the high-resolution surface models of underlying hydrostratigraphic units not yet completed (tops of the Eau Claire, Ironton-Galesville, Potosi-Franconia, Prairie du Chien-Eminence, Ancell, Galena-Platteville, and Maquoketa Units). Specifically, data from this first-iteration model of the Silurian-Devonian Carbonate Unit were used as an upper constraint in adjusting provisional high-resolution surface models of the listed underlying units. Since the Silurian-Devonian Carbonate Unit underlies the Upper Bedrock Unit, it provides a more restrictive upper constraint on plausible elevations of top of deeper units than the previously developed high-resolution surface model of the top of the Upper Bedrock Unit model and permits more accurate modeling of the tops of the deeper units. But because development of the first-iteration high-resolution surface model of the top of the Silurian-Devonian Carbonate Unit itself required use of the high-resolution surface model of the top of the Mt. Simon Unit—a unit that is stratigraphically far-removed from the Silurian-Devonian Carbonate Unit, a second-iteration high-resolution surface model of the top of the Silurian-Devonian Carbonate Unit was developed after the high-resolution surface model of the top of the Maquoketa Unit was completed. With the more restrictive constraint of the Maquoketa Unit model employed for identification of lower stratigraphic violations, rather than the model of the top of the Mt. Simon Unit, the second-iteration high-resolution surface model of the top of the Silurian-Devonian Carbonate Unit is somewhat more accurate than the first-iteration model.

Error incurred by using the first-iteration high-resolution model—and not the second-iteration model—of the top of the Silurian-Devonian Carbonate Unit as an upper constraint on plausible values of high-resolution surface models of underlying hydrostratigraphic units is insignificant. With only a single, essentially irrelevant exception, the sets of points adjusted as stratigraphic violations of the upper constraint are precisely the same for provisional high-resolution surface models of these underlying hydrostratigraphic units whether the first-iteration or second-iteration high-resolution model of the Silurian-Devonian Carbonate Unit is used as an upper constraint. The exception is the high-resolution surface model of the top of the Maquoketa Unit, for which use of the second-iteration high-resolution model as an upper constraint would have added a single point—located in the model farfield—to the set of over 69,000 points adjusted as stratigraphic violations. Thus, the first-iteration high-resolution model was not only a better tool than the high-resolution surface model of the more stratigraphically distant Upper Bedrock Unit for identifying implausibly high elevations in provisional high-resolution surface models of underlying units, but it was essentially as good a tool for this purpose as the second-iteration model.

The Silurian-Devonian Carbonate Unit is absent or exposed at the bedrock surface in a large portion of the regional model domain, and for these areas, source data for the first-iteration high-resolution model of the top of the Silurian-Devonian Carbonate Unit were obtained from previously developed high-resolution surface models of the tops of the Mt. Simon Unit and Upper Bedrock Unit, respectively (Figure C-12). Structure-contour mapping was employed elsewhere, for the most part. This mapping includes an unpublished structure-contour map of the top of the Silurian-Devonian Carbonate Unit in Illinois and areas to the west (USGS, Wisconsin District, personal communication, 2002) and published maps of the structure of the top of the Traverse Group in Michigan (Catacosinos et al., 1990) and the Muscatatuck Group in Indiana (Rupp, 1991).

Since faulting has affected the top of the Silurian-Devonian Carbonate Unit, the inverse-distance algorithm (Table C-5) was employed for interpolation of the source data, with breaklines included in a .bln file developed from the shapefile containing the five fault features discussed previously (Section C.1.1.3). The provisional first-iteration high-resolution surface model of the top of the Silurian-Devonian Carbonate Unit was then adjusted using the high-resolution surface models of tops of the Upper Bedrock Unit and Mt. Simon Unit as upper and lower constraints, respectively. Because the first-iteration high-resolution surface model of the top of the Silurian-Devonian Carbonate Unit was not employed in developing the irregular-grid model of the unit, an active-cell high-resolution surface model of the first-iteration model of the unit was not generated.

C.1.5.6. Top of Eau Claire Unit

Structure-contour mapping of the top of the Eau Claire Formation in Illinois, Wisconsin, and areas west of the Mississippi River was digitized and employed as source data for development of the high-resolution surface model of the top of the Eau Claire Unit (Figure C-13). Contours digitized from an unpublished structure-contour map of the top of the Eau Claire (USGS, Wisconsin District, personal communication, 2002) were employed in Wisconsin, a portion of central Illinois, and areas west of the Mississippi River. These contours were edited to correct stratigraphic violations of digitized structure contours of adjacent hydrostratigraphic units and for consistency with structure-contour maps of other units in the vicinity of mapped areas of absence. The unpublished USGS mapping was not employed as source data in northern Illinois, where published structure-contour mapping of the top of the Eau Claire (Visocky et al., 1985) was used. Structure contours digitized from the Eau Claire structure map of Visocky et al. (1985) were augmented with additional contours, positioned using professional judgment in a high-priority area encompassing the model nearfield and the Plum River Fault and Sandwich Fault Zone. Contours digitized from the unpublished USGS mapping showing Eau Claire structure in central Illinois were edited to adjust contour positions to those along the southern border of the northern Illinois area where the data of Visocky et al. (1985) were used.

Eau Claire top-elevation data for Michigan, Indiana, and a part of central Illinois were synthesized using isopach maps, structure-contour maps, and the previously generated high-resolution surface model of the top of the Mt. Simon Unit.

Eau Claire elevation data for Michigan were synthesized by effectively adding a digitized isopach map of the Eau Claire Formation (Bricker et al., 1983) to a digitized structure-contour map of the top of the Mt. Simon Sandstone (Bricker et al., 1983) that was augmented with additional contours, positioned using professional judgment between the locations of the published contours. This technique is discussed in reference to the generation of interpolation source data for the high-resolution surface model of the base of the Mt. Simon Unit. Although Bricker et al. (1983) published a structure-contour map of the top of the Eau Claire Formation in Michigan, this map was not employed because it includes numerous and severe stratigraphic violations of their structure-contour map of the top of the Mt. Simon Sandstone. Because the intersection points generated through the process were relatively thinly distributed across the lower peninsula of Michigan, the additional step was taken of hand-contouring a structure-contour map of the top of the Eau Claire based on the intersection points, in the form of a polyline-shapefile. This hand-contoured map honors the synthesized Eau Claire elevation data and was constructed using the structure-contour map of the top of the Mt. Simon Sandstone (Bricker et al., 1983) as a guide to the configuration of the top of the Eau Claire.

Since published structure-contour mapping of the top of the Eau Claire Formation is not available for a small portion of central Illinois within the regional model domain, and since the unpublished USGS mapping does not cover this area, Eau Claire top-elevation data were synthesized for that area by subtracting a digitized isopach map of the Ironton and Galesville Sandstones (Emrich, 1966) from a structure-contour map of the Ironton Sandstone (Emrich, 1966). This subtraction was accomplished using the same approach of calculating Eau Claire top elevation at points of intersection of polylines digitized from the structure-contour and isopach maps. Only the point-shapefile containing the intersection points was used as interpolation source data for the central Illinois area. A hand-contoured map based on the intersection points was not developed.

Eau Claire top-elevation data were also synthesized for the area of Indiana where a published Eau Claire structure-contour map is not available. To accelerate the process of synthesizing elevation data, an approach based on summation of interpolated elevation and structure data was employed for this area. An isopach map of the Eau Claire Formation (Rupp, 1991) was digitized as a polyline shapefile. An ArcGIS tool was then employed to export the vertices of the polyline-shapefile as a point-feature shapefile, and a different ArcGIS tool was used to add the x- and y-coordinates of the point features to the attribute table of the exported point-shapefile. These point data were then exported in text format (procedure Arc-k), and this file was used as input data for interpolation in Surfer of Eau Claire Formation thickness in Indiana.

A kriging algorithm was employed for the interpolation of the thickness data in Surfer (Table C-9). The output grid was designed so that interpolation results were generated for the same (x, y) coordinate pairs as all other interpolations conducted for the project, but only for those locations within the northern Indiana portion of the regional model domain. Interpolation results—a model of the thickness of the Eau Claire Formation in Indiana—were exported as a text file which was then imported into ArcGIS and saved in point-shapefile format. Cross validation statistics for the interpolation of Indiana Eau Claire thickness data are shown in Table C-10.

The attribute table of the resulting Eau Claire thickness model contained fields for the x- and y-coordinates of each point in the output grid as well as the interpolated Eau Claire thickness at the point. An additional field was added for a unique numerical index calculated from the x- and y-coordinates using the formula described previously (page C-22). Since all the interpolations were constrained so as to give results at a consistent set of locations, this index field of the Eau Claire thickness model was employed to join the attribute table of the Eau Claire thickness model to that of the previously generated high-resolution surface model of the top of the Mt. Simon Unit, which also contained the index. A field was added to the attribute table of the Eau Claire thickness model to contain the estimated Mt. Simon Unit top elevation at each point, and this field was populated with the Mt. Simon top elevations from the joined attribute table. The table join was then removed. A final field was added to the attribute table of the Eau Claire thickness model to contain an estimate of the elevation of the top of the Eau Claire Unit, and these elevations were calculated by adding the estimated top elevation of the top of the Mt. Simon Unit at each point to the estimated thickness of the Eau Claire Formation and thus generate a provisional model of the elevation of the top of the Eau Claire Unit in Indiana. These data were prepared for use as source data for interpolation of Eau Claire top elevation across the entire model domain in the same way as described previously—namely, by erasing points from buffer areas along state boundaries and by exporting the data in text format.

Structure contours were estimated using professional judgment for the entire area of Lake Michigan within the regional model domain. The contours were constructed to depict a simple surface, with minimal added perturbations, that completely honors the Eau Claire top-elevation data in surrounding areas as shown in Figure C-13.

Interpolation source data for areas of bedrock-surface exposures of the Eau Claire Unit were generated by selecting and exporting point-features located within these exposures from the previously developed high-resolution surface model of the top of the Upper Bedrock Unit. Similarly, interpolation source data for areas of absence of the Eau Claire Unit were generated by selecting and exporting point-features located within these areas from the previously developed high-resolution surface model of the top of the Mt. Simon Unit.

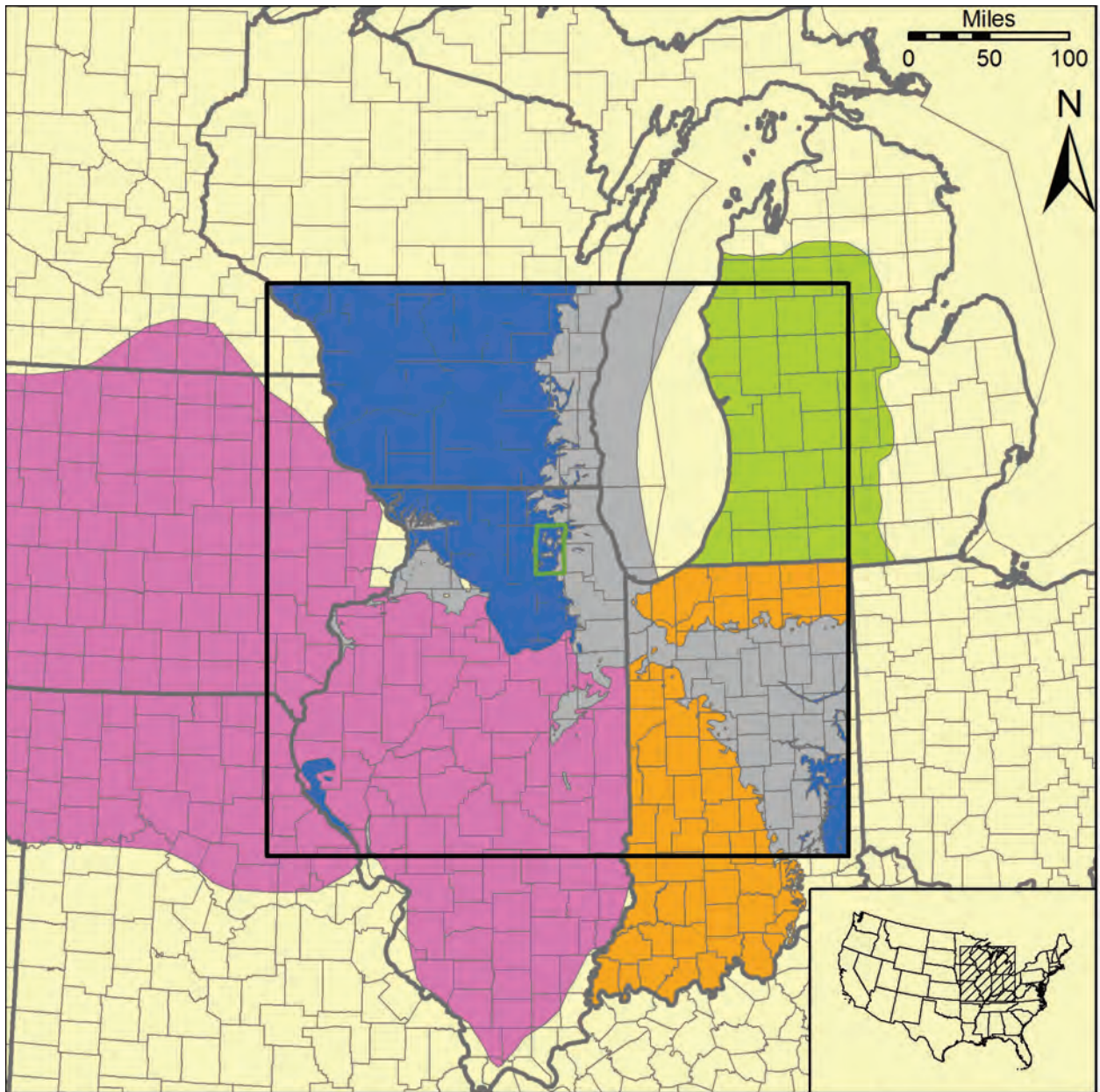
The inverse-distance algorithm (Table C-5) was employed for interpolation of the source data with breaklines included in a .bln file developed from the shapefile containing the five fault features discussed previously (Section C.1.1.3). The provisional high-resolution surface model of the top of the Eau Claire Unit was then adjusted using the first-iteration high-resolution surface model of the top of the Silurian-Devonian Carbonate Unit and the high-resolution surface model of the top of the Mt. Simon Unit as upper and lower constraints, respectively. The portion of the resulting high-resolution surface model of the top of the Eau Claire Unit west of the Mississippi River was then erased to create the active-cell high-resolution surface model of the top of the Eau Claire Unit.

Table C-9. Parameters of Kriging Algorithm Used for Interpolation of Eau Claire Formation Thickness Data Having Output Grid Coincident with Northern Indiana

<i>Gridding Method</i>	<i>Kriging</i>
Kriging Type	Point
Polynomial Drift Order	0
Kriging std. deviation grid	no
Output Grid	
Minimum x	3539000 ft
Maximum x	4269000 ft
Minimum y	2236000 ft
Maximum y	3203500 ft
x and y spacing	2500 ft
Semi-Variogram Model	
Component Type	Linear
Anisotropy Angle	0
Anisotropy Ratio	1
Variogram Slope	1
Search Parameters	
Search Ellipse Radius #1	1200000 ft
Search Ellipse Radius #2	1200000 ft
Search Ellipse Angle	0
Number of Search Sectors	8
Maximum Data Per Sector	8
Maximum Empty Sectors	4
Minimum Data	3
Maximum Data	64

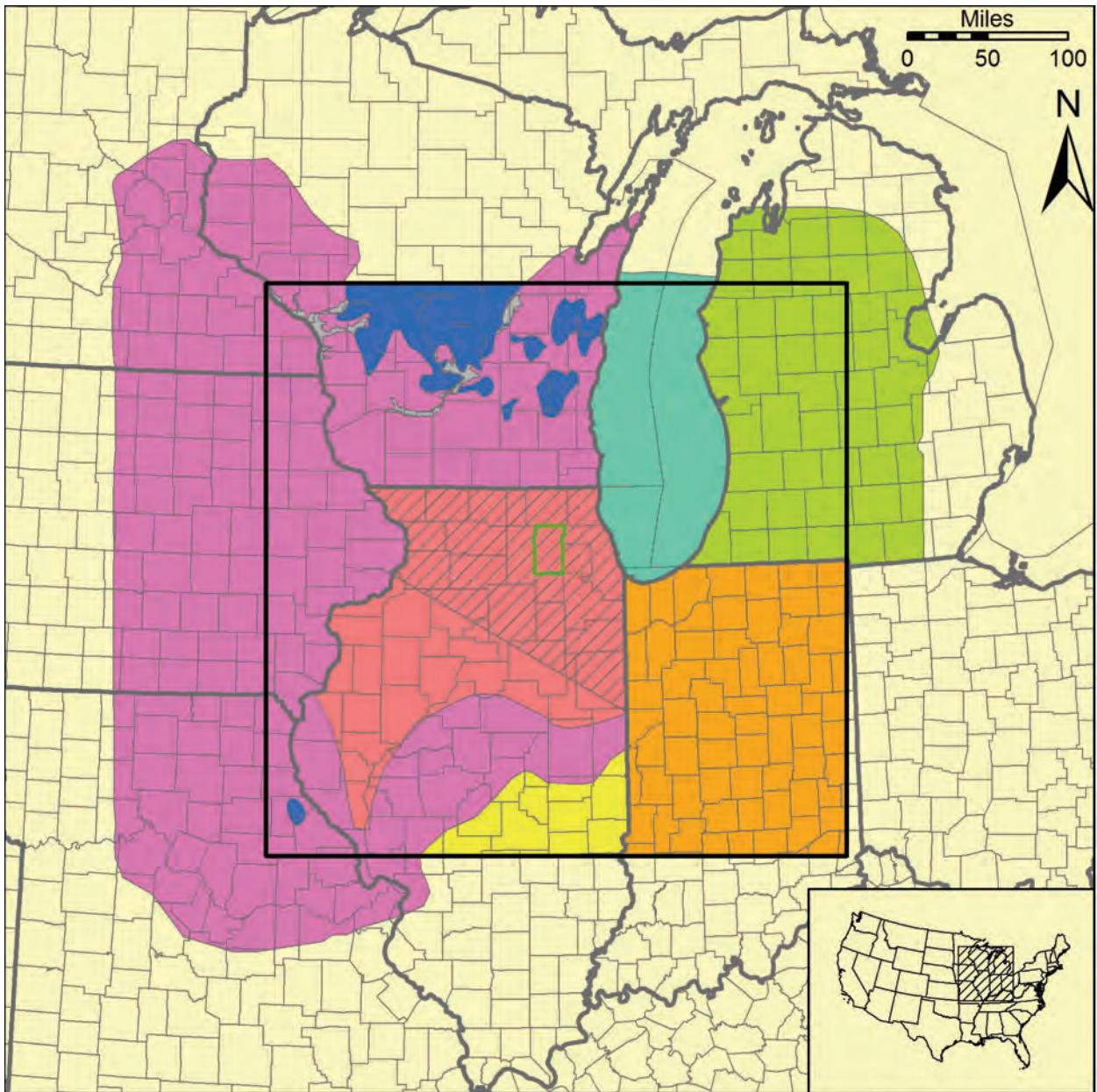
Table C-10. Cross-Validation Statistics for Interpolations of Thickness Data

<i>Thickness Model</i>	<i>Univariate Cross-Validation Statistics</i>			<i>Inter-Variable Correlation with Residual Z at Validation Points</i>		
	<i>Median Abs. Deviation of Residual Z</i>	<i>Mean of Residual Z</i>	<i>Root Mean Square of Residual Z</i>	<i>X</i>	<i>Y</i>	<i>Z</i>
Maquoketa Group (Central Illinois)	0.003	0.002	0.678	-0.027	-0.049	-0.144
Utica Shale (Michigan)	0.097	-0.022	0.372	-0.020	0.042	-0.060
Ancell Group (Indiana)	0.033	0.011	0.122	0.065	0.126	-0.132
Davis Formation (Indiana)	0.119	0.006	2.320	-0.020	-0.007	-0.035
Potosi Dolomite (Indiana)	0.236	0.026	0.709	0.034	0.016	-0.060
Ironton and Galesville Sandstones (Indiana)	0.044	0.048	0.601	0.139	-0.169	-0.272
Eau Claire Formation (Indiana)	0.059	0.003	0.188	0.079	-0.007	-0.076



- | | | |
|---|--|--|
| <p>High-resolution model of Upper Bedrock Unit (Silurian-Devonian Carbonate Unit bedrock-surface exposures)</p> <p>High-resolution model of top of Mt. Simon Unit (Silurian-Devonian Carbonate Unit absent)</p> <p>Traverse Gp top structure (Catacosinos et al., 1990)</p> | <p>Muscatatuck Gp top structure (Rupp, 1991)</p> <p>Silurian-Devonian Carbonate Unit top structure (US Geological Survey, WI Dist, personal communication, 2002)</p> | <p>Surfer output grid (regional model domain)</p> <p>Kane County</p> |
|---|--|--|

Figure C-12. Sources of data for first-iteration high-resolution surface model of top of Silurian-Devonian Carbonate Unit.













- | | | | | | |
|---|--|---|---|---|--|
|  | High-resolution model of Upper Bedrock Unit (Eau Claire Unit bedrock-surface exposures) |  | Ironton Ss top structure minus Ironton-Galesville Ss thickness (Emrich, 1966) |  | Surfer output grid (regional model domain) |
|  | High-resolution model of top of Mt. Simon Unit (Eau Claire Unit absent) |  | Eau Claire Fm top structure (Visocky et al., 1985), augmented where hatched |  | Kane County |
|  | Mt. Simon Ss top structure (augmented) plus Eau Claire Fm thickness (Bricker et al., 1983) |  | Eau Claire Fm top structure (US Geological Survey, WI Dist, personal communication, 2002), edited | | |
|  | High-resolution model of top of Mt. Simon Unit plus Eau Claire Fm thickness (Rupp, 1991) |  | Estimated | | |

Figure C-13. Sources of data for high-resolution surface model of top of Eau Claire Unit.

C.1.5.7. Top of Ironton-Galesville Unit

Elevation data digitized from published and unpublished structure-contour mapping of the top of the Ironton-Galesville Sandstone and its equivalents were employed as source data for development of the high-resolution surface model of the top of the Ironton-Galesville Unit in much of Illinois, Wisconsin, and areas west of the Mississippi River (Figure C-14). Contours digitized from an unpublished structure-contour map of the top of the Ironton-Galesville (USGS, Wisconsin District, personal communication, 2002) were employed in Wisconsin, a portion of central Illinois, and areas west of the Mississippi River. These contours were edited to correct stratigraphic violations of digitized structure contours of adjacent hydrostratigraphic units and for consistency with structure-contour maps of other units in the vicinity of mapped areas of absence. The unpublished USGS mapping was not employed as source data in northern Illinois, where published structure-contour mapping of the top of the Ironton-Galesville (Visocky et al., 1985) was used. Structure contours digitized from the Ironton Sandstone structure map of Visocky et al. (1985) were augmented with additional contours, positioned using professional judgment in a high-priority area encompassing the model nearfield and the Plum River Fault and Sandwich Fault Zone. Contours digitized from the unpublished USGS mapping showing Ironton-Galesville structure in central Illinois were edited to adjust contour positions to those along the southern border of the northern Illinois area where the data of Visocky et al. (1985) were used. In a small portion of central Illinois not covered by the unpublished USGS mapping or the mapping of Visocky et al. (1985), elevation data were obtained by digitizing a structure-contour map of the top of the Ironton Sandstone by Emrich (1966).

Ironton-Galesville elevations in Michigan were synthesized by effectively subtracting a digitized isopach map of the Franconia Formation (Bricker et al., 1983) from a digitized structure-contour map of the top of the Franconia Formation (Bricker et al., 1983). This technique is discussed in reference to the generation of interpolation source data for the high-resolution surface model of the base of the Mt. Simon Unit. Although Bricker et al. (1983) published a structure-contour map of the top of the Ironton-Galesville in Michigan, this map was not employed because it includes numerous and severe stratigraphic violations of their structure-contour maps of the tops of the Eau Claire Formation and even the deeper Mt. Simon Sandstone. Because the intersection points generated through the process were relatively thinly-distributed across the lower peninsula of Michigan, the additional step was taken of hand-contouring a structure-contour map of the top of the Ironton-Galesville based on the intersection points, in the form of a polyline-shapefile. This hand-contoured map honors the synthesized Ironton-Galesville elevation data and was constructed using the structure-contour map of the top of the Franconia Formation (Bricker et al., 1983) as a guide to the configuration of the top of the Ironton-Galesville.

Ironton-Galesville top-elevation data were also synthesized for the area of Indiana within the regional model domain, where an Ironton-Galesville structure-contour map is not available, using an approach based on summation of interpolated thickness data and the previously generated high-resolution surface model of the Eau Claire Unit. This technique is discussed in reference to the development of interpolation source data for high-resolution surface model of the top of the Eau Claire of Indiana. The thickness model of the Ironton-Galesville employed in this process was generated by interpolation of point data generated from a digitized isopach map of the Ironton-Galesville Sandstone (Becker et al., 1978) that was augmented with additional isopachs positioned between published isopachs using professional judgment. A kriging

algorithm was employed for the interpolation (Table C-11). Cross validation statistics for the interpolation of Indiana Ironton-Galesville thickness data are shown in Table C-10.

Structure contours were estimated using professional judgment for the entire area of Lake Michigan within the regional model domain. The contours were constructed to depict a simple surface with minimal added perturbations that completely honors the Mt. Simon top-elevation data in surrounding areas as shown in Figure C-14.

Interpolation source data for areas of bedrock-surface exposure of the Ironton-Galesville Unit were generated by selecting and exporting point-features located within these exposures from the previously developed high-resolution surface model of the top of the Upper Bedrock Unit. Similarly, interpolation source data for areas of absence of the Ironton-Galesville Unit were generated by selecting and exporting point-features located within these areas from the previously developed high-resolution surface model of the top of the Eau Claire Unit.

The inverse-distance algorithm (Table C-5) was employed for interpolation of the source data with breaklines included in a .bln file developed from the shapefile containing the five fault features discussed previously (Section C.1.1.3). The provisional high-resolution surface model of the top of the Ironton-Galesville Unit was then adjusted using the first-iteration high-resolution surface model of the top of the Silurian-Devonian Carbonate Unit and the high-resolution surface model of the top of the Eau Claire Unit as upper and lower constraints, respectively. The portion of the resulting high-resolution surface model of the top of the Ironton-Galesville Unit west of the Mississippi River was then erased to create the active-cell high-resolution surface model of the top of the Ironton-Galesville Unit.

C.1.5.8. Top of Potosi-Franconia Unit

Compilation of source data for development of the high-resolution surface model of the top of the Potosi-Franconia Unit presented several challenges owing to a lack of published and unpublished structure-contour maps of the horizon. Contours digitized from an unpublished structure-contour map of the top of the Potosi-Franconia Unit (USGS, Wisconsin District, personal communication, 2002) were employed in parts of Wisconsin, a portion of central Illinois, and areas west of the Mississippi River (Figure C-15). These contours were edited to correct stratigraphic violations of digitized structure contours of adjacent hydrostratigraphic units and for consistency with structure-contour maps of other units in the vicinity of mapped areas of absence. A published structure-contour map of the bottom of the Ancell Group (Visocky et al., 1985) was employed as source data in parts of Illinois where subcrop mapping of the Tiptecanoe Sequence (Willman et al., 1975) suggests that the Ancell rests on the Potosi-Franconia Unit. In other areas of the regional model domain, elevation data were synthesized using thickness data or were obtained from previously generated high-resolution surface models of other surfaces.

In parts of Illinois where the Potosi-Franconia Unit is not overlain by the Ancell Group and that were not covered by the unpublished USGS mapping with sufficient detail, elevation data were synthesized by effectively adding digitized isopach maps of the Franconia Formation and Potosi Dolomite (Willman et al., 1975) to available structure-contour mapping of the Ironton Sandstone. This technique is discussed in reference to the generation of interpolation source data for the high-resolution surface model of the base of the Mt. Simon Unit. For development of Potosi-Franconia interpolation source data in Illinois, however, the technique was applied twice. It was first applied to sum the thicknesses of the Franconia Formation and Potosi Dolomite at intersections of digitized isopachs of the two units. A hand-contoured isopach map of the combined interval, in the form of a polyline-shapefile, was then constructed based on the intersection points. The hand-contoured map of the summed thicknesses of the Franconia and

Potosi was then added to digitized structure-contour mapping of the top of the Ironton Sandstone from Visocky et al. (1985) and Emrich (1966). In much of northern Illinois, the thickness of the Potosi-Franconia Unit was added to a digitized version of the Ironton Sandstone structure-contour map of Visocky et al. (1985) that was augmented with additional contours, positioned using professional judgment in a high-priority area encompassing the model nearfield and the Plum River Fault and Sandwich Fault Zone. In a small part of central Illinois, the Potosi-Franconia thickness was added to a digitized version of the Ironton structure map of Emrich (1966). All of the intersection points estimated using Ironton structure data from Emrich (1966) and Visocky et al. (1985) and Franconia Formation and Potosi Dolomite thickness data from Willman et al. (1975) were then hand-contoured to honor the intersection points and the structure-contour map of the bottom of the Ancell Group mentioned in the preceding paragraph. A smaller contour-interval was employed in the high-priority area of northern Illinois where the Ironton structure map of Visocky et al. (1985) was augmented.

Contours digitized from the unpublished structure-contour map of the top of the Potosi-Franconia Unit (USGS, Wisconsin District, personal communication, 2002) were edited for consistency with the structure contours developed by the process discussed in the preceding paragraph.

Potosi-Franconia Unit elevation data for Michigan were synthesized by effectively adding a digitized isopach map Trempealeau Formation (Bricker et al., 1983) to a digitized structure-contour map of the top of the Franconia Formation (Bricker et al., 1983). The same technique of identification of intersections of isopachs and structure contours was employed for this addition process as discussed previously (page C-35). Although Bricker et al. (1983) published a structure-contour map of the top of the Trempealeau Formation in Michigan, this map was not employed because it includes numerous and severe stratigraphic violations of their structure-contour maps of other lithostratigraphic units. A hand-contoured structure-contour map of the top of the Potosi-Franconia Unit in Michigan was constructed, in the form of a polyline-shapefile, based on the intersection points and on structure-contour maps of the tops of the Franconia Formation and Prairie du Chien Group (Bricker et al., 1983).

It is acknowledged that the Trempealeau Formation of Michigan does not correlate directly to the Potosi Dolomite of Illinois. The Trempealeau Formation, rather, contains equivalents of both the Potosi Dolomite and the Eminence Formation of Illinois, units which cannot be distinguished in Michigan. Use of the Trempealeau Formation isopach map to define the top of the Potosi-Franconia Unit in Michigan thus has the consequence of the high-resolution surface model of the top of the Potosi-Franconia Unit being defined in Michigan by the equivalent of the Eminence Formation, a unit that is otherwise assigned to the Prairie du Chien-Eminence Unit. The resulting high-resolution surface model of the top of the Potosi-Franconia Unit does not uniformly depict the top of the Potosi Dolomite and equivalents, then. For purposes of groundwater flow modeling, this shortcoming of the geologic model is acceptable because the lithologies of the units above and below the problematic contact—equivalents of the Potosi Dolomite, Eminence Formation, and Prairie du Chien Group of Illinois—are all predominantly dolomite and are hydraulically similar.

Potosi-Franconia top-elevation data were also synthesized for the area of Indiana within the regional model domain. Thickness models of two lithostratigraphic units—the Davis Formation and the Potosi Dolomite—were added to the high-resolution surface model of the top of the Ironton-Galesville Unit to synthesize the Potosi-Franconia Unit top elevations in Indiana. The thickness models of the Davis Formation and Potosi Dolomite employed in this process

were both generated by interpolation, using a kriging algorithm (Table C-12)), of point data generated from digitized isopach maps of the Davis Formation (Rupp, 1991) and Potosi Dolomite (Droste and Patton, 1985). Cross validation statistics for the interpolation of Indiana Potosi and Davis thickness data are shown in Table C-10.

Like the Trempealeau Formation of Michigan, the Potosi Dolomite of Indiana does not correlate directly to the Potosi Dolomite of Illinois. Rather, the Potosi of Indiana contains equivalents of both the Potosi Dolomite and the Eminence Formation of Illinois, which cannot be distinguished in Indiana. Use of the Indiana Potosi Dolomite isopach map to define the top of the Potosi-Franconia Unit in Indiana thus has the consequence of the high-resolution surface model of the top of the Potosi-Franconia Unit being defined in Indiana by the equivalent of the Eminence Formation, a unit that is otherwise assigned to the Prairie du Chien-Eminence Unit. As mentioned previously in regard to use of the Trempealeau Formation isopach map in Michigan, for purposes of groundwater flow modeling, this shortcoming of the geologic model is acceptable because the lithologies of the units above and below the problematic contact—equivalents of the Potosi Dolomite, Eminence Formation, and Prairie du Chien Group of Illinois—are all predominantly dolomite and are hydraulically similar.

Interpolation source data for areas of bedrock-surface exposure of the Potosi-Franconia Unit were generated by selecting and exporting point-features located within these exposures from the previously developed high-resolution surface model of the top of the Upper Bedrock Unit. Similarly, interpolation source data for areas of absence of the Potosi-Franconia Unit were generated by selecting and exporting point-features located within these areas from the previously developed high-resolution surface model of the top of the Ironton-Galesville Unit.

Structure contours were estimated using professional judgment for the entire area of Lake Michigan within the regional model domain. The contours were constructed to depict a simple surface, with minimal added perturbations, that completely honors the Mt. Simon top-elevation data in surrounding areas as shown in Figure C-15.

The inverse-distance algorithm (Table C-5) was employed for interpolation of the source data with breaklines included in a .bln file developed from the shapefile containing the five fault features discussed previously (Section C.1.1.3). The provisional high-resolution surface model of the top of the Potosi-Franconia Unit was then adjusted using the first-iteration high-resolution surface model of the top of the Silurian-Devonian Carbonate Unit and the high-resolution surface model of the top of the Ironton-Galesville Unit as upper and lower constraints. The portion of the resulting high-resolution surface model of the top of the Potosi-Franconia Unit west of the Mississippi River was then erased to create the active-cell high-resolution surface model of the top of the Potosi-Franconia Unit.

Table C-11. Parameters of Kriging Algorithm Used for Interpolation of Ironton-Galesville Thickness Data Having Output Grid Coincident with Northern Indiana

<i>Gridding Method</i>	<i>Kriging</i>
Kriging Type	Point
Polynomial Drift Order	0
Kriging std. deviation grid	no
Output Grid	
Minimum x	3539000 ft
Maximum x	4269000 ft
Minimum y	2236000 ft
Maximum y	3203500 ft
x and y spacing	2500 ft
Semi-Variogram Model	
Component Type	Linear
Anisotropy Angle	0
Anisotropy Ratio	1
Variogram Slope	1
Search Parameters	
No Search (use all data)	

Table C-12. Parameters of Kriging Algorithm Used for Interpolation of Davis Formation, Potosi Dolomite, and Ancell Group Thickness Data Having Output Grid Coincident with Northern Indiana

<i>Gridding Method</i>	<i>Kriging</i>
Kriging Type	Point
Polynomial Drift Order	0
Kriging std. deviation grid	no
Output Grid	
Minimum x	3539000 ft
Maximum x	4269000 ft
Minimum y	2236000 ft
Maximum y	3203500 ft
x and y spacing	2500 ft
Semi-Variogram Model	
Component Type	Linear
Anisotropy Angle	0
Anisotropy Ratio	1
Variogram Slope	1
Search Parameters	
Search Ellipse Radius #1	1200000 ft
Search Ellipse Radius #2	1200000 ft
Search Ellipse Angle	0
Number of Search Sectors	8
Maximum Data Per Sector	8
Maximum Empty Sectors	6
Minimum Data	3
Maximum Data	64

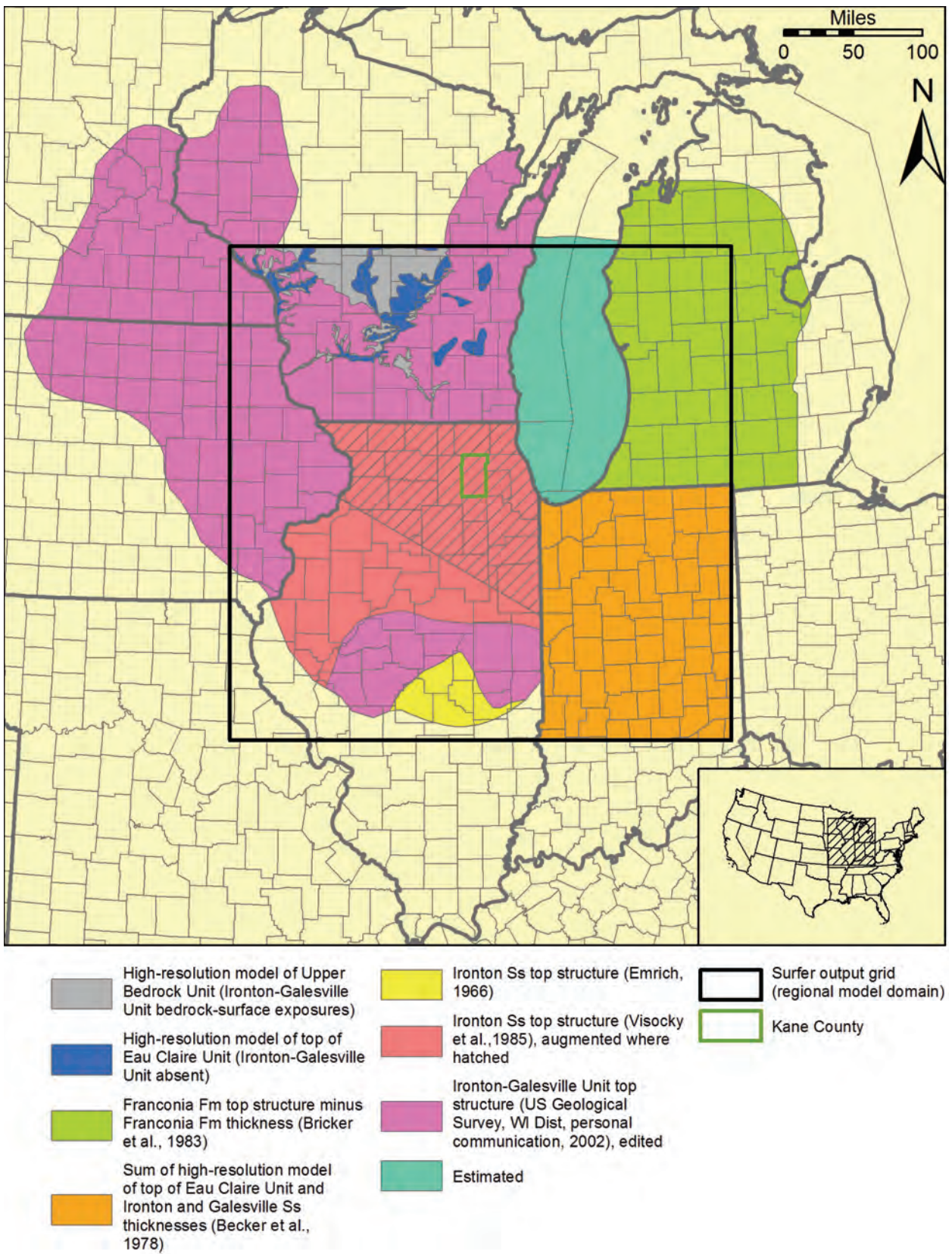
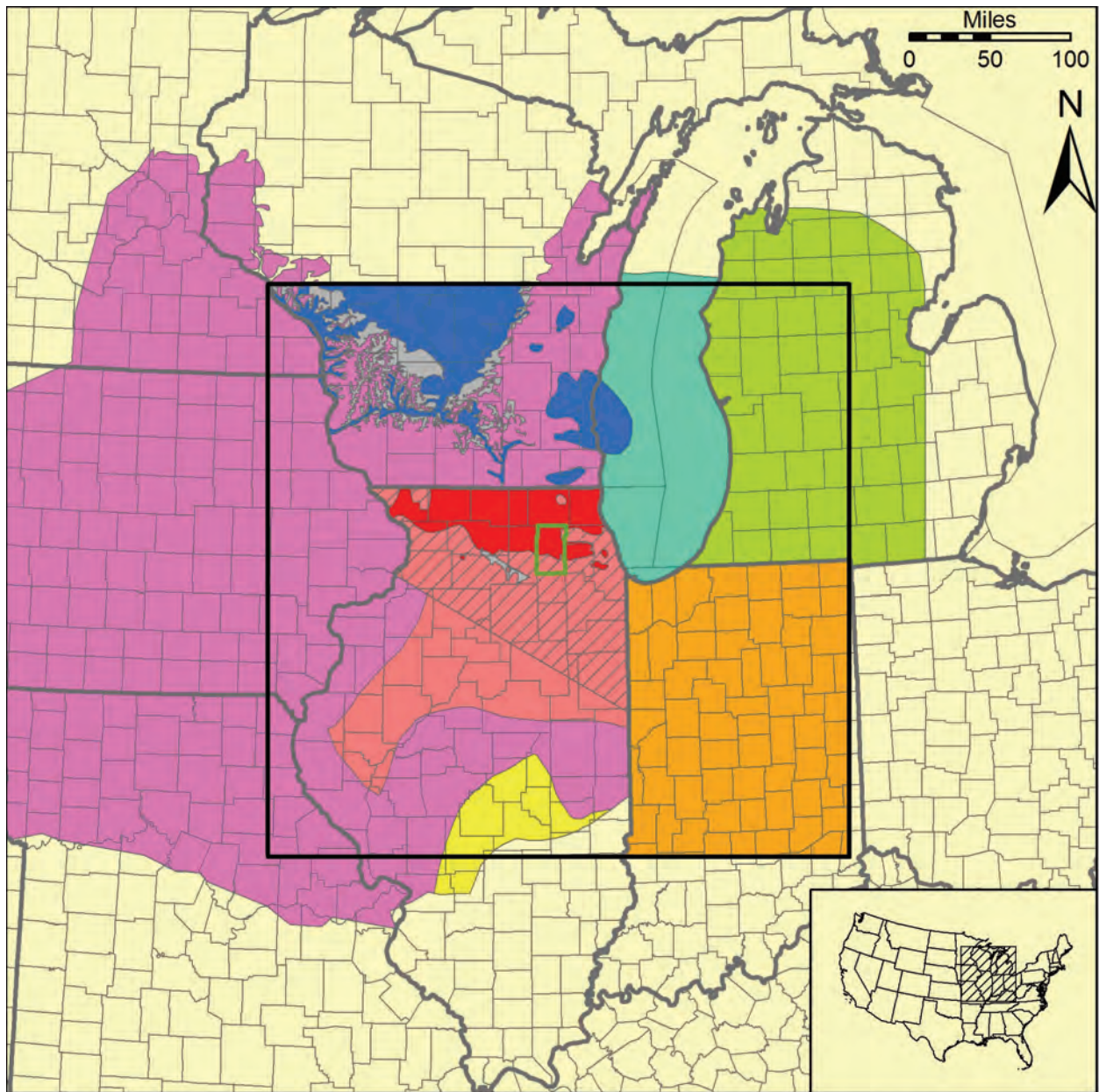


Figure C-14. Sources of data for high-resolution surface model of top of Ironton-Galesville Unit.



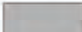




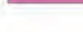





- | | | | | | |
|---|--|---|---|---|---|
|  | High-resolution model of Upper Bedrock Unit (Potosi-Franconia Unit bedrock-surface exposures) |  | Ancell Gp bottom structure (Visocky et al., 1985) |  | Potosi-Franconia Unit top structure (US Geological Survey, WI Dist, personal communication, 2002), edited |
|  | High-resolution model of top of Ironton-Galesville Unit (Potosi-Franconia Unit absent) |  | Ironton Ss top structure (Emrich, 1966) plus Franconia Fm and Potosi DI thicknesses (Willman et al., 1975) |  | Estimated |
|  | Franconia Fm top structure plus Trempealeau Fm thickness (Bricker et al., 1983) |  | Ironton Ss top structure plus Franconia Fm and Potosi DI thicknesses (Willman et al., 1975), smaller contour interval where hatched |  | Surfer output grid (regional model domain) |
|  | High-resolution model of top of Eau Claire Unit plus Davis Fm and Potosi DI thicknesses (Rupp, 1991) | | |  | Kane County |

Figure C-15. Sources of data for high-resolution surface model of top of Potosi-Franconia Unit.

C.1.5.9. Top of Prairie du Chien-Eminence Unit

Elevation data digitized from published and unpublished structure-contour mapping of the top of the Prairie du Chien Group and equivalent horizons were employed as source data for development of the high-resolution surface model of the top of the Prairie du Chien-Eminence Unit in most of the regional model domain (Figure C-16). Contours digitized as a polyline-shapefile from an unpublished structure-contour map of the top of the Prairie du Chien-Eminence Unit (USGS, Wisconsin District, personal communication, 2002) were employed in portions of Wisconsin, Illinois, and Lake Michigan as well as areas west of the Mississippi River. These contours were edited to correct stratigraphic violations of digitized structure contours of adjacent hydrostratigraphic units and for consistency with structure-contour maps of other units in the vicinity of mapped areas of absence. A published structure-contour map of the bottom of the Ansell Group (Visocky et al., 1985) was digitized as a polyline-shapefile for source data in parts of Illinois covered by the map where subcrop mapping of the Tippecanoe Sequence (Willman et al., 1975) suggests that the Ansell rests on the Prairie du Chien Group. Contours digitized from the unpublished USGS mapping showing Prairie du Chien structure in central Illinois were edited to adjust contour positions to those along the southern border of the northern Illinois area where the data of Visocky et al. (1985) were used. The Prairie du Chien structure-contour map of Bricker et al. (1983) was digitized as a polyline-shapefile for source data in the lower peninsula of Michigan and adjacent areas of the Great Lakes. Finally, the Prairie du Chien structure-contour map of Rupp (1991) was digitized as a polyline-shapefile for source data in Indiana.

Interpolation source data for areas of bedrock-surface exposure of the Prairie du Chien-Eminence Unit were generated by selecting and exporting point-features located within these exposures from the previously developed high-resolution surface model of the top of the Upper Bedrock Unit. Similarly, interpolation source data for areas of absence of the Prairie du Chien-Eminence Unit were generated by selecting and exporting point-features located within these areas from the previously developed high-resolution surface model of the top of the Potosi-Franconia Unit.

Structure contours were estimated using professional judgment for part of the area of Lake Michigan within the regional model domain. The contours were constructed to depict a simple surface, with minimal added perturbations, that completely honors the Mt. Simon top-elevation data in surrounding areas as shown in Figure C-16.

The inverse-distance algorithm (Table C-5) was employed for interpolation of the source data with breaklines included in a .bln file developed from the shapefile containing the five fault features discussed previously (Section C.1.1.3). The provisional high-resolution surface model of the top of the Prairie du Chien-Eminence Unit was then adjusted using the first-iteration high-resolution surface model of the top of the Silurian-Devonian Carbonate Unit and the high-resolution surface model of the top of the Potosi-Franconia Unit as upper and lower constraints, respectively. The portion of the resulting high-resolution surface model of the top of the Prairie du Chien-Eminence Unit west of the Mississippi River was then erased to create the active-cell high-resolution surface model of the top of the Prairie du Chien-Eminence Unit.

C.1.5.10. Top of Ancell Unit

Contours digitized from an unpublished structure-contour map of the top of the Ancell Unit (USGS, Wisconsin District, personal communication, 2002) were employed as interpolation source data for the high-resolution surface model of the Ancell Unit in parts of Wisconsin, a portion of central Illinois, and areas west of the Mississippi River (Figure C-17). These contours were edited to correct stratigraphic violations of digitized structure contours of adjacent hydrostratigraphic units and for consistency with structure-contour maps of other units in the vicinity of mapped areas of absence. The unpublished USGS mapping was not employed as source data in northern Illinois, where published structure-contour mapping of the top of the Ancell Group (Visocky et al., 1985) was used. Contours digitized from the unpublished USGS mapping showing Ancell Unit structure in central Illinois were edited to adjust contour positions to those along the southern border of the northern Illinois area where the data of Visocky et al. (1985) were used.

Interpolation source data for the lower peninsula of Michigan were synthesized by effectively adding the thicknesses of the St. Peter Sandstone and Glenwood Formation, digitized as polyline-shapefiles from maps by Bricker et al. (1983), to the elevation of the top of the Prairie du Chien Group, also digitized as a polyline shapefile from a map by Bricker et al. (1983). This technique is discussed in reference to the generation of interpolation source data for the high-resolution surface model of the base of the Mt. Simon Unit. For development of Ancell interpolation source data in Michigan, however, the technique was applied twice. It was first applied to sum the thicknesses of the Glenwood Formation and St. Peter Sandstone at intersections of digitized isopachs of the two units. A hand-contoured isopach map of the combined interval was then constructed, in the form of a polyline-shapefile, based on the intersection points. The hand-contoured isopach map of the summed thicknesses of the Glenwood Formation and St. Peter Sandstone was then added to the digitized structure-contour mapping of the top of the Prairie du Chien Group. The intersection points of the isopachs and structure contours, representing the estimated elevation of the top of the Ancell Group, were then used, together with the Prairie du Chien structure map (Bricker et al., 1983), as the basis for a hand-contoured structure-contour map of the top of the Ancell Group, in the form of a polyline-shapefile. This synthesized structure contour map of the top of the Ancell Group was employed for interpolation source data for the high-resolution surface model of the top of the Ancell Unit.

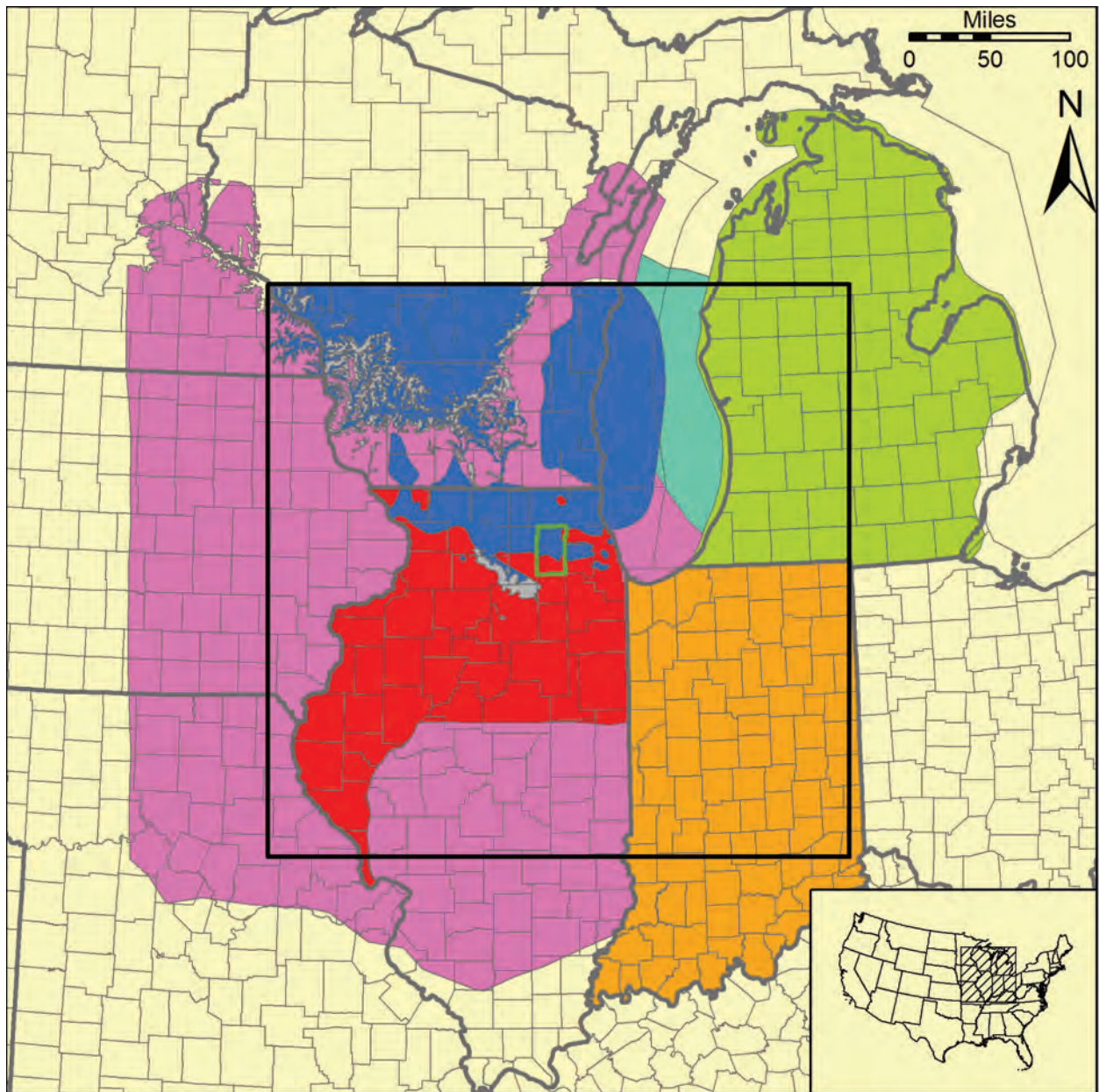
Ancell Unit top-elevation data were also synthesized for the area of Indiana within the regional model domain, where an Ancell Group structure-contour map is not available, using an approach based on summation of interpolated thickness data and the previously generated high-resolution surface model of the Prairie du Chien Eminence Unit. This technique is discussed in reference to the development of interpolation source data for high-resolution surface model of the top of the Eau Claire of Indiana. The thickness model of the Ancell Group employed in this process was generated by interpolation of point data generated from a digitized isopach map of the Ancell Group (Rupp, 1991). A kriging algorithm was employed for the interpolation (Table C-12). Cross validation statistics for the interpolation of Indiana Ancell Group thickness data are shown in Table C-10.

Interpolation source data for areas of bedrock-surface exposure of the Ancell Unit were generated by selecting and exporting point-features located within these exposures from the previously-developed high-resolution surface model of the top of the Upper Bedrock Unit. Similarly, interpolation source data for areas of absence of the Ancell Unit were generated by

selecting and exporting point-features located within these areas from the previously-developed high-resolution surface model of the base of the Prairie du Chien-Eminence Unit.

Structure contours were estimated using professional judgment for part of the area of Lake Michigan within the regional model domain. The contours were constructed to depict a simple surface, with minimal added perturbations, that completely honors the Ancell Unit top-elevation data in surrounding areas as shown in Figure C-17.

The inverse-distance algorithm (Table C-5) was employed for interpolation of the source data with breaklines included in a .bln file developed from the shapefile containing the five fault features discussed previously (Section C.1.1.3). The provisional high-resolution surface model of the top of the Ancell Unit was then adjusted using the first-iteration high-resolution surface model of the top of the Silurian-Devonian Carbonate Unit and the high-resolution surface model of the top of the Prairie du Chien-Eminence Unit as upper and lower constraints, respectively. The portion of the resulting high-resolution surface model of the top of the Ancell Unit west of the Mississippi River was then erased to create the active-cell high-resolution surface model of the top of the Prairie du Chien-Eminence Unit.












- | | | | | | |
|---|--|---|---|---|--|
|  | High-resolution model of Upper Bedrock Unit (Prairie du Chien-Eminence Unit bedrock-surface exposures) |  | Prairie du Chien Gp top structure (Rupp, 1991) |  | Surfer output grid (regional model domain) |
|  | High-resolution model of top of Potosi-Franconia Unit (Prairie du Chien-Eminence Unit absent) |  | Ancell Gp bottom structure (Visocky et al., 1985) |  | Kane County |
|  | Prairie du Chien Gp top structure (Bricker et al., 1983) |  | Prairie du Chien Gp top structure (US Geological Survey, WI Dist, personal communication, 2002), edited | | |
| | |  | Estimated | | |

Figure C-16. Sources of data for high-resolution surface model of top of Prairie du Chien-Eminence Unit.

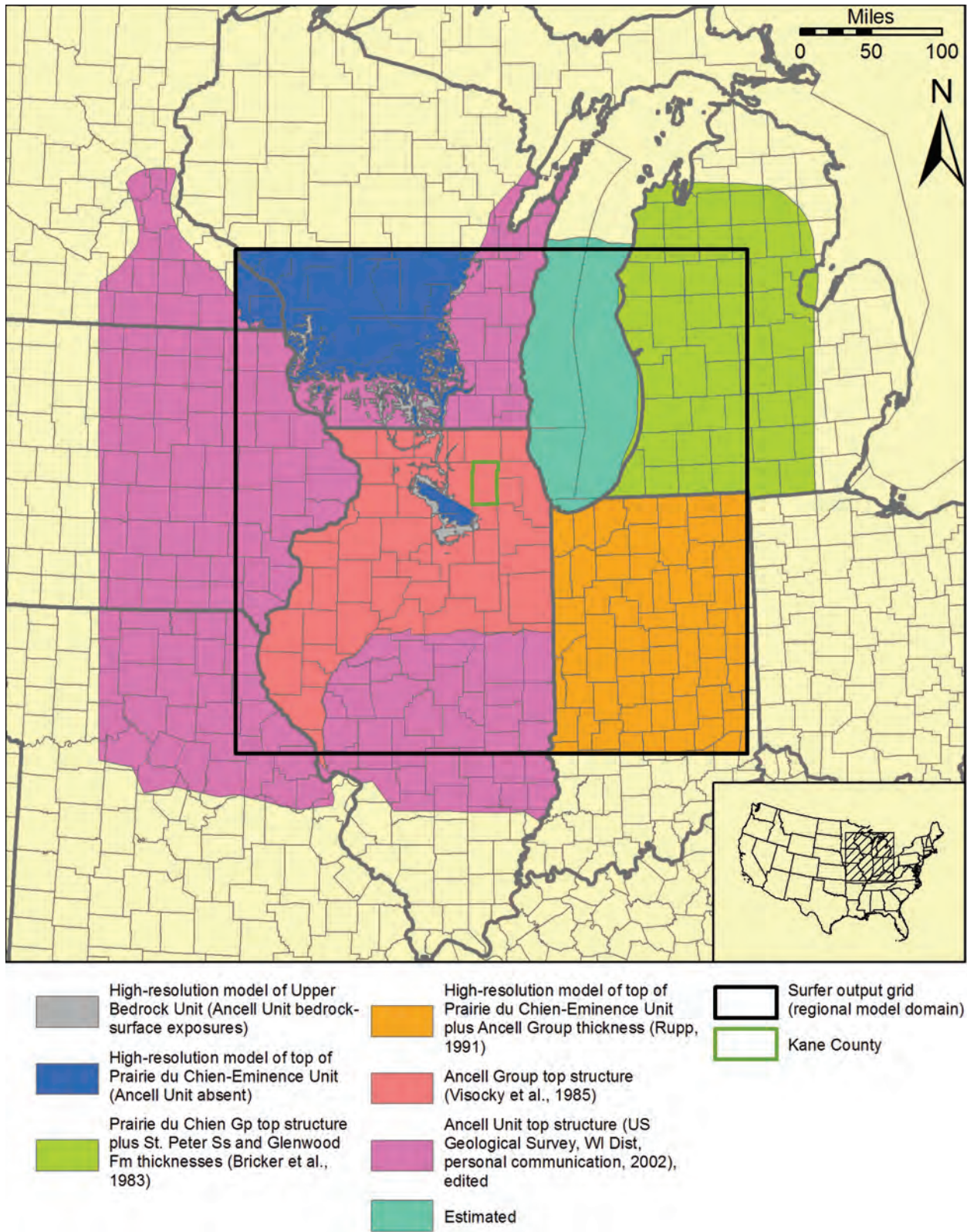


Figure C-17. Sources of data for high-resolution surface model of top of Ancell Unit.

C.1.5.11. Top of Galena-Platteville Unit

Elevation data digitized from published and unpublished structure-contour mapping of the top of the Galena Group and equivalent horizons were employed as source data for development of the high-resolution surface model of the top of the Galena-Platteville Unit in most of the regional model domain (Figure C-18). Contours digitized as a polyline-shapefile from an unpublished structure-contour map of the top of the Galena-Platteville Unit (USGS, Wisconsin District, personal communication, 2002) were employed in portions of Wisconsin, Illinois, and Lake Michigan as well as areas west of the Mississippi River. These contours were edited to correct stratigraphic violations of digitized structure contours of adjacent hydrostratigraphic units and for consistency with structure-contour maps of other units in the vicinity of mapped areas of absence. A published structure-contour map of the top of the Galena Group (Visocky et al., 1985) was digitized as a polyline-shapefile for source data in parts of Illinois covered by the map. Contours digitized from the unpublished USGS mapping showing Galena-Platteville structure in central Illinois were edited to adjust contour positions to those along the southern border of the northern Illinois area where the data of Visocky et al. (1985) were used. The Trenton Formation structure-contour map of Catacosinos et al. (1990) was digitized as a polyline-shapefile for interpolation source data in the lower peninsula of Michigan. Finally, the Trenton Group structure-contour map of Rupp (1991) was digitized as a polyline-shapefile for source data in Indiana.

Interpolation source data for areas of bedrock-surface exposure of the Galena-Platteville Unit were generated by selecting and exporting point-features located within these exposures from the previously-developed high-resolution surface model of the top of the Upper Bedrock Unit. Similarly, interpolation source data for areas of absence of the Galena-Platteville Unit were generated by selecting and exporting point-features located within these areas from the previously-developed high-resolution surface model of the top of the Ansell Unit.

Structure contours were estimated using professional judgment for part of the area of Lake Michigan within the regional model domain. The contours were constructed to depict a simple surface, with minimal added perturbations, that completely honors the Galena-Platteville Unit top-elevation data in surrounding areas as shown in Figure C-18.

The inverse-distance algorithm (Table C-5) was employed for interpolation of the source data with breaklines included in a .bln file developed from the shapefile containing the five fault features discussed previously (Section C.1.1.3). The provisional high-resolution surface model of the top of the Galena-Platteville Unit was then adjusted using the first-iteration high-resolution surface model of the top of the Silurian-Devonian Carbonate Unit and the high-resolution surface model of the top of the Ansell Unit as upper and lower constraints, respectively. The portion of the resulting high-resolution surface model of the top of the Galena-Platteville Unit west of the Mississippi River was then erased to create the active-cell high-resolution surface model of the top of the Galena-Platteville Unit.

C.1.5.12. Top of Maquoketa Unit

Elevation data digitized from published and unpublished structure-contour mapping of the top of the Maquoketa Group were employed as source data for development of the high-resolution surface model of the top of the Maquoketa Unit in much of the regional model domain (Figure C-19). Contours digitized as a polyline-shapefile from an unpublished structure-contour map of the top of the Maquoketa Unit (USGS, Wisconsin District, personal communication,

2002) were employed in portions of Wisconsin and Illinois as well as areas west of the Mississippi River.

These contours were edited to correct stratigraphic violations of digitized structure contours of adjacent hydrostratigraphic units and for consistency with structure-contour maps of other units in the vicinity of mapped areas of absence. A published structure-contour map of the top of the Maquoketa Group (Visocky et al., 1985) was digitized as a polyline-shapefile for source data in parts of Illinois covered by the map. Contours digitized from the unpublished USGS mapping showing Maquoketa structure in central Illinois were edited to adjust contour positions to those along the southern border of the northern Illinois area where the data of Visocky et al. (1985) were used. A Maquoketa Group structure-contour map by Rupp (1991) was digitized as a polyline-shapefile for source data in Indiana.

Maquoketa Unit top-elevation data were synthesized for the area of Michigan within the regional model domain, where a Maquoketa Group structure-contour map is not available, using an approach based on summation of interpolated thickness data and the previously generated high-resolution surface model of the Galena-Platteville Unit. This technique is discussed in reference to the development of interpolation source data for high-resolution surface model of the top of the Eau Claire of Indiana. The thickness model of the Maquoketa Group employed in this process was generated by interpolation of point data generated from a digitized isopach map of the Utica Shale (a Maquoketa Group equivalent) (Western Michigan University Department of Geology, 1981). A kriging algorithm, with a rectangular output grid covering southwestern Michigan and adjacent Lake Michigan, was employed for the interpolation (Table C-13). Cross validation statistics for the interpolation of Michigan Utica Shale thickness data are shown in Table C-10. Synthesized Maquoketa Unit elevation data for the Lake Michigan portion of the output grid—an area not covered by the Utica Shale thickness map by the Western Michigan University Department of Geology (1981) and therefore of dubious accuracy—were erased and not used as interpolation source data.

Interpolation source data for a portion of the regional model domain in central Illinois were also synthesized using the technique described on page C-42 by summing the high-resolution surface model of the Galena-Platteville Unit with a model of the thickness of the Maquoketa Group based on a polyline shapefile of the thickness of the Maquoketa Group digitized from isopach mapping by Willman et al. (1975). This part of central Illinois is not covered by the published or unpublished structure-contour mapping discussed previously. A kriging algorithm, with a rectangular output grid enclosing the part of central Illinois lacking Maquoketa elevation data, was employed for the interpolation (Table C-14). Cross validation statistics for the interpolation of central Illinois Maquoketa Group thickness data are shown in Table C-10. Synthesized Maquoketa Unit elevation data generated through this process for areas covered by the unpublished USGS Maquoketa Group structure-contour mapping were erased and not used as interpolation source data.

Interpolation source data for areas of bedrock-surface exposure of the Maquoketa Unit were generated by selecting and exporting point-features located within these exposures from the previously-developed high-resolution surface model of the top of the Upper Bedrock Unit. Similarly, interpolation source data for areas of absence of the Maquoketa Unit were generated by selecting and exporting point-features located within these areas from the previously developed high-resolution surface model of the top of the Galena-Platteville Unit.

Structure contours were estimated using professional judgment for part of the area of Lake Michigan within the regional model domain. The contours were constructed to depict a

simple surface, with minimal added perturbations, that completely honors the Maquoketa Unit top-elevation data in surrounding areas as shown in Figure C-19.

The inverse-distance algorithm (Table C-5) was employed for interpolation of the source data with breaklines included in a .bln file developed from the shapefile containing the five fault features discussed previously (Section C.1.1.3). The provisional high-resolution surface model of the top of the Maquoketa Unit was then adjusted using the first-iteration high-resolution surface model of the top of the Silurian-Devonian Carbonate Unit and the high-resolution surface model of the top of the Galena-Platteville Unit as upper and lower constraints, respectively. The portion of the resulting high-resolution surface model of the top of the Maquoketa Unit west of the Mississippi River was then erased to create the active-cell high-resolution surface model of the top of the Maquoketa Unit.

C.1.5.13. Top of Silurian-Devonian Carbonate Unit (Second Iteration)

The second-iteration model of the top of the Silurian-Devonian Carbonate Unit was developed from largely the same interpolation source data as the first-iteration model (page C-40) with two differences (Figure C-20). First, source data for areas of absence of the Silurian-Devonian Carbonate Unit were generated by selecting and exporting point-features within these areas from the previously developed high-resolution surface model of the top of the Maquoketa Unit, not the top of the Mt. Simon Unit as used for the first-iteration model. Second, interpolation source data derived from the unpublished structure-contour map of the top of the Silurian-Devonian Carbonate Unit (USGS, Wisconsin District, personal communication, 2002) and from the structure-contour map of the top of Muscatatuck Group in Indiana (Rupp, 1991) were trimmed to reduce file sizes and interpolation time. The reduction in input data was found to have no significant impact on the accuracy of the interpolation results.

The inverse-distance algorithm (Table C-5) was employed for interpolation of the source data with breaklines included in a .bln file developed from the shapefile containing the five fault features discussed previously (Section C.1.1.3). The provisional second-iteration high-resolution surface model of the top of the Silurian-Devonian Carbonate Unit was then adjusted using the high-resolution surface model of the top of the Upper Bedrock Unit and the high-resolution surface model of the top of the Maquoketa Unit as upper and lower constraints, respectively. The portion of the resulting second-iteration high-resolution surface model of the top of the Silurian-Devonian Carbonate Unit west of the Mississippi River was then erased to create the active-cell second-iteration high-resolution surface model of the top of the Silurian-Devonian Carbonate Unit.

Table C-13. Parameters of Kriging Algorithm Used for Interpolation of Utica Shale Thickness Data Having Output Grid Coincident with Southwestern Michigan Part of Regional Model Domain

<i>Gridding Method</i>	<i>Kriging</i>
Kriging Type	Point
Polynomial Drift Order	0
Kriging std. deviation grid	no
Output Grid	
Minimum x	3724000 ft
Maximum x	4269000 ft
Minimum y	3186000 ft
Maximum y	4116000 ft
x and y spacing	2500 ft
Semi-Variogram Model	
Component Type	Linear
Anisotropy Angle	0
Anisotropy Ratio	1
Variogram Slope	1
Search Parameters	
Search Ellipse Radius #1	1200000 ft
Search Ellipse Radius #2	1200000 ft
Search Ellipse Angle	0
Number of Search Sectors	8
Maximum Data Per Sector	8
Maximum Empty Sectors	6
Minimum Data	3
Maximum Data	64

Table C-14. Parameters of Kriging Algorithm Used for Interpolation of Utica Shale Thickness Data Having Output Grid Coincident with Part of the Regional Model Domain in Central Illinois

<i>Gridding Method</i>	<i>Kriging</i>
Kriging Type	Point
Polynomial Drift Order	0
Kriging std. deviation grid	no
Output Grid	
Minimum x	2579000 ft
Maximum x	3551500 ft
Minimum y	1831000 ft
Maximum y	3106000 ft
x and y spacing	2500 ft
Semi-Variogram Model	
Component Type	Linear
Anisotropy Angle	0
Anisotropy Ratio	1
Variogram Slope	1
Search Parameters	
Search Ellipse Radius #1	1700000 ft
Search Ellipse Radius #2	1700000 ft
Search Ellipse Angle	0
Number of Search Sectors	8
Maximum Data Per Sector	8
Maximum Empty Sectors	6
Minimum Data	3
Maximum Data	64

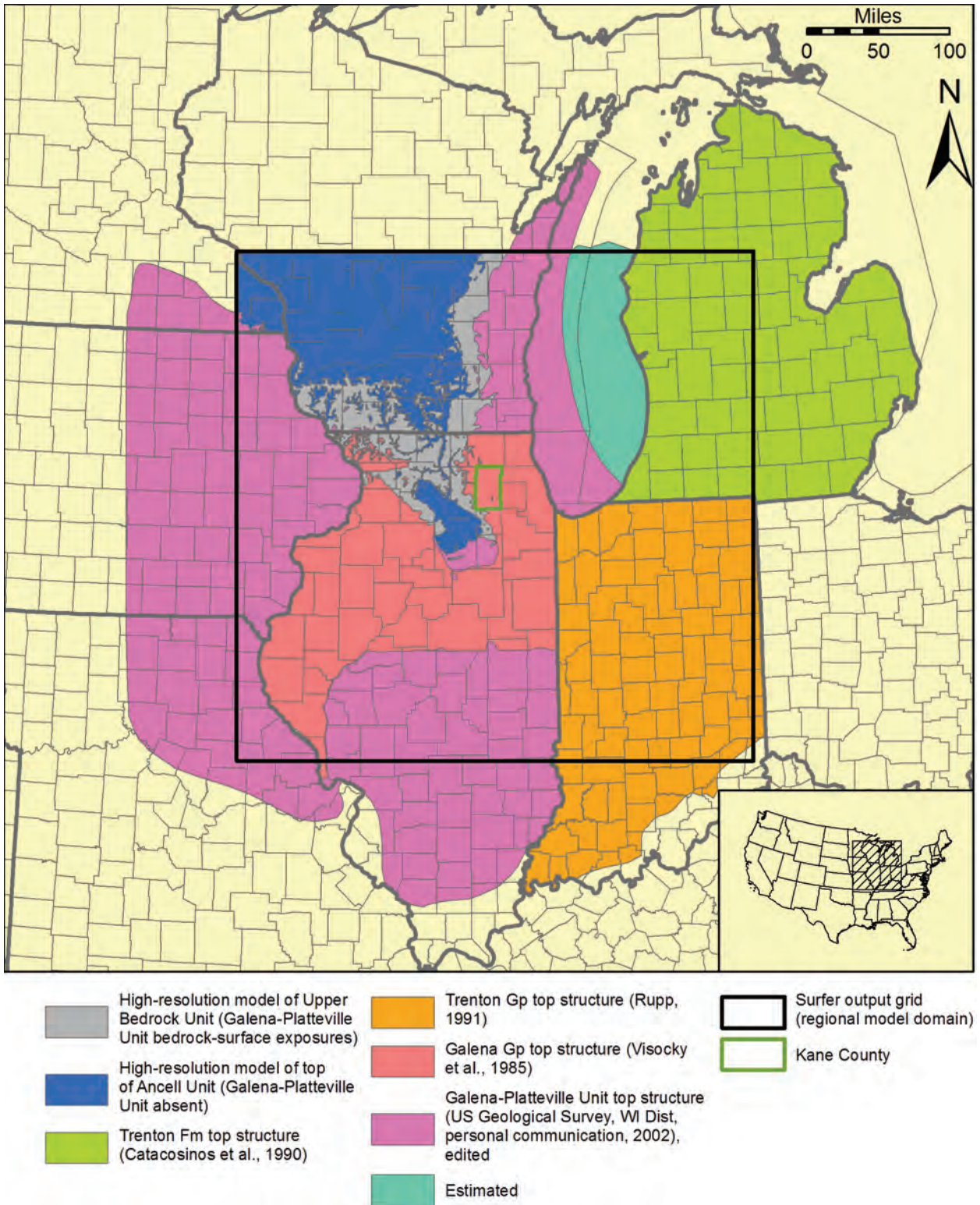
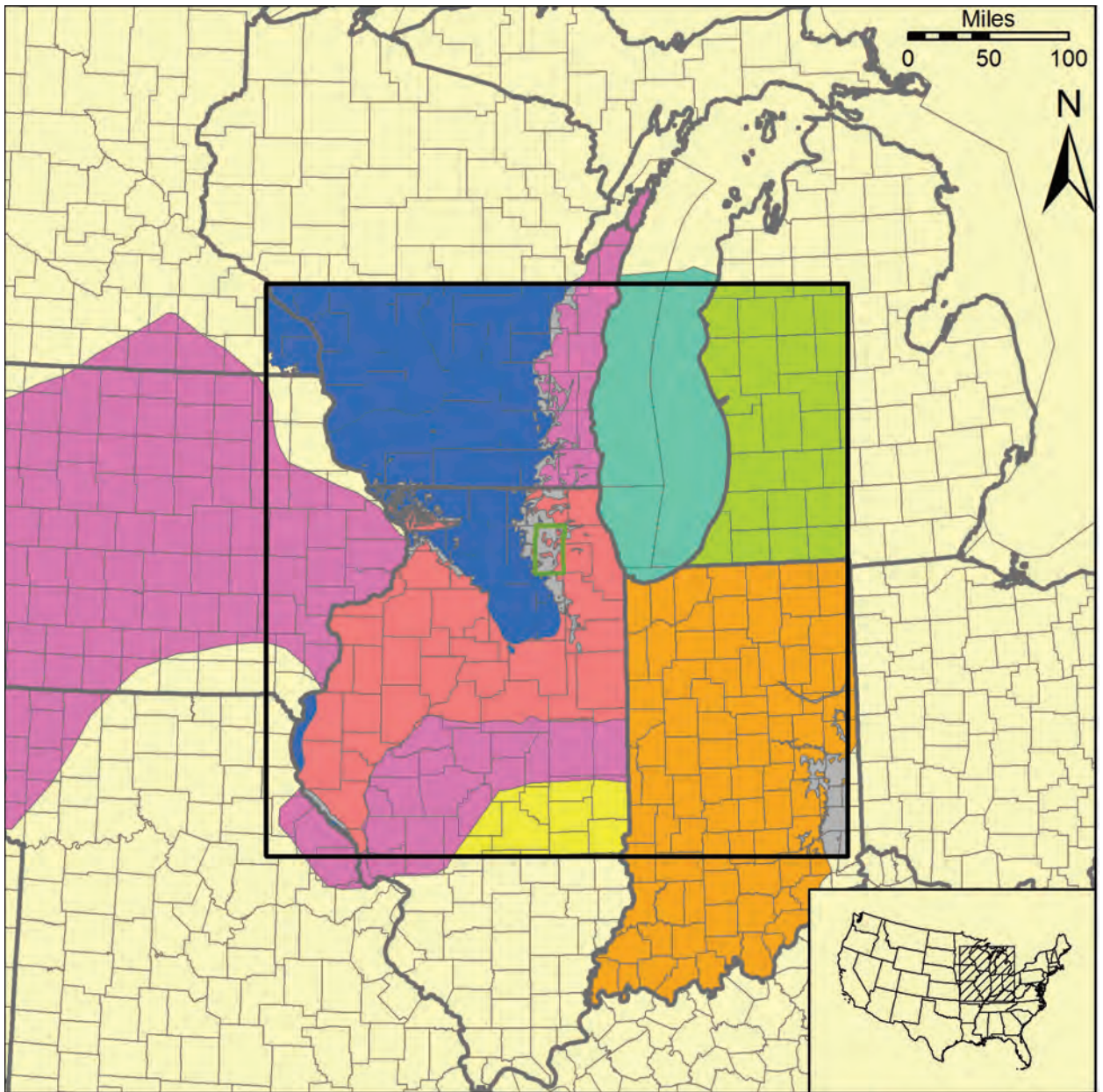


Figure C-18. Sources of data for high-resolution surface model of top of Galena-Platteville Unit.










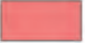


- | | | | | | |
|---|--|---|--|---|--|
|  | High-resolution model of Upper Bedrock Unit (Maquoketa Unit bedrock-surface exposures) |  | Maquoketa Gp top structure (Rupp, 1991) |  | Estimated |
|  | High-resolution model of top of Galena-Platteville Unit (Maquoketa Unit absent) |  | High-resolution model of top of Galena-Platteville Unit plus Maquoketa Gp thickness (Willman et al., 1975) |  | Surfer output grid (regional model domain) |
|  | High-resolution model of top of Galena-Platteville Unit plus Utica Shale thickness (Western Michigan University Department of Geology, 1981) |  | Maquoketa Gp top structure (Visocky et al., 1985) |  | Kane County |
|  | Maquoketa Unit top structure (US Geological Survey, WI Dist, personal communication, 2002), edited | | | | |

Figure C-19. Sources of data for high-resolution surface model of top of Maquoketa Unit.

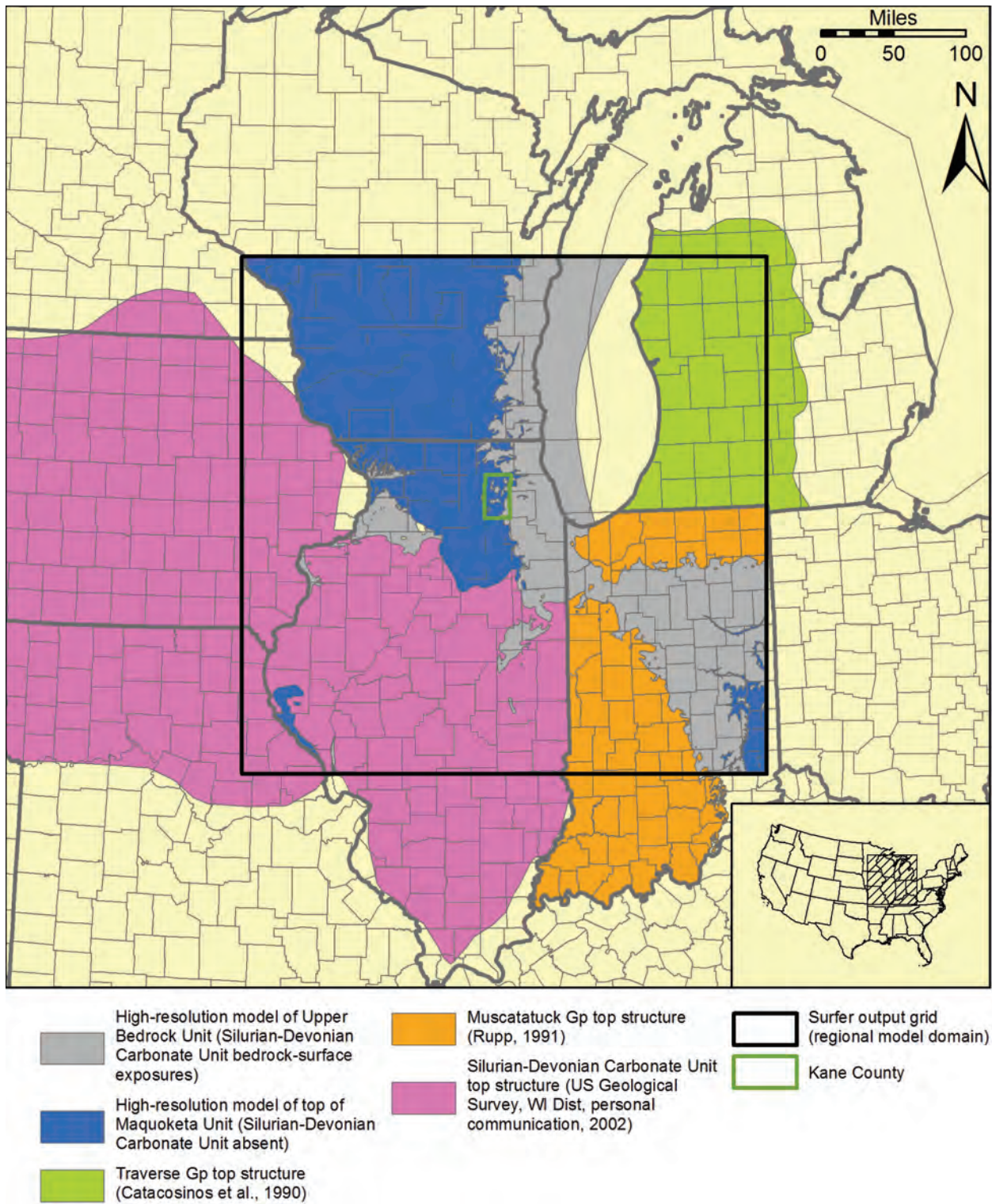


Figure C-20. Sources of data for second-iteration high-resolution surface model of top of Silurian-Devonian Carbonate Unit.

C.2. Irregular-Grid Geologic Model

An *irregular-grid geologic model* was developed from the completed high-resolution geologic model. The irregular-grid geologic model is a set of 12 *irregular-grid surface models*, each of which consists of estimates, for each active cell in the irregular finite-difference groundwater flow modeling grid, of the elevation of the top or bottom of a hydrostratigraphic unit. The 12 modeled surfaces are the tops of each of the 11 hydrostratigraphic units together with the bottom of the Mt. Simon Unit. Each irregular-grid surface model is adjusted to provide a minimum thickness of each hydrostratigraphic unit in areas of absence of the unit. These minimum thicknesses reflect the number of model layers devoted to each hydrostratigraphic unit and a 1-foot minimum thickness for each layer (Figure C-21). For example, since three model layers are devoted to the Silurian-Devonian Carbonate Unit, the minimum thickness of the Silurian-Devonian Carbonate Unit, based on a 1-foot thickness for each model layer, is 3 ft. The minimum thickness of most hydrostratigraphic units is 1 foot, since most hydrostratigraphic units are represented by only a single model layer.

Development of the irregular grid geologic model was begun using the *spatial join* utility of ArcGIS to join a polygon-shapefile of modeling grid with the active-cell high-resolution model of the top of each unit. This utility joins the attributes of two GIS layers based on the location of the features in the layers and was employed to develop a *provisional irregular-grid surface model* from each of the active-cell high-resolution surface models. The spatial-join process calculates the average elevation of the top of the unit, using elevations from the active-cell high-resolution surface model of the unit as input for each active cell in the model grid (Figure C-22). Since the active-cell high-resolution surface model includes estimated elevations at grid nodes spaced 2500 ft apart, the precise grid-cell dimensions in the model nearfield, the calculated average elevation in the model nearfield is based on a single elevation estimate. Average values calculated for larger grid cells in the model farfield are based on as many as 1024 values from the high-resolution surface model. Input data for the spatial join process was restricted to the *active-cell* high-resolution surface model to omit estimated elevations from the trans-Mississippi area, where the high-resolution model is less accurate.

The output of the spatial join process is a new polygon-shapefile with the same polygons as the modeling grid shapefile. This shapefile is referred to in this report as a *provisional irregular-grid surface model*. The attribute table of the new shapefile contains the calculated average elevation of the top of the hydrostratigraphic unit. The spatial join process was carried out 12 times to develop a provisional irregular-grid surface model of the top of each hydrostratigraphic unit as well as one of the bottom of the Mt. Simon Unit.

The average elevation of the top of each of the horizons covered by the 12 provisional irregular-grid surface models was indexed with a unique integer assigned to each cell of the modeling grid. This index was used to combine the 12 provisional irregular-grid surface models into a single Microsoft Excel (Microsoft Corporation, 2003) spreadsheet for manipulation of the average elevation data to accommodate the required minimum thickness of 1 foot per model layer. The spreadsheet contained a row for each grid cell, identified by the index value, and the average elevation of each of the 12 horizons from the provisional irregular-grid surface models of the horizons. From the elevation data, thicknesses of each of the 11 hydrostratigraphic units were calculated. Then, starting with the Quaternary Unit and working downward through the stratigraphic succession, the calculated thickness, based on the provisional irregular-grid surface modeling, was compared with the minimum thickness required to represent the unit in the regional groundwater flow model (Figure C-21). If the provisional thickness of the unit was less

than the required thickness, the bottom elevation of the unit (which is, in turn, the top elevation of the underlying unit) was recalculated as the top elevation minus the required thickness, shifting its position slightly downward. The spreadsheet rows highlighted in yellow in Figure C-23 illustrate this adjustment for a set of 20 grid cells. For cells where the provisional thickness of the Quaternary Unit was less than 3 ft, the top elevation of the Upper Bedrock Unit was recalculated as the top elevation of the Quaternary Unit minus 3 ft (1 ft for each of the three model layers representing the Quaternary Unit). Adjustment of the each unit made use of the top elevation recalculated in the adjustment of the immediately overlying unit. Thus, following on the example above, the elevation of the top of the Silurian-Devonian Carbonate Unit was recalculated as the top elevation of the Upper Bedrock Unit (after adjusting for a 3 ft minimum thickness of the Quaternary Unit) minus 1 ft.

With the completion of the adjustment, each provisional irregular-grid surface model was converted to the (final) irregular-grid surface model of the unit. Note that the provisional irregular-grid surface model of the top of the Quaternary Unit was unchanged, but all other provisional irregular-grid surface models were subject to adjustment. The set of adjusted elevations defining the geometry of the 11 hydrostratigraphic units is referred to as the irregular-grid geologic model.

C.3. Irregular-Grid Geologic Model to Geologic Framework of Regional Groundwater Flow Model

Conversion of the irregular-grid geologic model to the geologic framework of the regional model required that top elevations of individual model layers be calculated for each hydrostratigraphic unit modeled as two or more layers. For example, elevations of the top of model layers 5, 6, and 7, which represent the Silurian-Devonian Carbonate Unit, had to be calculated from the elevations of the tops of the Silurian-Devonian Carbonate Unit and the Maquoketa Unit included in the irregular-grid geologic model (Figure C-21). This arithmetic manipulation of the irregular-grid geologic model was carried out in Microsoft Excel for each hydrostratigraphic unit and each cell of the irregular model.

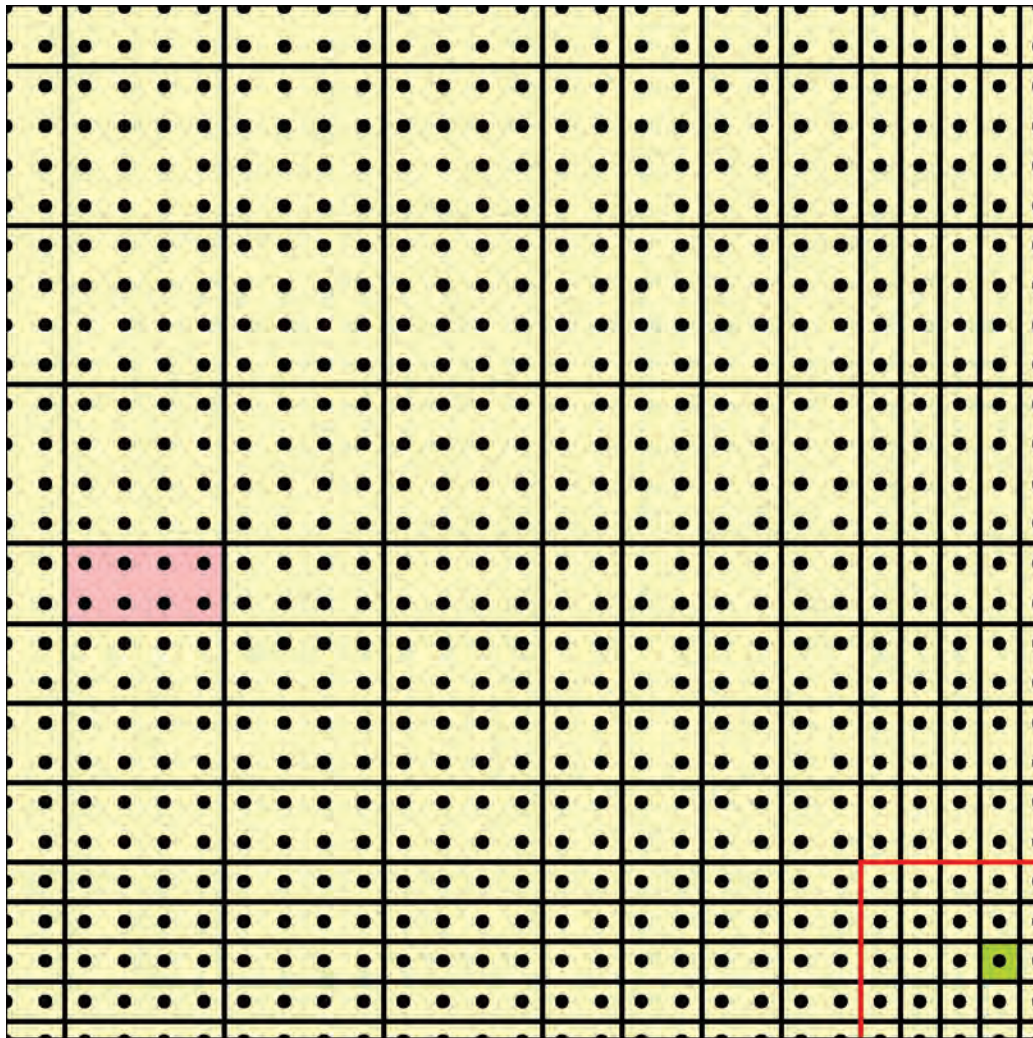
For hydrostratigraphic units represented by two or more model layers, the thickness of each individual model layer representing the unit was calculated for each cell by dividing the total thickness of the hydrostratigraphic unit, as represented in the irregular-grid geologic model, by the number of model layers devoted to the hydrostratigraphic unit (Figure C-21). Each of the model layers representing the hydrostratigraphic unit was thereby assigned an equal thickness. Thus the thickness of the three model layers representing the Silurian-Devonian Carbonate Unit in a cell was calculated as the difference in elevation between the tops of the Silurian-Devonian Carbonate Unit and the Maquoketa Unit divided by three. This layer thickness value was then employed to calculate the elevation of the tops of the model layers representing the hydrostratigraphic unit. Following on the example already begun, the elevation of the top of the model layer 6—the middle of three layers representing the Silurian-Devonian Carbonate Unit—was calculated by subtracting the layer thickness from the elevation of the top of the Silurian-Devonian Carbonate Unit. The elevation of layer 7 was calculated by multiplying the model layer thickness by 2 and subtracting the product from the elevation of the top of the Silurian-Devonian Carbonate Unit. The elevation of the top of model layer 5 is equivalent to the elevation of the top of the Silurian-Devonian Carbonate Unit.

After top elevations were assigned to all 20 layers in the regional model, the elevation data, indexed by grid cell, were exported from Microsoft Excel in text format and then imported

into Groundwater Vistas (Environmental Simulations Inc., 2005) as the geologic framework of the regional model.

HYDROSTRATIGRAPHIC UNIT	MODEL LAYER
Quaternary Unit (QT)	1
	2
	3
Upper Bedrock Unit (UB)	4
Silurian-Devonian Carbonate Unit (SD)	5
	6
	7
Maquoketa Unit (MQ)	8
	9
Galena-Platteville Unit (GP)	10
	11
Ancell Unit (AN)	12
Prairie du Chien-Eminence Unit (PE)	13
Potosi-Franconia Unit (PF)	14
Ironton-Galesville Unit (IG)	15
Eau Claire Unit (EC)	16
Mt Simon Unit (MS)	17
	18
	19
	20

Figure C-21. Relationship of hydrostratigraphic units to model layers.







- Data point, high-resolution surface model
- 
 Finite difference cell, model nearfield: provisional irregular-grid average from spatial join based on one value from high-resolution surface model
- 
 Finite difference cell, model farfield: provisional irregular-grid average from spatial join based on eight values from high-resolution surface model
- 
 Regional model nearfield
- 
 Finite-difference cell

Figure C-22. Calculation of average values for finite-difference cells through spatial-join process.

Microsoft Excel - irreg_mod_corr_for_min_m.xls

Types a question for help: [?]

	A	B	C	D	E	F	G
	INDEX	ELEV_QUATERNARY_NOT_ADJUSTED	ELEV_UPPER_BEDROCK_NOT_ADJUSTED	THK_QUATERNARY_NOT_ADJUSTED	ELEV_QUATERNARY_ADJUSTED	ELEV_UPPER_BEDROCK_ADJUSTED	THK_QUATERNARY_ADJUSTED
2	9721	405.1204781	395.3222029	395.3222029	405.1204781	395.3222029	9.79827523
3	9722	397.9242902	389.5717109	389.5717109	397.9242902	389.5717109	8.35257929
4	9723	389.5624298	383.7129609	383.7129609	389.5624298	383.7129609	5.84046895
5	9724	380.7889519	377.6730159	377.6730159	380.7889519	377.6730159	3.11593599
6	9725	389.9065197	388.5519986	1.3545231	389.9065197	386.9065197	3
7	9726	349.7244907	349.7244907	0	349.7244907	346.7244907	3
8	9727	339.3193865	339.3193865	0	339.3193865	336.3193865	3
9	9728	333.6243769	331.4404289	2.18394805	333.6243769	330.6243769	3
10	9729	326.9569474	313.2083291	13.74861828	326.9569474	313.2083291	13.74861828
11	9730	318.9687135	290.056745	28.91196851	318.9687135	290.056745	28.91196851
12	9731	308.4153324	269.2098221	39.20551032	308.4153324	269.2098221	39.20551032
13	9732	294.7988669	245.2019751	49.59691174	294.7988669	245.2019751	49.59691174
14	9733	279.8427484	225.0049898	54.83775854	279.8427484	225.0049898	54.83775854
15	9734	271.8402467	214.3482231	57.49202354	271.8402467	214.3482231	57.49202354
16	9735	263.4599315	209.1371537	54.32277783	263.4599315	209.1371537	54.32277783
17	9736	239.3924503	205.7915945	33.60085586	239.3924503	205.7915945	33.60085586
18	9737	271.9575099	224.3031895	47.65432039	271.9575099	224.3031895	47.65432039
19	9738	413.6384667	298.4361583	115.2023084	413.6384667	298.4361583	115.2023084
20	9739	559.0020744	416.8644858	142.1375886	559.0020744	416.8644858	142.1375886
21	9740	685.3879813	452.7327493	232.655232	685.3879813	452.7327493	232.655232
22							
23							
24							
25							
26							
27							
28							
29							
30							
31							
32							
33							
34							
35							
36							
37							
38							
39							
40							
41							
42							
43							
44							
45							
46							
47							

Sheet1 / backup / Sheet3 /

Ready

Figure C-23. Example of correction of provisional irregular-grid model to accommodate required minimum model layer thickness of 1 foot per model layer.

C.4. References

Becker, L.E., A.J. Hreha and T.A. Dawson. 1978. *Pre-Knox (Cambrian) Stratigraphy in Indiana*. Indiana Department of Natural Resources Geological Survey 57, Bloomington, IN.

Bricker, D.M., R.L. Milstein and J. C.R. Reszka. 1983. *Selected Studies of Cambro-Ordovician Sediments within the Michigan Basin*. Michigan Department of Natural Resources Geological Survey Division Report of Investigation 26, Lansing, MI.

Buschbach, T.C. 1964. *Cambrian and Ordovician Strata of Northeastern Illinois*. Illinois State Geological Survey Report of Investigation 218, Urbana, IL.

Cannon, W.F., T.H. Kress, D.M. Sutphin, G.B. Morey, J. Meints and R.D. Barber-Delach. 1997. Digital Geologic Map and Mineral Deposits of Minnesota, Wisconsin, and Michigan (Version 3.0) (Downloadable GIS Data). *United States Geological Survey*, <http://pubs.usgs.gov/of/1997/of97-455/> (accessed April 4, 2006).

Catacosinos, P.A. and P.A. Daniels, Jr. 1991. Stratigraphy of Middle Proterozoic to Middle Ordovician formations of the Michigan basin. In *Early sedimentary evolution of the Michigan basin*, 53-71. Edited by P.A. Catacosinos and P.A. Daniels. Geological Society of America Special Paper 256. Geological Society of America, Boulder, CO.

Catacosinos, P.A., P.A. Daniels, Jr. and W.B. Harrison, III. 1990. Structure, Stratigraphy, and Petroleum Geology of the Michigan Basin. In *Interior Cratonic Basins*, 561-601. Edited by M.W. Leighton, D.R. Kolata, D.F. Oltz and J.J. Eidel. American Association of Petroleum Geologists Memoir 51. American Association of Petroleum Geologists, Tulsa, OK.

Droste, J.B. and J.B. Patton. 1985. *Lithostratigraphy of the Sauk Sequence in Indiana*. Indiana Department of Natural Resources Geological Survey Occasional Paper 47, Bloomington, IN.

Droste, J.B. and R.H. Shaver. 1983. *Atlas of Early and Middle Paleozoic Paleogeography of the Southern Great Lakes Area*. Indiana Department of Natural Resources Geological Survey 32, Bloomington, IN.

Emrich, G.H. 1966. *Ironton and Galesville (Cambrian) Sandstones in Illinois and Adjacent Areas*. Illinois State Geological Survey Circular 403, Urbana, IL.

Environmental Simulations Inc. 2005. Groundwater Vistas Version 4.19.

Environmental Systems Research Institute. 2005. ArcGIS - Version 9.1.

Feinstein, D.T., T.T. Eaton, D.J. Hart, J.T. Krohelski and K.R. Bradbury. 2003. *Regional aquifer model for southeastern Wisconsin; Report 1: Data collection, conceptual model development, numerical model construction, and model calibration*. Wisconsin Geological and Natural History Survey administrative report prepared for Southeastern Wisconsin Regional Planning Commission.

Golden Software Inc. 2002. Surfer - Version 8.

Gray, H.H., C. Ault, S. Keller and D. Harper. 2002. BEDROCK_GEOL_MM48_IN: Bedrock Geology of Indiana (Indiana Geological Survey, 1:500,000, Polygon Shapefile). *Indiana Geological Survey*, http://igs.indiana.edu/arcims/statewide/dload_page/geology.html (accessed April 4, 2006).

Herzog, B.L., B.J. Stiff, C.H. Chenoweth, K.L. Warner, J.B. Sieverling and C. Averly. 1994. *Buried Bedrock Surface of Illinois*. Illinois State Geological Survey Illinois Map 5, Champaign, IL.

Illinois Department of Natural Resources. 1996a. Bedrock Geology, Illinois Geographic Information System, Volume I (GIS Data on CD-ROM). *Illinois Department of Natural Resources* (May 1996).

Illinois Department of Natural Resources. 1996b. Bedrock Topography, Illinois Geographic Information System, Volume I (GIS Data on CD-ROM). *Illinois Department of Natural Resources* (May 1996).

Kolata, D.R., T.C. Buschbach and J.D. Treworgy. 1978. *The Sandwich Fault Zone of Northern Illinois*. Illinois State Geological Survey Circular 505, Urbana, IL.

Microsoft Corporation. 2003. Microsoft Office Excel 2003.

National Oceanic and Atmospheric Administration Satellite and Information Service. 1996. Bathymetry of Lake Michigan. *National Oceanic and Atmospheric Administration*, <http://map.ngdc.noaa.gov/website/mgg/greatlakesbathy/viewer.htm> (accessed August 9, 2005).

Rupp, J.A. 1991. *Structure and Isopach Maps of the Paleozoic Rocks of Indiana*. Indiana Department of Natural Resources Geological Survey Special Report 48, Bloomington, IN.

Visocky, A.P., M.G. Sherrill and K. Cartwright. 1985. *Geology, Hydrology, and Water Quality of the Cambrian and Ordovician Systems in Northern Illinois*. Illinois State Geological Survey and Illinois State Water Survey Cooperative Groundwater Report 10, Champaign, IL.

Western Michigan University Department of Geology. 1981. *Hydrogeologic Atlas of Michigan prepared for United States Environmental Protection Agency, Underground Injection Control Program*. Western Michigan University, Kalamazoo, MI.

Willman, H.B., E. Atherton, T.C. Buschbach, C. Collinson, J.C. Frye, M.E. Hopkins, J.A. Lineback and J.A. Simon. 1975. *Handbook of Illinois Stratigraphy*. Illinois State Geological Survey Bulletin 95, Urbana, IL.

Wisconsin Geological and Natural History Survey and Wisconsin Department of Administration State Planning Office. 1976. *Glacial Deposits of Wisconsin, Sand and Gravel Resource Potential*. Wisconsin Geological and Natural History Survey Land Resources Analysis Program Map 10, Madison, WI.

Young, H.L. 1992. *Summary of Ground-Water Hydrology of the Cambrian-Ordovician Aquifer System in the Northern Midwest, United States*. United States Geological Survey Professional Paper 1405-A, Washington, DC.